GUIDELINES AND STANDARDS

Guidelines for the Echocardiographic Assessment of the Right Heart in Adults and Special Considerations in Pulmonary Hypertension: Recommendations from the American Society of Echocardiography

Monica Mukherjee, MD, MPH, FASE, Chair, Lawrence G. Rudski, MDCM, FASE, Co-Chair, Karima Addetia, MD, FASE, Jonathan Afilalo, MD, MSc, Michele D'Alto, MD, PhD, Benjamin H. Freed, MD, FASE, Lynsy B. Friend, ACS, RCS, FASE, Luna Gargani, MD, PhD, Julia Grapsa, MD, PhD, FASE, Paul M. Hassoun, MD, Lanqi Hua, RDCS, FASE, Jiwon Kim, MD, FASE, Valentina Mercurio, MD, PhD, Rajan Saggar, MD, and Anton Vonk-Noordegraaf, MD, PhD, *Baltimore, Maryland; Montreal, Quebec, Canada; Chicago, Illinois; Naples and Pisa, Italy; Lebanon, New Hampshire; London, United Kingdom; Boston, Massachusetts; New York, New York; Los Angeles, California; and Amsterdam, the Netherlands*

Right heart adaptation to pulmonary hypertension (PH) is a critical determinant of clinical outcomes, morbidity, and mortality in patients with or at risk for cardiopulmonary disease. The World Symposium on Pulmonary Hypertension recently redefined PH as a mean pulmonary arterial pressure >20 mm Hg, based on a wealth of epidemiologic evidence underscoring the significant impact of even mildly elevated mean pulmonary artery pressures on major adverse clinical events. The lowered diagnostic threshold for PH has renewed interest in echocardiography and its critical role in early detection and screening, refined hemodynamic evaluation, and longitudinal monitoring. However, the systematic assessment of the right heart remains inconsistent, largely due to the predominant focus on left heart evaluation, limited familiarity with right heart ultrasound techniques, and a paucity of reference data defining normal right heart size and function. A systematic, comprehensive ultrasound-based assessment of the right heart offers valuable diagnostic insights for in screening at-risk populations, PH classification, risk stratification, monitoring therapeutic response, and informing prognostication, thereby improving clinical outcomes. (J Am Soc Echocardiogr 2025;38:141-86.)

Keywords: Echocardiography, Right heart, Right atrium, Right ventricle, Pulmonary hypertension, Prognosis

From the Johns Hopkins University School of Medicine, Baltimore, Maryland (M.M., P.M.H.); Division of Cardiology, Azrieli Heart Center, Jewish General Hospital, McGill University, Montreal, Quebec, Canada (L.G.R., J.A.); University of Chicago Heart and Vascular Center, Chicago, Illinois (K.A.); Department of Cardiology, Monaldi Hospital, Naples, Italy (M.D.); Division of Cardiology, Northwestern University Feinberg School of Medicine, Chicago, Illinois (B.H.F.); Dartmouth Hitchcock Medical Center, Lebanon, New Hampshire (L.B.F.); Department of Surgical, Medical and Molecular Pathology and Critical Care Medicine, University of Pisa, Pisa, Italy (L.G.); the Department of Cardiology, Guys and St. Thomas NHS Trust, London, United Kingdom (J.G.); Massachusetts General Hospital, Harvard University School of Medicine, Boston, Massachusetts (L.H.); Division of Cardiology, Weill Cornell Medicine, New York, New York (J.K.); the Department of Translational Medical Sciences, Federico II University of Naples, Naples, Italy (V.M.); the Lung and Heart-Lung Transplant and Pulmonary Hypertension Programs, David Geffen School of Medicine, University of California, Los Angeles, Los Angeles, California (R.S.); and the Department of Pulmonary Medicine, Amsterdam UMC Vrije Universiteit Amsterdam, Amsterdam, the Netherlands (A.V.-N.).

Attention ASE Members:

Login at "www.ASELearningHub.org to earn continuing medical education credit through an online activity related to this article. Certificates are available for immediate access upon successful completion of the activity and postwork. This activity is free for ASE Members, and $40 for nonmembers.

TABLE OF CONTENTS

Abbreviations

2DE = Two-dimensional echocardiography

3DE = Three-dimensional echocardiography

AccT = Acceleration time

ACHD = Adult congenital heart disease

AF = Atrial fibrillation

AFTR = Atriofunctional tricuspid regurgitation

ASE = American Society of Echocardiography

BSA = Body surface area

CMR = Cardiac magnetic resonance

CO = Cardiac output

CT = Computed tomography

CW = Continuous-wave

ERS = European Respiratory Society

ESC = European Society of Cardiology

ET = Ejection time

FAC = Fractional area change

FDG = 2-deoxy-2-[^{18}F]-fluorodeoxyglucose

FTR = Functional tricuspid regurgitation

HVd = Hepatic vein diastolic wave velocity

HVs = Hepatic vein systolic wave velocity

IVC = Inferior vena cava

IVCT = Isovolumetric contraction time

IVRT = Isovolumetric relaxation time

IVS = Interventricular septum

LV = Left ventricular

LVEDP = Left ventricular end-diastolic pressure

LVEI = Left ventricular eccentricity index

LVOT = Left ventricular outflow tract

MOD = Method of discs

MPA = Main pulmonary artery

mPAP = Mean pulmonary artery pressure

MPI = Myocardial performance index

PA = Pulmonary artery

PAEDP = Pulmonary artery end-diastolic pressure

PAH = Pulmonary arterial hypertension

Echocardiography is the diagnostic tool of choice in the comprehensive assessment of the right heart, largely based on the 2010 American Society of Echocardiography (ASE) guidelines,[1] which drew much needed attention to the importance of essential imaging techniques and established reference values of normality. However, an important diagnostic challenge in the classification of pulmonary hypertension (PH) is distinguishing pre-capillary PH from post-capillary PH due to left-sided heart disease. Advancements in Doppler-based techniques for noninvasive hemodynamic estimation, combined with the functional assessment of right heart remodeling in response to increased afterload, have established echocardiography as an essential first-line imaging modality. Furthermore, echocardiography is a widely available clinical tool that demonstrates practicality, repeatability, and value in serial monitoring of therapeutic interventions in PH given its high specificity and positive predictive value.[1]

The present document replaces the 2010 ASE right heart guidelines,[1] providing updated normative values and severity grading for relevant right heart echocardiographic parameters on the basis of a comprehensive review of published large epidemiologic cohorts, as shown in Table 1. Furthermore, this document places special emphasis on evaluating the right heart in the context of individuals with pulmonary vascular disease (PVD) at risk for and with PH, across World Symposium on Pulmonary Hypertension (WSPH) subtypes[2,3]

Specifically, the purposes of the present guidelines document are as follows:

1. Describe the updated PH classification and how the right heart adapts to emerging PVD, focusing on structural and functional changes in response to increased afterload.
2. Define the optimal acoustic windows and echocardiographic views and parameters required for right heart evaluation.
3. Provide reference values to define normality and grade abnormality on the basis of a critical review of the literature.
4. Present recommendations on the assessment of tricuspid valve (TV) and pulmonic valve (PV) disease and special considerations in PH.

PASP = Pulmonary artery systolic pressure

PCWP = Pulmonary capillary wedge pressure

PET = Positron emission tomography

PH = Pulmonary hypertension

PLAX = Parasternal long-axis

PR = Pulmonic regurgitation

PS = Pulmonic stenosis

PSAX = Parasternal short-axis

PV = Pulmonic valve

PVD = Pulmonary vascular disease

PVR = Pulmonary vascular resistance

PW = Pulsed-wave

RA = Right atrial

RAP = Right atrial pressure

RAV = Right atrial volume

RHC = Right heart catheterization

RV = Right ventricular

RVEDA = Right ventricular end-diastolic area

RVEDV = Right ventricular end-diastolic volume

RVEF = Right ventricular ejection fraction

RVESA = Right ventricular end-systolic area

RVESV = Right ventricular end-systolic volume

RVFW = Right ventricular free wall

RVFWS = Right ventricular free wall strain

RVGLS = Right ventricular global longitudinal strain

RVH = Right ventricular hypertrophy

RVOT = Right ventricular outflow tract

RVSP = Right ventricular systolic pressure

RVWT = Right ventricular wall thickness

5. Propose standard image acquisition and reporting for right-sided measures in clinical practice.
6. Establish the essential role for echocardiography in screening, detection, monitoring of therapeutic response, and prognostication of PH.

A. QUALITATIVE AND QUANTITATIVE ASSESSMENT OF THE RIGHT HEART

Given the complex geometric configuration of the right heart, which varies in shape with loading conditions, such as PH, heart failure, and valvular heart disease, the comprehensive qualitative and quantitative assessment of chamber size is essential. Figure 1 demonstrates the recommended imaging windows for comprehensive right heart chamber assessment. Table 2 summarizes recommendations for image acquisition of essential right heart chamber size with representative illustrations.

Right Atrium

The right atrium (RA) is the least studied cardiac chamber, yet its importance has been well documented across various conditions. A contemporary meta-analysis underscored the clinical value of RA area as a simple reproducible measure that is significantly associated with clinical worsening, morbidity, and mortality in PH.[4] RA size is also an integral component of existing PH screening and risk stratification algorithms in patients at risk for and with PH.[2,3]

A thorough evaluation of RA chamber size and function is crucial in the assessment of the right heart. Anatomically, the RA is composed of an appendage and a vestibule, which includes the fossa ovalis, crista terminalis, and Eustachian valve. The RA chamber is best imaged from a modified right ventricular (RV)–focused view,[1,5] focused on optimizing atrial visualization. First,

STE = Speckle-tracking echocardiography

SV = Stroke volume

TAPSE = Tricuspid annular plane systolic excursion

TCO = Tricuspid closure-open interval

TDI = Tissue Doppler imaging

TEE = Transesophageal echocardiography

TMAD = Tissue motion annular displacement

TR = Tricuspid regurgitation

TV = Tricuspid valve

TVA = Tricuspid valve annulus

UEA = Ultrasound enhancing agent

VTI = Velocity-time integral

WSPH = World Symposium on Pulmonary Hypertension

the right heart is visualized from the apical four chamber view, and the transducer is moved laterally to ensure complete visualization of the RV free wall (RVFW) throughout the cycle, as shown in Figure 2. To obtain the RA-focused view, the proble is then tilted superiorly (upward) and medially (toward the sternum) to maximize visualization of the entire RA chamber. The depth, focus, and gain settings can be adjusted to enhance endocardial border definition and frame rate and optimize image quality. Employing an atrial-focused view has been shown to improve area and volumetric measurements of the RA chamber, comparable with volumetric assessment by three-dimensional echocardiography (3DE).[6]

RA volume (RAV) can be evaluated using the single-plane method of discs (MOD) or the area-length approach. Compared directly against the single-plane MOD, volumes obtained using the area-length approach are often larger. Since a standardized orthogonal plane for the RA is not available to enable biplane volume measurements, volumes derived using the single-plane MOD method is recommended. RAV measurements using the MOD approach are more accurate compared to linear measurements, although they may be enlarged in normal subjects, such as athletes and men, even after indexing to body surface area (BSA). RA enlargement should be considered abnormal when contextual factors such as patient demographics and clinical history suggest underlying pathology or when associated findings, such as impaired RA function, significant tricuspid regurgitation (TR), or signs of elevated RA pressure (RAP), are present. Similar to the left atrium, increased RAV is a better reflection of chronic filling conditions and RV diastolic dysfunction.[1,2]

Three-dimensional echocardiography (3DE)–derived RAV is obtained from the RA-focused apical view using multibeat full-volume acquisition and tend to be larger than volumes derived using two-dimensional echocardiographic (2DE) methodology. However, although 3DE-based RAV provides detailed volumetric and functional RA assessments, its clinical application is still emerging and it is not yet widely recommended for standard clinical use.

Key Points

- The RA is best imaged from the apical four-chamber view at the end of ventricular systole and tilting upwards to maximize visualization of the superior aspect of the chamber. The single plane MOD is the best approach to assess RAV.
- Normal thresholds are RA area < 19 cm^2, RAV index (MOD) < 30 mL/m^2, and RAV index (area-length) < 32 mL/m^2.
- An enlarged RA chamber can be seen in normal subjects, even after indexing to BSA. When abnormal, RA dilatation reflects chronic elevations in filling pressures and RV diastolic dysfunction.

Recommendation

> 1. Given its inclusion in screening algorithms for PH and prognostic significance, RA area and/or RAV indexed to BSA should be included in standard echo reporting.

Right Ventricle

In normal subjects, the RV assumes a flattened, pear-shaped appearance consisting of three major anatomic components: (1) the inlet portion, comprising the TV and subvalvular apparatus and the papillary muscles; (2) the trabeculated apical myocardium; and (3) the infundibulum or conus, encompassing the smooth-walled RV outflow tract (RVOT) beneath the PV. By 2DE, no single geometric model can capture all three components in a single plane and therefore, multiple imaging planes are required for a comprehensive quantitative assessment, as shown in Figure 1. Qualitatively, the RV should appear no more than two-thirds the size of the left ventricular (LV) with relative predominance of the LV apex from the apical four-chamber view.[1,5]

Acquisition techniques for RV quantitative measures are further detailed in Table 2, however two important considerations should be emphasized. First, RV linear measurements obtained from the parasternal views are variable depending on transducer angulation and the rib interspace from which they were acquired. Second, RV basal, midventricular, and longitudinal dimensions should be obtained in end-diastole from the apical RV-focused view, ensuring that the lateral wall is visualized throughout the cardiac cycle (Figure 2). The RV-focused view has been shown to provide more reproducible measurements of RV size and function than the conventional apical four-chamber view.[7] With maladaptation of the right heart chambers seen in progressive high afterload states such as PH,[8,9] the longitudinal linear dimension should be adjusted to represent the distance from the displaced apex perpendicularly to the tricuspid valve annulus (TVA), parallel to the interventricular septum (IVS).

The RV wall thickness (RVWT) is preferentially measured from the subcostal view in end-diastole. RVWT measurements may be obtained from the 2DE-directed linear measures and/or M-mode imaging from the anteromedial aspect of the free wall, halfway between the TVA and papillary muscles. Subcostal acoustic windows are advantageous in patients with PH and significant lung disease, enabling right heart imaging without interference from bone or lung artifacts. The subcostal approach is also useful for patients who cannot be positioned in the lateral decubitus position. However, subcostal imaging may be challenging due to the relatively thin RVFW and prominent trabeculations of the RV cavity. In these cases, RVWT can be measured from the parasternal long-axis (PLAX) view. Increased RVWT can be seen in PH across WSPH classes depending on the time course, underlying disease etiology, disease duration, and the degree of adaptation.[9-12] However, increased RVWT is a nonspecific finding and can also be seen in infiltrative and inherited cardiomyopathies.

In addition to linear dimensions, RV size can be measured by area and volume using 2DE and 3DE, respectively, from the RV-focused view, as detailed in Table 2. For both 2DE-derived RV end-diastolic area (RVEDA) and RV end-systolic area, and 3DE-derived RV end-diastolic volume (RVEDV) and RV end-systolic volume (RVESV), the endocardial border should be traced such that the papillary muscles, trabeculations, and moderator band are included within the measurements. When feasible, RV volumetric measures should be obtained using 3DE techniques, as there is no simplified method to calculate RV volumes using 2DE alone.[13] To obtain a full 3DE volume data set of the entire chamber, imaging is performed at minimal depth and with a limited sector size. Although most dedicated RV analytic software automatically identifies the timing of end-diastole and end-systole, the maximum and minimum RV chamber sizes and endocardial borders should be manually verified.

When compared with cardiac magnetic resonance (CMR) imaging, RV volumes are slightly underestimated by echocardiography.[14-17] Intervendor and intersoftware discrepancies may also contribute to variability in RV volume measurements.[18] Studies have consistently shown that women have smaller RV volumes compared with men, even when adjusted for BSA,[18-21] and are smallest among Asian adults.[22] There is conflicting data, however, regarding the impact of physiologic aging on 3DE-derived RV volumes. A prior study of 507 healthy volunteers found a 5 mL/decade decrease in RVEDV and a 3 mL/decade decrease in RVESV.[19] However, a more recent meta-analysis suggests that the overall change per decade is smaller, with a reduction of 1-2 mL/decade for both RVEDV and RVESV,[18] Additionally, data from the World Alliance Societies of Echocardiography (WASE) has suggested that there are no significant differences in these parameters with age.[22]

Key Points

> - Quantitative measures of RV chamber size are readily obtained using standard parasternal short-axis (PSAX) and PLAX views and from the apical RV-focused view.
> - RVWT should be obtained from the anteromedial aspect of the free wall using the subcostal view by direct 2DE measures and/or M-mode imaging. If technically difficult, the PLAX view can also be used for RVWT measurements.
> - The normal value for RVWT is <5 mm.
> - 3DE-derived RV volumes can be can be obtained using dedicated software from a full-volume data set, although they may be underestimated compared with CMR.

Recommendations

> 1. RV chamber quantification should be performed from the parasternal windows and the apical RV-focused view, ensuring that the RVFW is visualized throughout the cardiac cycle.
> 2. Critical measures for reporting include at least one quantitative measure of RV chamber size, typically the basal dimension obtained from the RV-focused apical four-chamber view. However, multiple measures may be necessary in select populations.
> 3. RVWT should be reported if abnormal.

Interventricular Septum

The morphology and phasic function of the IVS are closely linked to contractility, hemodynamic conditions, electric conduction, and the intricate interplay between the two ventricles.[23] IVS morphology can be assessed visually on M-mode imaging, 2DE, and 3DE. The

Table 1 Summary of reference limits for recommended measures of right heart structure and function

Variable	Normal Reference Value	Abnormality Grading		
		Mild	Moderate	Severe
Chamber dimension				
RA major dimension, cm	<5.4	≥5.4 to ≤5.8	>5.8 to ≤6.3	>6.3
RA minor dimension, cm	<4.2	≥4.2 to ≤4.7	>4.7 to ≤5.1	>5.1
RA area, cm^2	<19	≥19 to ≤22	>22 to ≤24	>24
RAV index (method of disks), mL/m^2	<30	≥30 to ≤36	>36 to ≤41	>41
RAV index (area-length method), mL/m^2	<33	≥33 to ≤38	>39 to ≤44	>44
RA end-systolic volume index (3D method), mL/m^2	<42	≥42 to ≤49	>49 to ≤57	>57
RA end-diastolic volume index (3D method), mL/m^2	<20	≥20 to ≤23	>23 to ≤27	>27
RV diameter basal, cm	<4.1	≥4.1 to ≤4.4	>4.4 to ≤4.9	>4.9
RV diameter basal index, cm/m^2	<2.4	≥2.4 to ≤2.6	>2.6 to ≤2.9	>2.9
RV diameter midventricular, cm	<3.5	≥3.5 to ≤3.8	>3.8 to ≤4.2	>4.2
RV diameter longitudinal, cm	<8.2	≥8.2 to ≤8.9	>8.9 to ≤9.6	>9.6
RVOT PLAX diameter, cm	<3.3	≥3.3 to ≤3.5	>3.5 to ≤3.9	>3.9
RVOT PSAX proximal diameter, cm	<3.4	≥3.4 to ≤3.8	>3.8 to ≤4.1	>4.1
RVOT PSAX distal diameter, cm	<2.9	≥2.9 to ≤3.0	>3.0 to ≤3.3	>3.3
RVWT, cm	<0.5	≥0.5 to ≤0.7	>0.7 to ≤0.9	>0.9
RV end-systolic area, cm^2	<14	≥14 to ≤16	>16 to ≤19	>19
RV end-systolic area index, cm^2	<8	≥8 to ≤9	>9 to ≤11	>11
RV end-diastolic area, cm^2	<25	≥25 to ≤28	>28 to ≤32	>32
RV end-diastolic area index, cm^2	<14	≥14 to ≤15	>15 to ≤17	>17
3D end-systolic volume, mL	<66	≥66 to ≤77	>77 to ≤89	>89
3D end-systolic volume index, mL/m^2	<41	≥41 to ≤48	>48 to ≤55	>55
3D end-diastolic volume, mL	<130	≥130 to ≤150	>150 to ≤170	>170
3D end-diastolic volume index, mL/m^2	<90	≥90 to ≤103	>103 to ≤115	>115
PA, cm	<2.5	≥2.5 to ≤3.0	>3.0 to ≤3.5	>3.5
RV systolic function				
TAPSE, cm	>1.7	≤1.7 to ≥1.3	≤1.3 to >1.0	≤1.0
Tissue Doppler S′ velocity, cm/s	>9.5	≤9.5 to ≥7.2	≤7.2 to > 5.0	≤5.0
Tissue Doppler RV MPI	<0.55	≥0.55 to <0.62	≥0.62 to <0.70	≥0.70
Pulsed Doppler RV MPI	<0.40	≥0.40 to <0.49	≥0.49 to <0.57	≥0.57
FAC, %	>35	≤35 to >29	≤29 to >22	≤22
3D RVEF, %	>45	≤45 to <39	≤39 to ≥32	<32
RV longitudinal free wall strain (three segment), %*	>20	≤20 to <15	<15 to ≥11	<11
RV longitudinal global strain (six segment), %*	>17	≤17 to >13	≤13 to >9	≤9
RV diastolic function				
RV E/A ratio	≥0.8 to <2.0	<0.8 Impaired relaxation	0.8 to 2.1 Pseudonormal	>2.1 Restrictive
RV e′/a′ ratio	≥0.5 to <1.8	≥1.8 to ≤2.1	>2.1 to ≤2.4	≥2.5
RV E/e′ ratio	<6.0	≥6.0 to ≤7.3	>7.3 to ≤8.4	≥8.5
Deceleration time, ms	≥120 to ≤230	≥87 to <120	≥57 to <87	≤57
Hemodynamics				
TRV maximum, m/s[†]	<2.8	≥2.8[†] to ≤3.1	≥3.2 to ≤3.5	≥3.6
RVSP, mm Hg	≤34	≥35 to ≤49	≥50 to ≤69	≥70
RAP, mm Hg	≥0 to <5 (mean 3)	≥5 to <10 (mean 8)	≥10 to <15	≥15
RVOT AccT, ms	>105	≥80 to ≤105	≥60 to <80	≤60

3D, three-dimensional; *AccT*, acceleration time; *FAC*, fractional area change; *PA*, pulmonary artery; *RA*, right atrium; *RAP*, right atrial pressure; *RAV*, right atrial volume; *RV*, right ventricle; *RVEF*, right ventricular ejection fraction; *RVOT*, right ventricular outflow tract; *RVSP*, right ventricular systolic pressure; *RVWT*, right ventricular wall thickness; *TAPSE*, tricuspid annular plane systolic excursion; *TRV*, tricuspid regurgitant velocity.

*Absolute values and ranges for strain are shown.

[†]Resting peak TRV of ≥2.9 or ≥2.8 m/s with at least two adjunctive echocardiographic signs suggests PH.
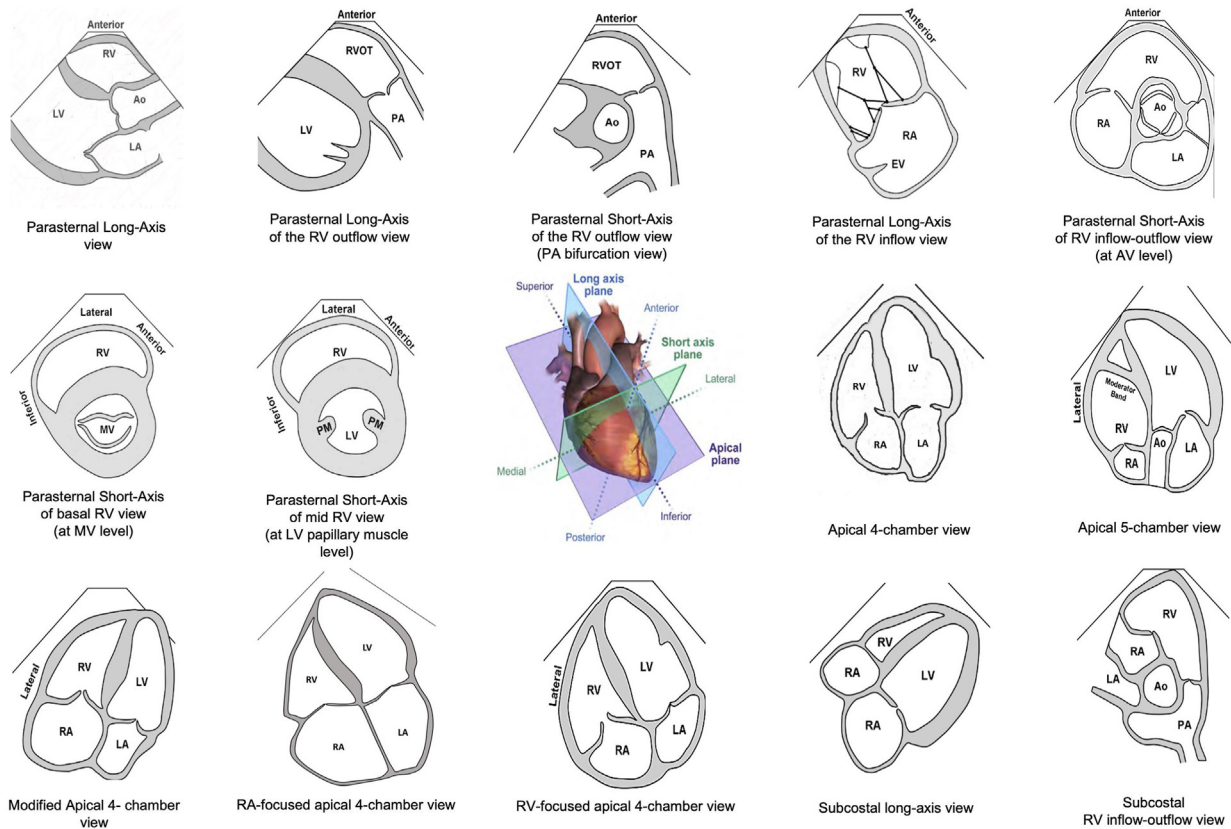
Figure 1 Standard transthoracic imaging planes for comprehensive right heart assessment. Several key views should be included in the standard echocardiographic assessment of the right heart. The PLAX view assesses RV internal diastolic dimension, while the parasternal RV outflow view quantifies mid and distal RVOT size, RVOT AccT, and the structure and function of the TV and PV. A high parasternal outflow view visualizes the proximal PA and PA bifurcation. The parasternal RV inflow view typically focuses on the anterior and septal tricuspid leaflets, while parasternal short-axis views can be used to assess the LV eccentricity index. The apical views (four-chamber, RA and RV focused) are essential for evaluating right heart chamber size and function. Hemodynamic assessment of RVSP often requires imaging planes such as the RV inflow, apical RV-focused, reversed four-chamber, and subcostal views. PAEDP and RVOT AccT are obtained from the parasternal RV outflow view. The subcostal long-axis view assesses RVWT, RA and RV size, hypertrophied infundibular muscle bundles, and provides alternative imaging planes for assessing the structure and function of the TV and PV, as well as evaluating for RVOT obstruction. The subcostal view is particularly useful in cases of congenital heart disease. Images provided by Lanqi Hua, RCDS. *Ao*, Aorta; *EV*, Eustachian valve; *LA*, left atrium; *MV*, mitral valve; *PM*, papillary muscle.
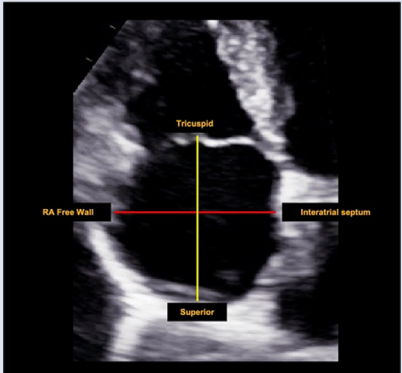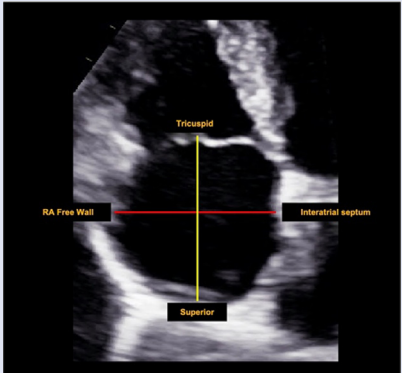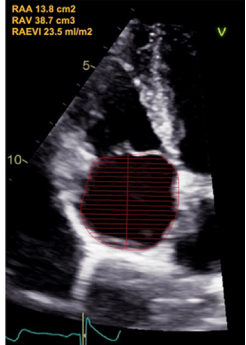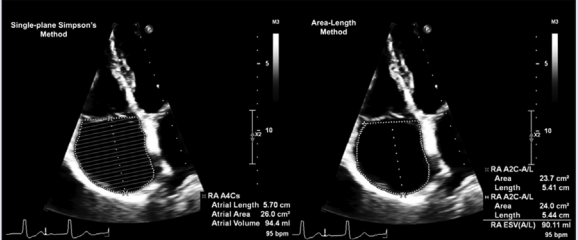
LV eccentricity index (LVEI) quantifies the change to the geometric and physiologic curvature of the septum throughout the cardiac cycle as a marker of RV loading conditions. The magnitude of IVS flattening is defined as the length ratio of two perpendicular LV dimensions, the LV anteroposterior and septolateral dimensions, from the PSAX view at the level of the papillary muscles, as shown in Table 2.

In normal hemodynamic states, the LVEI ratio is 1 in both end-systole and end-diastole, reflecting a roughly circular profile of the LV chamber throughout the cardiac cycle. An LVEI greater than 1 at end-diastole suggests RV volume overload. Common clinical scenarios leading to RV volume overload include significant pulmonic regurgitation (PR) and/or TR, and congenital conditions such as atrial septal defect and anomalous pulmonary venous drainage. RV pressure overload distorts the IVS predominately during RV end-systole and early LV diastole, resulting in LVEI > 1 at end-systole. Flattening of the LVEI in end-systole can occur in PH as well as conditions such as pulmonic stenosis (PS) and RVOT obstruction, even in the absence of elevated pulmonary pressures.

In contrast, an LVEI value >1 at both end-systole and end-diastole suggests elevated RV pressure with or without concomitant volume overload. Advanced PH and right heart failure may be associated with progressive flattening and distortion of the IVS, interventricular mechanical dyssynchrony, and LV underfilling.[24]

Abnormal LVEI is a common finding among patients with precapillary PH and an important prognostic marker in this population,[25-28] leading to the incorporation of this metric in clinical PH screening.[2,3] Quantifying LVEI reduces interobserver variability compared with subjective assessment; however is dependent on an accurate imaging plane and optimal visualization. Additionally, IVS morphology and function are best assessed without significant conduction abnormalities such as preexcitation and paced rhythms, after cardiac surgery, or in conditions that may result in ventricular interdependence, such as constrictive pericarditis.[23] Recent advances in postprocessing techniques demonstrate the feasibility of three-dimensional echocardiographic septal curvature analyses, allowing quantification of regional RV septal morphology.[29]

Table 2 Right heart quantitative chamber assessment

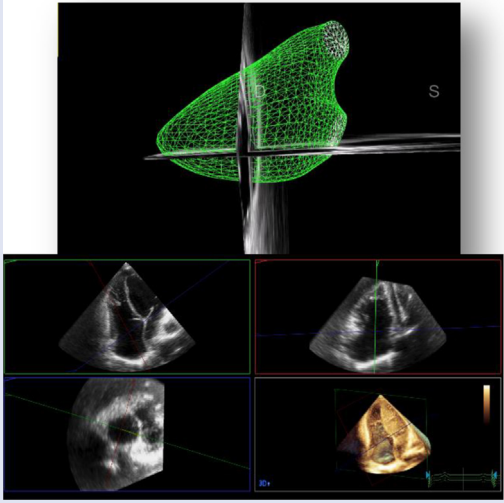| Variable	Image acquisition	Illustration
RA major dimension (long-axis, longitudinal), cm	From the dedicated RA-focused apical 4Ch view, linear RA dimensions are measured at the end of ventricular systole. The major (long-axis longitudinal, yellow line) dimension of the RA is from the center of the TVA to the center of the superior RA wall, parallel to the interatrial septum.	
RA minor dimension, (short axis, transverse), cm	The RA minor (transverse, red line) dimension is obtained from the midlevel of the RA free wall to the interatrial septum, perpendicular to the long axis of the chamber, excluding the RA appendage and venae cavae.	
RA end-systolic area, cm^2	The RA area is measured from the lateral aspect of the TVA to the septal aspect following the RA endocardium and excluding the IVC and superior vena cava and RA appendage.	
RA volume (2D and 3D), cm^3	2DE volumes are obtained from the dedicated RA-focused apical 4Ch view at the end of ventricular systole and can be calculated either by the single-plane Simpson's method or the area-length method. 2DE-derived RAV is typically smaller than those obtained by 3DE. Volumes should be indexed to BSA. 3DE datasets are usually obtained from the apical approach using a multi-beat full-volume acquisition.	

(Continued)

Table 2 (*Continued*)

Variable	Image acquisition	Illustration
RV chamber		
Basal, cm	From RV focused apical 4Ch view, the basal dimension is measured at end-diastole just beneath and parallel to the tricuspid annular plane from RVFW to the interventricular septum.	
Midventricular, cm	From approximately halfway between the tricuspid annular plane and the apex, the midventricular dimension is measured from RVFW to interventricular septum parallel to the tricuspid annular plane.	
Longitudinal, cm	The longitudinal dimension is measured just beneath the tricuspid annulus from the midpoint to the tip of the RV apex. However, this measurement is highly dependent on probe rotation, and it is important to avoid foreshortening. If the RV apex is displaced leftward, the measurement should be taken from the displaced apex to the midpoint of the basal dimension.	
RVEDA, cm^2	From the RV-focused apical 4Ch view, the endocardial border is traced in end-diastole from the lateral tricuspid annulus along the RVFW to the apex and back along the IVS toward the medial tricuspid annulus. The papillary muscles, trabeculations, and moderator band are all included in the cavity area.	
RVESA, cm^2	From the RV-focused apical 4Ch view, the endocardial border is traced in end-systole from the lateral tricuspid annulus along the free wall to the apex and back along the IVS toward the medial tricuspid annulus. The papillary muscles, trabeculations, and moderator band are all included in the cavity area.	
RV wall thickness, cm	From the subcostal view, the RVWT is measured in end-diastole at the level of the RV inflow (initial one-third of the RV chamber between the tricuspid annulus and papillary muscles), excluding trabeculations, papillary muscle and pericardial fat. RVWT can be measured by M-mode or 2DE-directed images. However, M-mode images can be confounded by the angle of insonation.	

(*Continued*)

Table 2 (*Continued*)

Variable	Image acquisition	Illustration
Interventricular septal morphology	EI is calculated as the ratio of two dimensions and is unitless. D1 is the septal-lateral dimension (red) perpendicular to the interventricular septum, dividing the ventricle in half. D2 is the anterior-posterior dimension (yellow) parallel to the IVS at the midpoint of the chamber. Both the RVEI and the LVEI are measured from the PSAX at the level of the papillary muscles in end-diastole and end-systole. EI = D2/D1 LVEI quantifies the presence of abnormal IVS curvature in RV volume overload (when measured at end-diastole) and RV pressure overload (when measured at end-systole). LVEI is calculated as D2/D1 and is abnormal if > 1. RVEI quantifies the presence of abnormal IVS curvature in RV volume overload (when measured at end-diastole) and RV pressure overload (when measured at end-systole). The RVEI = D2/D1 and is abnormal if > 1. LVEI is used more commonly than RVEI.	
RVOT Proximal diameter, cm	The proximal RVOT dimension can be measured at the end of diastole in both parasternal long-axis and cross-sectional imaging planes. RVOT measurements can differ by up to 40% between planes. The proximal RVOT dimension from the PLAX view is measured from RVFW to IVS, proximal to the aortic valve, transecting the RV chamber, and is referred to as the RVIDD when measured from this plane. From the PSAX, the proximal RVOT diameter is measured from RVFW the anterior aortic wall above the aortic valve, perpendicular to the RV chamber.	
Distal diameter, cm	The distal RVOT dimension is measured from the PA bifurcation PSAX view from lateral aortic wall to distal RVOT free wall just proximal to the pulmonary annulus in end-diastole. The distal RVOT dimension from this imaging plane is less variable.	
Pulmonary artery, cm	The PA dimensions are measured from the PA bifurcation PSAX view in end-diastole. The MPA dimension is measured halfway between the pulmonary annulus and the PA bifurcation. The left and right PA dimensions are measured at the proximal portion of the respective PA branch in end-diastole.	

Table 2 (*Continued*)

Variable	Image acquisition	Illustration
3D volumes	An ECG-gated 3DE dataset is acquired from an RV-focused apical 4Ch view by combining sub-volumes generated from 4 to 6 consecutive cardiac cycles. From the apical 4Ch view, the entire RVFW and apex should be included and breath holding can be used to avoid stitching artifact. If the RV-focused view is suboptimal, the subcostal view can also be used. If the rhythm is irregular, using a two-beat full-volume acquisition can also be used to avoid stitching artifact, although a two-beat acquisition may reduce temporal resolution. UEA should be considered when imaging quality is suboptimal.	

2DE, two-dimensional echocardiography; *3DE*, three-dimensional echocardiography; *4Ch*, four-chamber; *BSA*, body surface area; *EI*, eccentricity index; *IVC*, inferior vena cava; *IVS*, interventricular septum; *LVEI*, left ventricular eccentricity index; *PA*, pulmonary artery; *PLAX*, parasternal long axis; *PSAX*, parasternal short axis; *RA*, right atrium; *RAV*, right atrial volume; *RVEDA*, right ventricular end-diastolic area; *RVEI*, right ventricular eccentricity index; *RVESA*, right ventricular end-systolic area; *RVFW*, right ventricular free wall; *RVIDD*, right ventricular internal diastolic dimension; *RVOT*, right ventricular outflow tract; *RVWT*, right ventricular wall thickness; *TVA*, tricuspid valve annulus; *UEA*, ultrasound enhancing agents.

Key Points

- LVEI is the ratio of LV anteroposterior and LV septolateral dimensions measured from the PSAX view at the level of the papillary muscles and has prognostic value in PH.
- LVEI = 1 in both end-systole and end-diastole reflects a circular LV profile throughout the cardiac cycle and normal RV hemodynamic conditions.
- LVEI > 1 at end-diastole suggests RV volume overload.
- LVEI > 1 in end-systole suggests RV pressure overload.
- LVEI > 1 in end-systole and end-diastole suggests RV pressure overload with or without concomitant volume overload.

Recommendations

1. LVEI should be measured to evaluate the presence and extent of RV volume and/or pressure overload.
2. Quantification and reporting of LVEI should be included when abnormal.

Pulmonary Artery

Similar to the right heart chambers, the main pulmonary artery (MPA) dilates in response to volume and pressure overload, and 2DE quantification of MPA diameter can be used to refine PH risk prediction.[30] The MPA dimension is evaluated from a PSAX view, at the level of the aortic valve, and then angling upward visualize the MPA and proximal pulmonary artery (PA) bifurcation. MPA diameter should be measured in end-diastole halfway between the PV and the PA bifurcation. Although technically feasible in most patients, precise MPA measurement may be challenging because of parallel orientation of the arterial walls with the ultrasound beam and rib artifact. In addition to transthoracic approaches, several views during transesophageal echocardiography (TEE) allow the evaluation of the MPA and its main branches.[31]

A 2DE-derived MPA end-diastolic diameter of >25 mm is considered abnormal. However, data derived from computed tomography (CT) suggest a normative value for the systolic diameter of the MPA of 29 mm in men and 27 mm in women,[32] while CMR-derived normative values suggest a range of 21 to 33 mm in men and 19 to 31 mm in women.[33] The systolic diameter of the MPA and its size relative to the ascending aorta by cardiac CT angiography correlates with invasive pulmonary pressures.[32,34] By TEE, a ratio of MPA to the ascending aorta ≥ 1 has also been shown to identify patients with PH, with sensitivity of 84.3%, specificity of 83.9%, positive predictive value of 87.6%, negative predictive value of 81.1%, and area under the receiver operating characteristic curve of 0.91 compared with CT-based studies.[35]

Taken together, although absolute normative values may differ by modality and are generally smaller by 2DE compared with CT and CMR, 2DE-derived MPA diameter > 25 mm and/or MPA/ascending aorta ratio ≥ 1 are abnormal. It is also important to note that variability among 2DE, CT and CMR measurements can arise from differences in cardiac cycle timing, such as end-diastolic vs systolic phase acquisition, and recognition of these differences is essential for accurate interpretation across modalities. A dilated MPA may also be a nonspecific finding and can be seen in PH across WSPH classifications, chronic lung disease, connective tissue disorders (e.g., Marfan syndrome, Ehlers-Danlos syndrome), acute and chronic pulmonary embolism, and congenital heart disease (e.g., atrial septal defect, ventricular septal defect).

Key Points

- MPA dimensions can be readily obtained by 2DE and can aid in estimating PH probability.
- MPA end-diastolic diameter > 25 mm and/or a ratio of MPA to ascending aortic diameter ≥1 by 2DE are considered abnormal.

Recommendations

1. MPA diameter is measured in end-diastole halfway between the PV and the bifurcation of the MPA from the PSAX, PA-focused view as part of a standard examination.
2. MPA diameters should be reported when abnormal.

B. FUNCTIONAL ASSESSMENT OF THE RIGHT HEART

Comprehensive echocardiographic assessment of right heart function is performed from the apical four-chamber view, as shown in Figure 2. Table 3 summarizes recommendations for image acquisition of essential right heart functional parameters.

Right Atrial Strain and Emptying Function

The RA is a dynamic structure with complex phasic function throughout the cardiac cycle, reflecting the intricate interplay between RA function and RV systolic and diastolic performance. The principal role of the RA is to regulate RV filling, serving as a reflection of RV hemodynamic conditions, as well as systolic and diastolic function. There are three phases of RA function. The RA reservoir phase occurs during ventricular systole, when the RA serves as a reservoir for systemic venous return, governed primarily by atrial compliance and relaxation. Next is the conduit phase, occurring during early ventricular diastole, and is modulated by RV relaxation and chamber stiffness. The last phase is the RA booster phase during late diastole, when RV filling is augmented by atrial contraction and is influenced by atrial contractile properties.

Evaluating RA strain using speckle-tracking echocardiography (STE) is an emerging technique to assess phasic RA function. RA strain is quantified from an RA-focused apical four-chamber view, optimized to visualize the entire RA chamber, using dedicated software either during image acquisition or post-processing. The RA chamber should be visualized without foreshortening and ensuring that the endocardial borders are visualized throughout the cardiac cycle. Foreshortened images may overestimate RA strain. On most commercially available platforms, atrial dedicated STE software can be applied can be applied to the chamber from the atrial-focused apical four-chamber view.

RA reservoir strain values are higher than corresponding left atrial strain values and are also higher in women than men.[42] Higher RAV and diminished reservoir strain have been shown to predict clinical worsening and correlate with function status and hemodynamic derangements in precapillary PH.[36-39] STE-derived RA strain may also serve as an independent contributor to right heart performance and adaptation in PH.[40] Although it is a promising tool for the RA functional assessment, the clinical applicability of RA strain is limited by the lack of established reference values across diverse populations and broad reference ranges in healthy adults.[41-43]
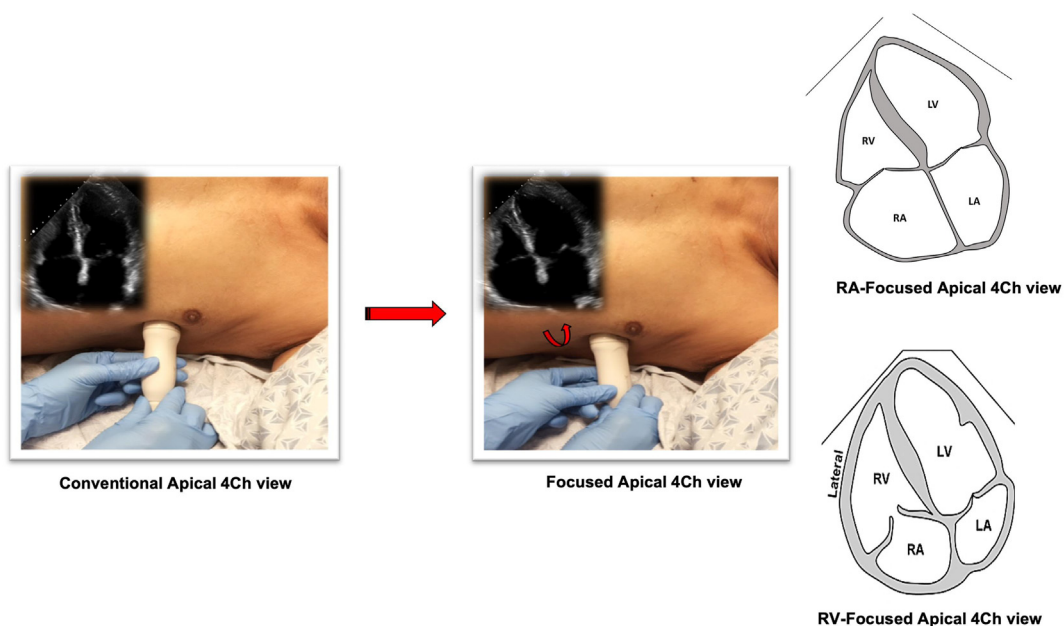

Figure 2 Approach to acquisition of the RA- and RV-focused views. To obtain the RV-focused apical 4Ch view, place the transducer at the apex, and rotate until the maximal RV chamber dimension is obtained. Often, the transducer must be positioned more laterally and tilted upward toward the RV, while ensuring that the RV apex is not foreshortened and that the left ventricular outflow tract or coronary sinus are not in plane. The RV chamber and free wall should be visualized throughout the cardiac cycle. To obtain the RA-focused view, start with the RV-focused apical 4Ch view. Then, tilt the probe superiorly (upward) and medially (toward the sternum) to maximize visualization of the entire RA chamber. The depth, focus, and gain settings can be adjusted to enhance endocardial border definition and optimize image quality. *4Ch*, four-chamber; *LA*, left atrium; *LV*, left ventricle; *RA*, right atrium; *RV*, right ventricle.

The RA function can also be measured by passive, active, and total emptying volumes and emptying fractions using 3DE methods. Recent data from the WASE study reveal significant differences in 3DE-derived RAV and functional parameters parameters stratified by sex, age, and race/ethnicity. sex, age, and race/ethnicity.[42] Although increased RAV measures and decreased emptying fractions may detect RA remodeling and dysfunction in PH,[44] this methodology has not been widely adopted in clinical practice.

Key Points

- RA strain is quantified from an RA-focused apical four-chamber view, optimized to visualize the entire RA chamber. Measurements can be made during image acquisition or post-processing using dedicated STE software.
- The three main phases of RA strain are the reservoir phase, conduit phase, and booster phase, each of which reflects the dynamic RA-RV relationship.
- Although largely a research tool, 3DE-derived total, passive, and emptying volumes and emptying fractions can also be used to assess RA phasic function.

Recommendations

1. Both STE- and 3DE-derived measures of RA phasic function have not yet been widely incorporated into clinical practice. However, these methods are important areas of active investigation and may have prognostic implications in PH and at-risk populations.
2. Although STE-derived RA strain is a promising tool for the assessment of dynamic RA phasic function, variability in normative values has limited its widespread clinical use.

Tricuspid Annular Plane Systolic Excursion

Tricuspid annular plane systolic excursion (TAPSE) measures RVFW longitudinal motion during the systolic phase of the cardiac cycle, as a surrogate of global RV systolic function. From the RV-focused view, the M-mode cursor is placed along the lateral TV annulus and aligned along the RVFW from base to apex, such that the cursor is parallel to annular motion. Focusing on the TVA using the zoom feature and increasing the sweep speed can improve TAPSE accuracy. The normal value for M-mode-derived TAPSE is >1.70 cm.

TAPSE primarily reflects tricuspid annular motion as a metric of RV longitudinal systolic function and should not be used in isolation without considering RV size and function, supportive findings, and the clinical context. Several common scenarios can lead to the underestimation of RV function by TAPSE, including suboptimal image quality, misalignment of the M-mode cursor with tricuspid annular motion, constrictive pericarditis, interference from indwelling pacemakers or catheters, and the postoperative state following cardiothoracic surgery.[45] TAPSE may overestimate RV function in the context of altered hemodynamics, right heart maladaptation,[46] and distortion of the tricuspid annulus with severe functional TR (FTR). In these cases, an abnormal TAPSE should be reported only if supported by adjunctive findings such as abnormal 3DE RV ejection fraction (RVEF) or fractional area change (FAC).

TAPSE can be combined with pulmonary artery systolic pressure (PASP), a marker of afterload, to assess RV contractile response to load, known as RV-PA coupling.[47] Validated against multibeat gold-standard pressure-volume assessment, the TAPSE/PASP ratio has demonstrated prognostic significance in a number of populations, including prediction of clinical outcomes in both pre- and postcapillary PH,[48-50] heart failure,[51] and in patients with COVID-19,[52,53] and predicts clinical outcomes in the transcatheter treatment of valvular heart disease.[54-56] In studies examining healthy individuals, the TAPSE/PASP ratio generally falls within the range of 0.5–0.7 mm/mmHg, with variations depending on factors such as age, sex, and specific methodologies used in each study.[57,59,69,163] However, in PH, a TAPSE/PASP ratio in the range of 0.3-0.4 mm/mm Hg is associated with RV-PA uncoupling as validated by pressure-volume loops and is linked to an increased mortality risk.[44,48,50]

Although less preferable to M-mode methodology, TAPSE can also be obtained using both STE and tissue Doppler imaging (TDI), known as tissue motion annular displacement (TMAD), and refers to the maximal systolic displacement of the lateral tricuspid annulus (Table 3). $TMAD_{TDI}$ has lower specificity and a greater number of false positives compared with $TMAD_{STE}$. Although $TMAD_{STE}$ overcomes some angle dependency, the lower frame rate may underestimate RV function when compared with M-mode-derived TAPSE.[58] These alternative techniques to derive TMAD are most valuable in situations in which M-mode is not feasible, such as during TEE.

Key Points

- TAPSE measurements should be reported on the basis of the quality of the measurement and in consideration of other parameters and clinical context. The normal TAPSE value is >1.70 cm.
- TAPSE accuracy varies in different scenarios and should be reported as normal or abnormal on the basis of compatible supporting findings.
- TAPSE/PASP ratio is a noninvasive physiologic index of RV-PA coupling that reflects RV contractile response to pulmonary afterload. A TAPSE/PASP ratio ranging between 0.3-0.4 mm / mm Hg is associated with RV-PA uncoupling and increased mortality risk.

Recommendations

1. TAPSE is obtained from the RV-focused view by placing the M-mode cursor along the lateral TV annulus and is a core component of the standard echocardiographic assessment of RV systolic function.
2. TAPSE values should be reported in the context of overall RV functional assessment.
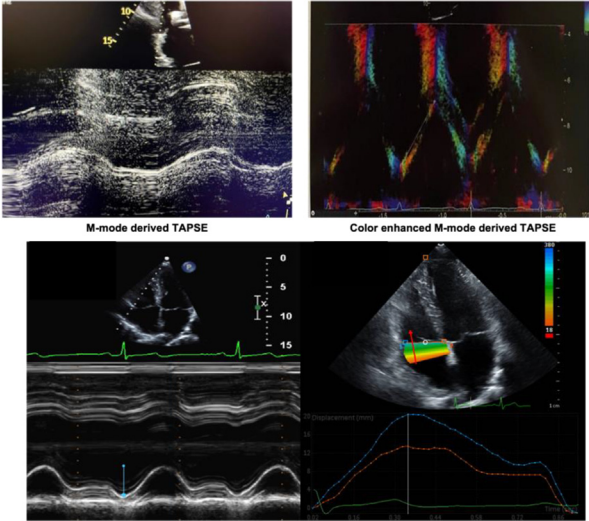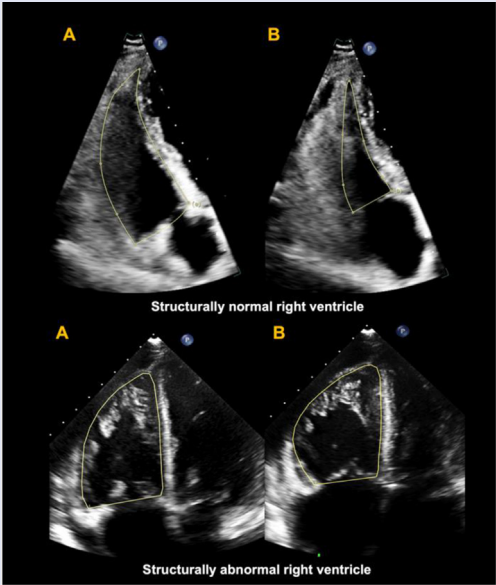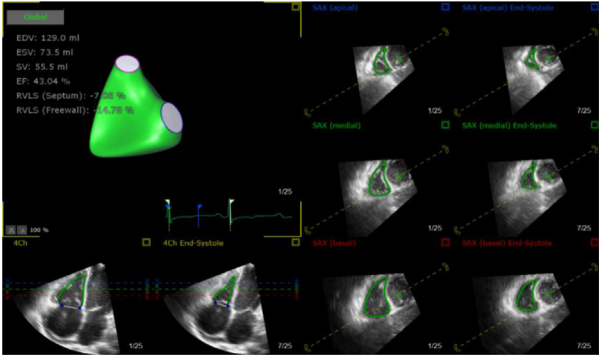
TDI S′ Velocity

TDI systolic (S′) velocity measures how fast the basal RVFW segment moves during peak systole, as a surrogate of RV longitudinal systolic function. TDI S′ velocity is obtained from the RV-focused view and placing the pulsed wave (PW) Doppler cursor along the lateral TVA and optimizing the sample volume set. The baseline should be optimized to allow for clear visualization and quantification of the peak systolic velocity above the baseline, and the early (e′) and late (a′) diastolic velocities below the baseline. A TDI systolic velocity >9.5 cm/s is normal.

Table 3 Right heart functional assessment

Variable	Image acquisition	Illustration
Right atrial strain, %	RA strain is measured from an RA-focused apical view, tracing from the lateral aspect of the tricuspid annulus to the septal aspect. The measurement excludes the area between the leaflets and the annulus, following the RA endocardium while avoiding the IVC, superior vena cava, and RA appendage. Care should be taken to prevent foreshortening of the RA, as this can lead to an overestimation of strain values. The RA curve provides measurements of reservoir strain (systemic venous return during ventricular systole), conduit strain (facilitating ventricular blood flow in early diastole), and booster strain (atrial contraction).	
Right atrial emptying volumes and function, %	RA function can be measured by passive, active, and total emptying volumes. Passive emptying function is influenced by atrial relaxation, chamber compliance, and stiffness Passive emptying function = (end-systolic RA volume) – (pre-A RA volume)/(end-systolic RA volume) Active emptying function is affected by atrial contractility, and = (pre-A RA volume) – (end-diastolic RA volume)/(pre-A RA volume). Total emptying function = (end-systolic RA volume) – (end-diastolic RA volume) / (end-systolic RA volume).	
Tissue Doppler S' velocity, cm/s	A TDI sample volume of 4 mm is placed at the base of RVFW along the lateral tricuspid annulus from the RV-focused 4Ch view. As this measurement is angle dependent, a maximum angle between the axis of contraction and ultrasound beam should be <20 degrees. TDI S' velocity is defined as the peak systolic velocity of the signal above the baseline (red dot).	

(Continued)

Table 3 (*Continued*)

Variable	Image acquisition	Illustration
TAPSE and TMAD, cm	TAPSE measures maximum apical excursion of the basal RVFW segment in systole by M-mode. To obtain, ensure that the M-mode cursor intersects the lateral tricuspid annulus and RV apex throughout the cardiac cycle, and maintains parallel alignment with annular motion from the RV-focused apical 4Ch view. Color Doppler can also be used to enhance TAPSE quality and measurement accuracy. TAPSE can also be obtained using STE and TDI imaging techniques. Tissue motion annular displacement (TMAD) refers to the maximal systolic displacement of the lateral tricuspid annulus. $TMAD_{TDI}$ measures the peak velocity (S') of the tissue motion at the tricuspid annulus compared to baseline using TDI. $TMAD_{STE}$ tracks the peak annular displacement.	
FAC, %	FAC measures RV chamber area percentage change between end-diastole (A) and end-systole (B) by tracing the RV endocardium from the lateral tricuspid annulus, along the RVFW to the apex, and then along the IVS to the medial tricuspid annulus, along the from the RV-focused apical 4Ch view. The papillary muscles, trabeculations, and moderator band are all included in the cavity area.	
3D RVEF, %	3DE RVEF, derived from RVEDV and RVESV using specialized software, offers a geometrically unbiased assessment of RV systolic function. Accurate measurement requires manual delineation of end-diastolic and end-systolic frames, including the moderator band and trabeculations, to account for RV volumes. 3DE measurements are dependent on adequate 2DE visualization of the entire RV chamber from the RV-focused apical 4Ch throughout the cardiac cycle. Breath hold should be used to avoid stitching artifact.	

Table 3 (*Continued*)

Variable	Image acquisition	Illustration
RVOT VTI, cm	RVOT VTI can be used to assess RV SV and CO. $SV = [(\pi r^2) \times VTI_{RVOT}]$ $CO = [(SV \times HR)/1,000]$ To obtain, a PW Doppler signal is placed within the RVOT, just proximal to the PV. In normal subjects (**A**), the contour of the PW Doppler profile is a smooth, domelike signal with a peak velocity occurring in mid-systole, consistent with the high compliance and low resistance of the pulmonary vascular bed. With progressive afterload elevation, the shape of the PW Doppler velocity profile changes and becomes more triangular. First, the RVOT AccT will become shorter with the peak velocity occurring in early to mid-systole (**B**). There may also be mid-systolic notching (**C**) of the PW Doppler signal (W sign) that is associated with elevated pulmonary vascular impedance and diminished compliance. In advanced PH and RV failure, the PW Doppler signal will become diminished and reversed with a steep and rapid AccT suggesting rapid equilibration of RVOT and proximal PA pressures (**D**).	
RVOT AccT, msec	RVOT AccT is acquired from a PW cursor placed just proximal to the PV at end-expiration, starting from flow onset to peak pulmonary flow velocity from the PSAX PA bifurcation view. RVOT AccT represents the duration from flow initiation to peak velocity and shortens in PH due to increased vascular impedance.	
dP/dt, mm Hg/s	RV dP/dt represents the instantaneous rate of pressure rise over time and serves as a surrogate for global RV contractility. It is estimated using the ascending limb of the CW Doppler signal (red line) of the TR envelope at a sweep speed of 200 mm/s and measuring the time interval required for the TR velocity to increase from 1 to 2 m/s.	

(*Continued*)

Table 3 (*Continued*)

Variable	Image acquisition	Illustration
RV MPI (Tei Index)*	RV MPI (Tei Index) is an index of global RV performance that can be measured using either The PW Doppler method across the RVOT or the TDI method. A higher RV MPI value typically indicates impaired RV function, while a lower value suggests better function. RV MPI = (TCO-ET)/ET *PW Doppler Method* The PW cursor is placed across the RVOT from the PSAX PA bifurcation view. Ejection time (ET) is defined as the time from the onset to the cessation of flow. Tricuspid valve closure onset (TCO) is derived from PW Doppler by measuring the time interval between the end of the transtricuspid A wave and the beginning of the E wave. TCO can also be derived from CW Doppler by measuring the duration of the TR jet, although this method is less commonly used for assessing total cardiac timing intervals. Since these measurements are obtained from different imaging planes and cardiac cycles, it is important to acquire data from beats with similar R-R intervals to improve accuracy. *TDI Method* From the RV-focused apical 4Ch view, the TDI cursor is placed along the lateral tricuspid annulus. Each time interval is measured from a single beat. ET is defined as the time interval between the onset and cessation of the S' velocity. TCO is derived by measuring the time interval between the end of the TDI a' velocity to the onset of the e' velocity.	
6-Segment RVGLS and 3-Segment RVFWS, %	RVLSS can be measured by both color-coded TDI imaging and STE techniques. STE is less angle dependent compared with TDI and has better reproducibility. STE measures the global and regional strain from the RV-focused apical 4Ch view, ensuring adequate visualization of the entire RV chamber throughout the cardiac cycle. The optimal temporal resolution is in the range of 50 to 90 fps. By convention, RVGLS refers to the average strain derived from the six segments of the interventricular septum and the RVFW. 3-segment RVFWS refers to strain derived from the basal, midventricular, and apical RVFW segments alone. RVFWS is typically considered a more accurate measure of RV function, as it isolates RV contractility from the influence of LV contractility.	

3D, three-dimensional; *4Ch*, four-chamber; *AccT*, acceleration time; *CO*, cardiac output; *CW*, continuous wave; *EDV*, end-diastolic volume; *ESV*, end-systolic volume; *ET*, ejection time; *FAC*, fractional area change; *HR*, heart rate; *IVC*, inferior vena cava; *IVCT*, isovolumetric contraction time; *IVRT*, isovolumetric relaxation time; *MPI*, myocardial performance index; *PA*, pulmonary artery; *PSAX*, parasternal short-axis; *PW*, pulse-wave; *RA*, right atrium; *RV*, right ventricle; *RVEF*, right ventricular ejection fraction; *RVFW*, right ventricular free wall; *RVFWS*, right ventricular free wall strain; *RVGLS*, right ventricular global longitudinal strain; *RVLSS*, right ventricular longitudinal systolic strain; *RVOT*, right ventricular outflow tract; *STE*, speckle-tracking echocardiography; *SV*, stroke volume; *TAPSE*, tricuspid annular plane systolic excursion; *TCO*, tricuspid closure-opening; *TDI*, tissue Doppler imaging; *TMAD*, tissue motion annular displacement; *TR*, tricuspid regurgitation; *VTI*, velocity time integral.
*RV MPI is a dimensionless index

TDI S′ velocity may be underestimated with poor image quality, inadequate optimization of the Doppler gain or filter settings, misalignment of the Doppler beam with the plane of motion, or with suboptimal patient positioning. TDI S′ velocity may also underestimate RV function in the immediate postoperative period following pericardiectomy[45] and overestimate RV function if there is significant leftward tethering of the RV apex. Similar to TAPSE, TDI S′ velocity only assesses the basal lateral RVFW segment as a surrogate of global RV systolic function and should not be used in isolation but rather in conjunction with other supportive findings. TDI S′ velocity can also be used as an alternative numerator within echocardiographic RV-PA coupling ratios,[59] although it has not been shown to outperform TAPSE.

Key Points

- TDI S′ velocity is a marker of how fast the basal RVFW segment is moving during peak systole as a surrogate of RV systolic function. The normal value of TDI S′ velocity is >9.5 cm/s.
- The accuracy of TDI S′ values relies on adequate alignment of the Doppler beam along the plane of motion, image quality, and optimization of Doppler gain and filter settings. Values should be reported as normal or abnormal on the basis of compatible supporting findings.

Recommendation

1. TDI S′ velocity is obtained by placing the PW Doppler cursor along the basal RVFW and should be included in the standard echocardiographic assessment of RV systolic function.

Fractional Area Change

FAC is an echocardiographic measure of RV systolic function that correlates well with CMR-derived RVEF.[60] From an RV-focused apical four-chamber view, the RV endocardium is traced in end-systole and end-diastole from the lateral tricuspid annulus along the RVFW to the apex, then back along the IVS to the medial tricuspid annulus, including trabeculations and the moderator band.

$$RV\ FAC\ (\%) = [(RVEDA - RVESA)/RVEDA] \times 100.$$

The normal value of FAC is >35%. To enhance the accuracy of FAC measurements, the RV-focused apical four-chamber view should be optimized to maximize RV area and ensure consistent visualization of the endocardial borders throughout the cardiac cycle. If RV visualization is suboptimal despite image optimization, ultrasound enhancing agents (UEA) may be beneficial for endocardial border delineation. When administering UEA for LV opacification, it is recommended to include RV imaging as part of the standard protocol. It is also important that serial FAC assessments are performed in the same manner to improve accuracy.

However, there are several important considerations when using FAC as a metric of RV systolic function. First, the RVOT is not routinely visualized from the RV-focused view, and therefore the contribution of the outflow tract is not considered in FAC-based quantification of RV systolic function. The exclusion of the RVOT in FAC quantification may be of particular relevance in patients with adult congenital heart disease (ACHD), such as those with tetralogy of Fallot. In these cases, alternative quantitative metrics of RV function may have improved reliability.[61] Despite this limitation,

it is important to note that FAC, unlike TAPSE and TDI S′ velocity, reflects both RVFW longitudinal shortening and radial thickening. Additionally, FAC includes the contribution of the IVS in RV systolic assessment. FAC is especially useful in assessing RV systolic function when TDI S′ velocity and/or TAPSE are underestimated in the immediate postoperative period[45] or influenced by loading conditions and geometric remodeling, as previously described.[46,62] Within echocardiographic coupling ratios, FAC/PASP ratio may have improved prognostic value reflecting age- and sex-related geometric and functional adaptation to a given afterload.[50,59]

Key Points

- FAC is a marker of global RV systolic function that correlates well with RVEF by CMR. The normal value of FAC is >35%.
- FAC does not include the contribution of the RVOT to RV systolic function. However, it does reflect RVFW longitudinal shortening, radial thickening, and interventricular septal contractility.
- FAC is valuable for assessing RV function when other functional measures, such as TAPSE and TDI S′ velocity, are unreliable or can be used as supporting evidence.
- UEA can be used to enhance RV endocardial border definition for FAC quantification.

Recommendation

1. FAC is obtained from the RV-focused apical four-chamber view by tracing the endocardial border at end-systole and end-diastole, including trabeculations and the moderator band.
2. FAC is a standard component of a comprehensive 2DE examination and may provide important adjunctive information regarding RV systolic function.

RVOT Velocity-Time Integral and Acceleration Time

PW Doppler interrogation of the RVOT is a readily obtainable measurement that can calculate RV stroke work and stroke volume (SV) using the distal RVOT diameter (centimeters) and the RVOT velocity-time integral (VTI; centimeters) obtained by PW Doppler across the RVOT.

$$RV\ SV = [\pi \times (RVOT\ diameter/2)^2] \times RVOT\ VTI.$$

The RVOT VTI is obtained from the PSAX view at the level of the aortic valve with the probe tilted superiorly to optimize RVOT and proximal PA visualization. The PW Doppler cursor is placed within RVOT, just beneath the PV using a of 1 to 2 mm sample volume. The signal should be optimized by adjusting the wall filters, baseline, and scale to ensure adequate visualization of the entire systolic tracing. Similar to other Doppler-derived techniques, RVOT VTI is angle dependent and may be underestimated if the cursor is not parallel to flow. A RVOT VTI >18 cm is normal.

Using the RVOT VTI spectral Doppler signal, the RVOT acceleration time (AccT) is measured from the onset of flow to the point of peak pulmonary flow velocity. RVOT acceleration time (RVOT AccT) >105 ms is generally considered normal, based on epidemiologic studies in healthy populations.[63] However, RVOT AccT may be less reliable in patients with low or high heart rates (<60 and >100 beats/min) and should not be used in isolation as a measure of RV function.

The contour of the RVOT VTI profile may also provide insights into advancing PVD and elevated afterload, as shown in Table 3. In normal subjects, the RVOT VTI profile will be parabolic, peaking in mid-systole, indicating a highly compliant pulmonary vascular bed with low resistance. As pulmonary vascular resistance (PVR) progressively increases, the normal parabolic contour with a midsystolic peak becomes more triangular, with a shortened time to peak in early systole.[64] Increasing impedance to pulmonary flow can lead to notching in the mid-systolic phase of the RVOT velocity profile, known as the "W sign." In advanced stages of PH, the RVOT VTI signal contour becomes spiked, reflecting early RV systolic ejection and rapid equilibration of RV-PA pressures due to decreased PA compliance, and is accompanied by a reduced spectral signal envelope.

The RVOT VTI can also be used as an alternative numerator within echocardiographic RV-PA coupling ratios. Across the spectrum of PH, the RVOT VTI/PASP ratio correlates with invasive measures of PA compliance, can discriminate pre-capillary from post-capillary PH related to heart failure with preserved ejection fraction, and is associated with functional capacity.[60] More data are needed, however, to establish the utility of the RVOT VTI/PASP ratio in clinical practice.

Key Points

- The RVOT VTI is a PW Doppler–derived measure of RV stroke volume. A RVOT VTI > 18 cm is normal.
- The contour of the RVOT VTI Doppler profile changes from parabolic to triangular with advancing PVD and elevated PVR.
- From the PW signal, RVOT AccT can also be obtained from the onset to the point of peak pulmonary flow velocity. RVOT AccT > 105 ms is considered normal.

Recommendation

1. The RVOT VTI is obtained by placing 1- to 2-mm PW Doppler sample volume within the distal RVOT just beneath the PV from the PA bifurcation PSAX view and should be part of the standard echocardiographic assessment.

Right Ventricular dP/dt

The ratio of the instantaneous rate of pressure rise over time (dP/dt) is a validated index of RV contractility and global systolic function.[1] RV dP/dt can be estimated from the ascending limb of the continuous-wave (CW) Doppler signal of TR at a sweep speed of 200 mm/s and measuring the time interval required for the TR signal to increase in velocity from 1 to 2 m/s. Based on the modified Bernoulli equation, this represents a 12 mm Hg increase in pressure, from 4 to 16 mm Hg. When this value is divided by the interval during which pressure increased, the result is expressed in mm Hg/s. A RV dP/dt < 400 mm Hg/s is abnormal.[1] In precapillary PH, a decreased RV dP/dt is a strong predictor of mortality, independent of TAPSE.[65]

Despite a relatively simple acquisition, measurement, and calculation, RV dP/dt is load dependent and may be less accurate in patients with severe TR. There is also a paucity of data derived from normal subjects, which limits widespread clinical applicability.

Key Points

- RV dP/dt is the instantaneous rate of pressure rise over time and serves as a surrogate for global RV contractility. RV dP/dt < 400 mm Hg/s is abnormal.
- RV dP/dt is measured from the CW Doppler signal of TR and is the time interval during which TR velocity increases from 1 to 2 m/s.

Recommendation

1. RV dP/dt measurements can be considered in patients with RV dysfunction as adjunctive evidence to support other readily obtained echocardiographic measures. However, due to a lack of normative data, RV dP/dt is not recommended for routine practice.

Right Ventricular Myocardial Performance Index

The RV myocardial performance index (MPI), also known as the Tei index,[66] is an established parameter of global systolic and diastolic RV function, representing the relationship between the ejection and non-ejection phases. Following RV diastolic filling, isovolumic contraction begins. Isovolumetric contraction time (IVCT; milliseconds) reflects the interval between TV closure and PV opening. The next interval is RV ejection, corresponding to ventricular systole. RV ejection time (ET; milliseconds) measures the interval during which blood is ejected across the PV. The next interval reflects the time between PV closure and TV opening, termed the isovolumetric relaxation time (IVRT; milliseconds). RV MPI can be calculated using two formulas:

$$RV\ MPI = [(IVRT + IVCT)/ET]$$
or
$$RV\ MPI = [(TCO - ET)/ET],$$

where TCO is the tricuspid closure-open interval, comprising IVCT, ET, and IVRT. RV MPI is acquired through either PW Doppler or TDI methods and is dimensionless.

Using the PW Doppler approach, ET is assessed by placing the cursor across the RVOT and measuring the time from the onset to the cessation of flow. TCO is determined using either PW Doppler of the tricuspid inflow (time from the end of the transtricuspid A wave to the beginning of the E wave) or CW Doppler of the TR jet (time from the onset to the cessation of the jet). As the RVOT and tricuspid inflow measurements are derived from different images, beats with similar R-R intervals should be used to enhance accuracy. In the TDI method, each time interval is measured from a single beat by pulsing the lateral tricuspid annulus. However, these two methods result in different reference values due to inherent differences in acquisition and time interval calculation, leading to only moderate inter-method correlation.[1] A normal RV MPI is <0.40 by the PW Doppler method and <0.55 by the TDI method.

Key advantages of RV MPI include its practicality, as it does not rely on geometric assumptions or constraints related to right heart chamber remodeling, and its prognostic value in PH, correlating with changes in clinical status.[1] However, RV MPI is a dynamic measurement that reflects both myocardial function and loading conditions, rather than being purely indicative of intrinsic myocardial

performance. For example, increased preload and right heart congestion, such as fluid overload, can prolong IVCT and IVRT, leading to an increased RV MPI. Conversely, reduced preload can shorten these intervals. PH and increased afterload can also prolong IVCT and IVRT, resulting in a higher RV MPI, regardless of RV systolic function. Severe TR may decrease IVRT without affecting IVCT. Last, varying R-R intervals, such as in patients with atrial fibrillation (AF), can lead to variable ET and TCO measurements. The sensitivity of RV MPI to loading conditions, arrhythmia, and modest intermethod correlation have limited widespread clinical use.

Key Points

- RV MPI is a technically feasible, practical, and clinically useful technique for quantifying global RV function using either PW Doppler or TDI methods.
- Normal RV MPI is <0.40 ms (PW Doppler method) and <0.55 ms (TDI method) with moderate intermethod correlation.
- RV MPI is a dynamic, load-dependent measurement that varies with loading conditions and is also influenced by arrhythmias and R-R interval variability.

Recommendation

1. Although RV MPI is a practical tool with prognostic value in PH, it is not recommended as the sole quantitative method for evaluating RV function, because of load dependency.

Right Ventricular Longitudinal Systolic Strain

STE is an adjunctive echocardiographic tool that uses a software-based algorithm to derive regional and global function from the deformation of ultrasound–myocardial tissue interactions.[67] STE can be performed during image acquisition on the ultrasound machine or in postprocessing using vendor-dependent or vendor-independent dedicated strain software.

RV strain analysis is performed from the RV-focused apical four-chamber view, ensuring that the lateral RVFW is visualized throughout the cardiac cycle, most commonly gated with the R-R interval to identify the onset of systole. Peak systolic strain occurs at aortic valve closure. Reference points and the region of interest are placed along the lateral and medial tricuspid annulus, and the RV endocardial border is traced, including trabeculations and papillary muscles. These regions of interest can be either contoured manually or generated semiautomatically and manually adjusted as needed. Dedicated RV STE software should be used when possible, rather than using a LV strain analysis package with modification.

Nomenclature is important when reporting strain. RV global longitudinal strain (RVGLS) refers to the average strain of six segments, including the basal, midventricular, and apical segments of the RVFW and IVS. In contrast, RV free wall strain (RVFWS) refers to the average strain of the three segments of the basal, midventricular, and apical RVFW alone. Each segment is represented by a corresponding color-coded strain curve, with the average of these segments typically signified by a dotted strain curve. Peak longitudinal systolic strain is defined as the maximum systolic shortening, typically occurring at aortic valve closure. However, conduction delays and regional RV dysfunction can cause this peak to occur later, resulting in variability in the timing of peak strain. The rate of systolic shortening is defined as the systolic strain rate. Including the IVS in 6-segment

RVGLS measurements can lower absolute strain values compared to 3-segment RVFWS and does not differentiate the contribution of LV contractility to RV systolic function. On the basis of pooled data, strain values more negative than −20% to −25% for both RVFWS and RVGLS are generally considered as normal.[68]

However, there are several key factors that must be considered when using STE. First, STE is dependent on adequate endocardial visualization from an optimized RV-focused view throughout the cardiac cycle and is subject to reverberation artifact. Complex chamber geometry and operator delineation of endocardial borders may also influence the accuracy and reproducibility STE measures. For example, the inclusion of the RA or pericardium will result in underestimation of strain values. In addition, STE is limited by heart rate variability, which when rapid, can decrease temporal resolution. Similar to RV MPI, STE is a measure of myocardial function that is influenced by underlying hemodynamic conditions. Increased preload may result in higher strain measurements that are not necessarily indicative of enhanced RV systolic function. Conversely, increased afterload may depress strain measurements, even when intrinsic myocardial function is preserved.[69] Incorporating RVFWS as the numerator in echocardiographic RV-PA coupling ratios may enhance the accuracy of strain measures as a metric of RV function.[59,70] Lastly, established differences in vendor-dependent STE software may affect reproducibility and standardization.[41,71] Serial STE measures of RV contractility should be performed using the same vendor to allow for comparison. A wealth of data underscores the prognostic importance of regional and global RV strain across patient populations. We recommend integrating RV strain analysis into the standard assessment of RV function, particularly in PH and individuals at risk for PVD.

Key Points

- STE-derived RV strain is an important marker of regional and global RV function that may be abnormal when conventional measures are otherwise normal, suggesting subclinical RV dysfunction. The normal values for both RVFWS and RVGLS are more negative than −20% to −25%.
- RVGLS refers to 6-segment strain derived from the RVFW and IVS, while RVFWS refers to 3-segment strain derived from the basal, midventricular, and apical RVFW alone. RVFWS is a more accurate measure of RV systolic function without the contribution of LV contractility.

Recommendations

1. RV strain can be obtained on the ultrasound machine during or after image acquisition or in postprocessing with dedicated strain software.
2. From the RV-focused apical four-chamber view, the endocardial border of the RV chamber is traced, starting from the lateral tricuspid annulus, along the RVFW, and ending at the medial tricuspid annulus. Manual contouring may enhance delineation of regions of interest.
3. When feasible, RV strain should be performed as part of the standard echocardiographic examination for the clinical assessment, screening, and serial evaluation of patients with and at risk for PH.

C. HEMODYNAMICS

Table 4 summarizes recommendations for image acquisition, illustrations, and formulas to calculate echocardiographic estimates of right heart hemodynamics.

Right Atrial Pressure

Right atrial pressure is estimated by measuring the inferior vena cava (IVC) diameter at end-expiration, 0.5 to 3.0 cm proximal to the RA ostium and distal to the hepatic vein from the subcostal view, and observing IVC diameter variation with sniff and quiet respiration.[1,5] When observing respirophasic variation, it is important to verify that these changes do not reflect IVC translation into another imaging plane. M-mode measurements of the IVC allows for more accurate quantification of the IVC diameter and presence of respiratory variation given its superior temporal resolution. A normal IVC diameter is ≤2.1 cm, and the IVC collapses with sniff and quiet respiration.

The combination of the IVC end-diastolic dimension and respirophasic behavior provides reliable noninvasive RAP estimates. If the IVC diameter is normal and collapses ≥50% with sniff and quiet respiration, the RAP is normal (3 mm Hg; range, 0-5 mm Hg). If the IVC appears small and collapsed, the RAP is likely low (<3 mm Hg), suggestive of hypovolemia. An enlarged IVC diameter that does not collapse <50% with a sniff suggests an elevated RAP (15 mm Hg; range, 10-20 mm Hg). In cases in which the IVC is markedly enlarged (>2.5 cm) without respirophasic variation and evidence of spontaneous echo contrast or color flow reflux, a value of 20 mm Hg can be considered. In indeterminate cases, an intermediate value of 8 mm Hg (range, 5-10 mm Hg) may be used and integrated with secondary indices of elevated RAP. Indeterminate estimation of RAP is defined by two main scenarios in which either IVC diameter is normal and does not collapse or the IVC diameter is dilated and does collapse. A detailed algorithm for quantifying RAP is detailed in Figure 3.

Hepatic vein (HV) flow patterns provide complementary insights into RAP estimation. In cases of low or normal RAP, there is systolic predominance in the HV flow, such that the HV systolic wave velocity (HVs) is greater than the HV diastolic wave velocity (HVd). The HVs filling fraction equals HVs/(HVs + HVd), and a value <55% is a sensitive and specific sign of elevated RAP.[72] With elevated RAP, HVs predominance is lost, such that the HVs/HVd ratio is <1. Importantly, the HV vein flow velocities have been validated in mechanically ventilated patients, provided that the velocities are averaged over at least five consecutive beats and comprising at least one respiratory cycle.

In indeterminate cases, secondary indices to consider include RA enlargement, bulging of the interatrial septum into the left atrium throughout the cardiac cycle, the presence of a restrictive right-sided diastolic filling pattern, tricuspid E/e' ratio > 6, and HVd flow predominance quantified as a HVs filling fraction < 55%. In indeterminate cases, if none of these secondary indices are present, RAP can be downgraded to 3 mm Hg. If secondary indices are present, RAP can be upgraded to 15 mm Hg. If uncertainty remains, an intermediate value of 8 mm Hg should be used.

As the estimation of RAP relies on both IVC diameter and respirophasic variation, there may be circumstances in which an adequate sniff cannot be performed, and quiet respiration can be used. In patients on positive pressure ventilation, the degree of IVC collapse cannot be used to reliably estimate RAP, and if clinically relevant, RAP should be measured invasively, if feasible. Secondary indices can also be evaluated to determine if RAP is normal or elevated. However, if uncertain remains, an if uncertainty remains, an intermediate value of 8 mm Hg should be used. Generally, an IVC diameter ≤2.1 cm in an intubated patient is accurate in identifying patients with RAP < 10 mm Hg.[73]

IVC dilation can be normal in healthy young healthy adults and athletes. Caval enlargement is also common in pregnant women due to increased total blood volume. In these scenarios, evaluating for adjunctive evidence of elevated filling pressures and clinical correlation are necessary.

Key Points

- Specific RAP values, rather than ranges, should be reported to ensure standardization.
- RAP values of 3, 8, or 15 mm Hg are assigned using an IVC diameter cutoff of 2.1 cm and observing respirophasic variability with sniff.
- In indeterminate cases, an intermediate value of 8 mm Hg can be used, and secondary indices should be assessed.
- In patients who are unable to adequately perform a sniff, IVC diameter variability can be observed with quiet respiration.
- Special caveats include patients who cannot adequately perform a sniff, young healthy adults, athletes, pregnant women, and patients on positive pressure ventilation.

Recommendations

1. RAP is easily quantifiable and acquired by measuring the IVC diameter at end-expiration from the subcostal view, 0.5 to 3.0 cm proximal to the RA ostium.
2. RAP is estimated by visualizing the variation in IVC diameter with sniff and with quiet respiration using 2DE and M-mode imaging techniques.
3. RAP is an integral component of standardized reporting and should be acquired in all cases when possible and reported as a discrete number.
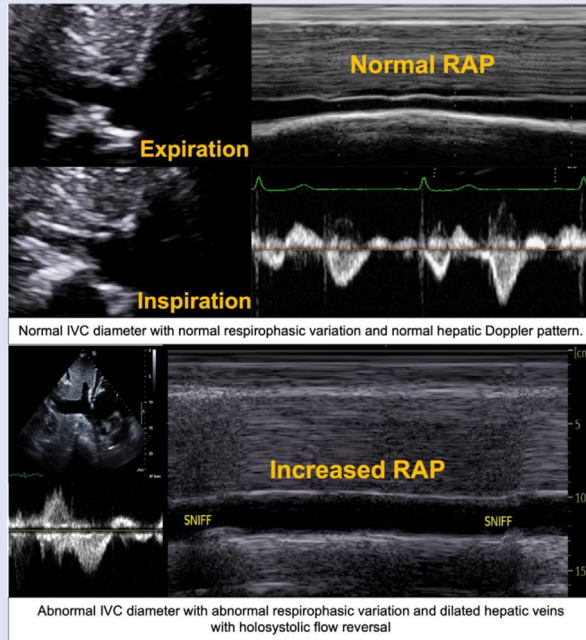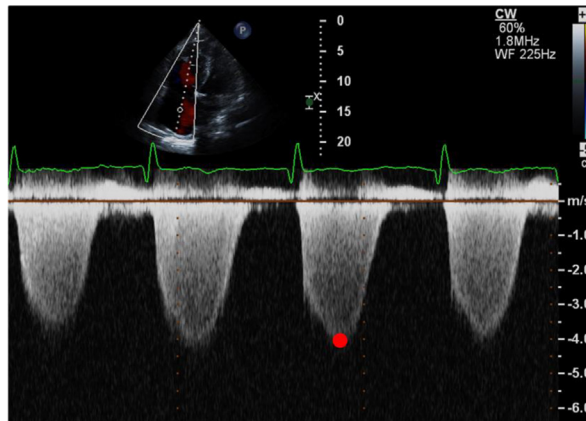
Right Ventricular Systolic Pressure

The RV systolic pressure (RVSP) is estimated from the peak TR jet velocity, using the simplified Bernoulli equation, and adding this value to the RAP estimate:

$$RVSP = [4 \times (\text{peak TR velocity})^2 + RAP].$$

In this equation, the peak TR velocity is obtained from the CW Doppler signal (expressed in meters per second), and RAP is estimated from IVC diameter and the degree of respirophasic variation.
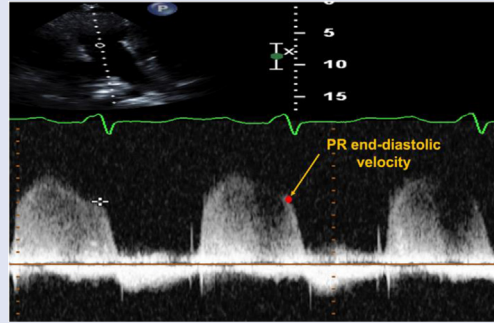
Table 4 Right heart hemodynamic assessment

Variable	Image acquisition	Illustration	Formulas
RAP, mm Hg	RAP is assessed by measuring IVC size and the collapsibility during normal breathing. IVC diameter is measured at end-expiration, approximately 0.5-3.0 cm proximal to the RA ostium, from the subcostal view. Collapsibility is determined by the change in IVC diameter during sniffing and quiet respiration.	 Normal IVC diameter with normal respirophasic variation and normal hepatic Doppler pattern. Abnormal IVC diameter with abnormal respirophasic variation and dilated hepatic veins with holosystolic flow reversal	3 mm Hg (range 0-5 mm Hg), IVC diameter ≤ 21 mm and ≥ 50% inspiratory collapse 8 mm Hg (range 5-10 mm Hg), IVC diameter ≤ 21 mm and < 50% collapse or an IVC diameter >21 mm and ≥ 50% collapse 15 mm Hg (range 10-20 mm Hg), IVC diameter > 21 mm and < 50% collapse 20 mm Hg, IVC diameter > 25 mm and < 50% collapse with dilated hepatic veins and adjunctive evidence of spontaneous echo contrast or color flow reflux within the vessel is suggestive of markedly elevated RAP, severe TR, or impaired venous return due to conditions such as right heart failure, RV diastolic dysfunction, or constrictive physiology.
RVSP, mm Hg	RVSP is calculated from the peak TR jet velocity, using the simplified Bernoulli equation, and adding this value to the RAP estimate. RVSP is equivalent to PASP in the absence of RVOT obstruction, PS, and/or proximal PA stenosis. To avoid overestimation of the spectral envelope, ensure that the peak systolic measurement is from the dense aspect of the spectral Doppler envelope. The optimal CW Doppler signal of the TR jet is characterized by a dense envelope, indicating a complete Doppler profile. To ensure accuracy and account for respirophasic variation, RVSP should be calculated by averaging at least three consecutive beats from the window with the highest velocities and the clearest Doppler envelope.		$\text{RVSP} = [4 \times (\text{peak TR velocity})^2 + \text{RAP}]$

(Continued)

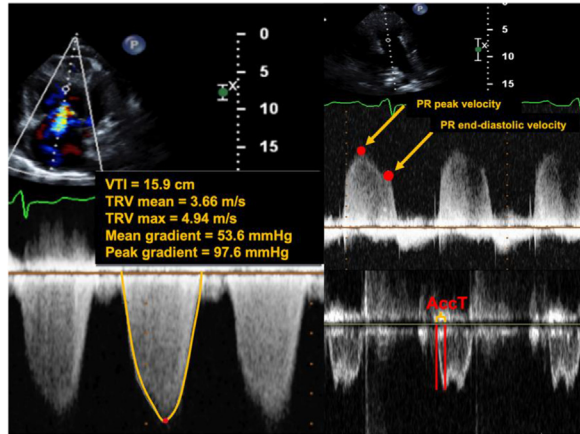|			
PAEDP, mm Hg	PAEDP is estimated by using the end-diastolic PR velocity, using the modified Bernoulli equation and adding this value to the RAP estimate. The optimal CW Doppler signal of the PR jet is characterized by a dense envelope, indicating a complete Doppler profile.	PR end-diastolic velocity	$PAEDP = [4*(\text{peak end-diastolic PR velocity})^2] + RAP$
mPAP, mm Hg	mPAP can be estimated using several equations. The most common is mPAP= [1/3 × (PASP) + 2/3 × (PAEDP)] Alternative formulas utilize either the RVOT AccT (msec) or peak PR velocity (m/s) to calculate mPAP. The VTI method involves tracing the envelope of the CW Doppler signal to obtain the area under the curve representing the regurgitant jet flow (v) which is then used in the modified Bernoulli equation $(4v^2)$ + RAP By invasive RHC, mPAP>20 mm Hg is considered abnormal.	 VTI = 15.9 cm TRV mean = 3.66 m/s TRV max = 4.94 m/s Mean gradient = 53.6 mmHg Peak gradient = 97.6 mmHg PR peak velocity PR end-diastolic velocity AccT	$mPAP = [1/3 \times (PASP) + 2/3*(PAEDP)]$ $mPAP = 79 - (0.45 \times AccT)$ $mPAP = 90 - (0.62 \times AccT)$ when AccT < 120 ms $mPAP = 4 \times (\text{early PR velocity})^2 + RAP$ $mPAP = VTI_{(TR)} + RAP$ $mPAP = [PASP \times 0.61] + 2$ mm Hg
PVR, Wood Units	Calculated by VTI_{RVOT} and the peak TR velocity, or by mPAP and PCWP.	 TR Vmax VTI RVOT	$PVR = [(\text{Peak TR velocity}/ VTI_{RVOT}) \times 10] + 0.16$ $PVR = (RVSP - PCWP)/CO$ $RVSP = [4 \times (\text{peak TR velocity})^2 + RAP]$ $PCWP = [1.24 \times (\text{mitral E/e' ratio}) + 1.9]$ $CO = [(\pi r^2) \times VTI_{RVOT}] \times HR$
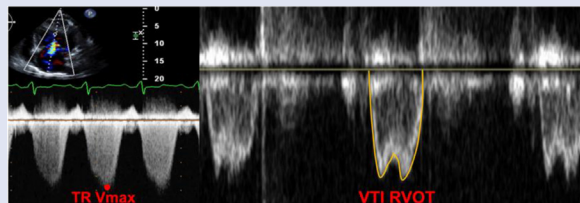
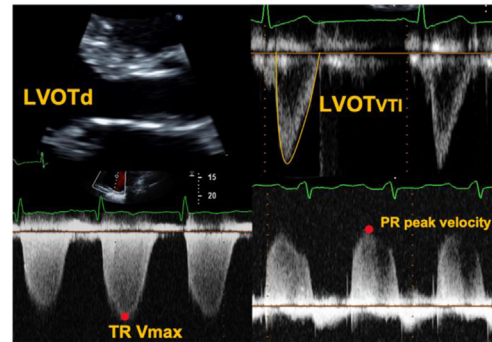| PCWP, mm Hg	There are two main methods to calculate PCWP:		
	Mitral Inflow Method Mitral valve inflow velocity is defined by the peak E velocity measured by PW Doppler at the leaflet tips of the mitral valve during diastole. Early diastolic e' velocities are obtained using TDI at the medial and lateral aspects of the mitral annulus, with the mean value taken from the lateral and medial aspects. If significant artifact or measurement error occurs, the best TDI value (lateral or medial) should be used. The ratio of mitral inflow E velocity to e' is then used in the following formula: PCWP=[1.24 x (mitral E/e') + 1.9]	 Mitral inflow method	PCWP=[1.24 x (mitral E/e') + 1.9]
	Stroke Volume Method SV is calculated as [SV=$\pi r^2 \times$ VTI$_{LVOT}$], where r is the radius (half the cross-sectional diameter) of the LVOT and VTI is the velocity time integral of the LVOT. PP is calculated as [PP=4 $\times$ (peak TRV)^2 $-$ (PR end-diastolic velocity)^2] The ratio of SV/PP is then used in the following formula: PCWP=[SV/PP]	 Stroke volume method	PCWP = [SV/PP] SV=[$\pi r^2 \times$ VTI$_{LVOT}$] PP=[4 $\times$ (peak TRV)^2 $-$ (PR end-diastolic velocity)^2]
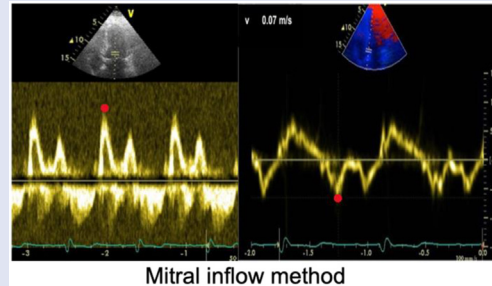
3D, three-dimensional; *4Ch*, four-chamber; *AccT*, acceleration time; *CO*, cardiac output; *CW*, continuous wave; *EDV*, end-diastolic volume; *ESV*, end-systolic volume; *ET*, ejection time; *FAC*, fractional area change; *HR*, heart rate; *IVC*, inferior vena cava; *IVCT*, isovolumetric contraction time; *IVRT*, isovolumetric relaxation time; *LVOTd*, LVOT dimension; *MPI*, myocardial performance index; *PA*, pulmonary artery; *PP*, pulse pressure; *PSAX*, parasternal short-axis; *PW*, pulse-wave; *RA*, right atrium; *RV*, right ventricle; *RVEF*, right ventricular ejection fraction; *RVFWS*, right ventricular free wall strain; *RVGLS*, right ventricular global longitudinal strain; *RVOT*, right ventricular outflow tract; *STE*, speckle-tracking echocardiography; *SV*, stroke volume; *TAPSE*, tricuspid annular plane systolic excursion; *TCO*, tricuspid closure-opening; *TDI*, tissue Doppler imaging; *TMAD*, tissue motion annular displacement; *TR*, tricuspid regurgitant; *Vmax*, maximum velocity; *VTI*, velocity time integral.
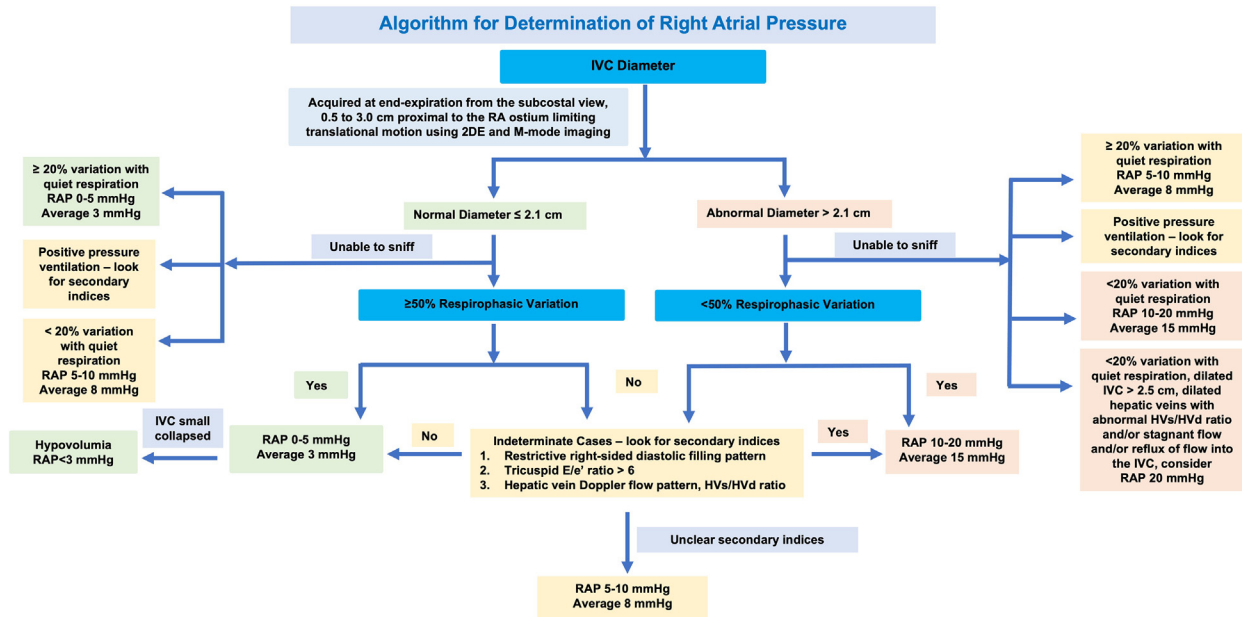
Figure 3 An algorithm for estimating RAP is shown, emphasizing key features including IVC diameter and respirophasic variation.

If RVSP is elevated, it is important to exclude obstruction at the level of the PV, or supra- or subpulmonic obstruction, especially in patients with ACHD (such as PS, RVOT obstruction, and/or proximal PA stenosis), or following PV surgery. In the absence of a gradient across the PV or RVOT, PASP is equal to RVSP. In post-surgical patients with ACHD, in the absence of residual RVOT obstruction or proximal PA stenosis, if the PASP is greater than two-thirds of the systemic blood pressure, pulmonary pressures are often severely elevated.

Technically adequate CW signals with well-defined Doppler envelopes can be obtained in most patients using a sweep speed of 100 mm/s. Inadequate TR signals frequently lead to underestimation or the inability to estimate RVSP accurately. If the Doppler signal is faint, image quality can be enhanced using agitated saline, blood-saline contrast, or UEA.[74] However, overgaining should be avoided, as this may lead to overestimation of TR velocities due to the amplification of noise or artifacts. To improve the accuracy of peak TR velocity measurements with or without contrast, the dense primary upper edge of the spectral envelope ("chin") should be measured rather than the faint aspects ("beard") of the signal profile.
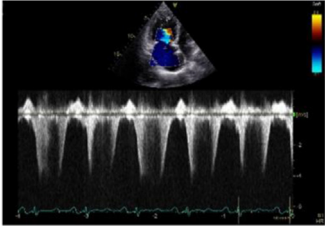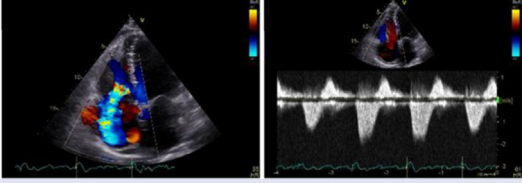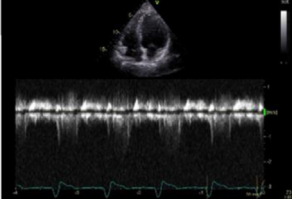
Misalignment of the CW Doppler signal that is not parallel to the direction of flow can also lead to underestimation or overestimation of RVSP due to angle-dependent velocity measurements errors. To improve accuracy, the TR signal should be obtained from multiple windows (e.g., RV inflow, apical 4-chamber, subcostal), and the highest velocity from these windows should be used to calculate RVSP. When possible, an average of three consecutive velocities should be used to reduce any beat-to-beat variability, which may reflect both instantaneous changes in RVSP and alterations in the TR jet direction as the heart moves during the respiratory cycle. In the setting of arrhythmia such as AF, the TR jet velocity should be averaged over five to 10 cardiac cycles rather than using the highest single velocity (e.g., the beat after a premature atrial or ventricular contraction or a pause), which will overestimate the TR velocity.

Several hemodynamic factors may also influence RVSP accuracy. In severe PH with right heart failure, reduced RV contractility and decreased PA compliance impair the ability of the RV to generate sufficient force, resulting in a diminished RV-PA pressure gradient and unreliable RVSP measurements. Assessing RVSP in the context of hemodynamically significant TR is also nuanced. Inadequate TR signal strength may underestimate RVSP, while severe TR with turbulent flow can result in a high velocity regurgitant signal leading to potential overestimation of RVSP. In FTR and/or malcoaptation of the tricuspid leaflets, the Doppler envelope can be truncated due to early equalization of RA-RV pressures as evidenced by laminar TR flow and a triangular CW Doppler signal contour,[75] leading to underestimation of the RA-RV gradient. Table 5 summarizes the main sources of error in the estimation of PASP.

A recent study investigating simultaneous invasive and noninvasive hemodynamics demonstrated that RV-RA gradients can be accurately calculated by the modified Bernoulli equation in patients with a parabolic TR velocity curve. In patients with more severe TR with a V-wave cutoff sign, the Bernoulli equation cannot be applied to determine the RV-RA gradient.[75] Table 5 summarizes the main sources of error in TR estimation.

A resting TR peak velocity of ≥2.9 m/s (RA-RV gradient of 34 mm Hg) suggests PH in the absence of RVOT obstruction.[76] To align with the updated WSPH definition of PH,[2,3] a peak TR velocity ≥ 2.8 m/s (RA-RV gradient of 31 mm Hg) with at least two other echocardiographic signs is suggestive of PH and warrants further investigation. These supporting measures include RV enlargement (eg, RV basal diameter greater than LV basal diameter), abnormal LVEI (>1.1), mid-systolic notching of the RVOT signal, end-diastolic PR velocity > 2.2 m/s, or signs of elevated RAP (IVC diameter > 2.1 cm or RA area > 18 cm^2). Clinicians should also consider the patient's age and body size when interpreting RVSP values near the upper limit of normal, as both healthy physiologic

Table 5 Common sources of error for hemodynamic assessment

Source of error	Underestimation	Overestimation
Significant RV failure and contractile dysfunction	X	
TR jet signal over-gaining		X
High output or hyperkinetic RV		X
Atrial fibrillation and velocity after a premature contraction or pause, if a higher velocity is used		X
Pulmonic stenosis		X
RAP estimation*	X	X
Limitations of the simplified Bernoulli equation	X	X
Unfavorable Theta angle >20 degrees (angle between ultrasound beam and direction of blood velocity)	X	

Significant TR with abnormal triangular CW Doppler contour	X	

Insufficient TR signal*	X	X

Caveat and common pitfalls
1. Measure the densest primary edge of the CW Doppler signal ("chin") and not the faint aspects ("beard") by optimizing the gain and brightness from multiple imaging planes. UEA, blood-saline contrast, and agitated saline can be used to augment the Doppler signal.
2. Position the ultrasound beam parallel to the direction of blood flow, ideally <20° Θ angle to minimize any error in velocity measurement.
3. If there is significant TR, the shape of the CW Doppler signal can help guide accuracy of RVSP estimates. A triangular CW Doppler contour will underestimate RVSP, while accuracy is improved with a parabolic Doppler contour.
4. Do not consider a velocity following a pause or premature contraction.
5. Consider the mean velocity across 5-7 beats in patients with arrhythmia.

AF, atrial fibrillation; *PS*, pulmonic stenosis; *PVD*, pulmonary vascular disease; *RAP*, right atrial pressure; *RV*, right ventricle; *RVSP*, right ventricular systolic pressure; *TR*, tricuspid regurgitation; *UEA*, ultrasound enhancing agent.
*Both right atrial pressure (RAP) estimates and inadequate tricuspid regurgitation (TR) signals can lead to overestimation or underestimation in hemodynamic assessments.

aging and increasing BSA can elevate RVSP values in this range without necessarily indicating PH.[77,78]

Key Points

- Using the modified Bernoulli equation, RVSP is estimated by the following formula: RVSP = [4 × (TR peak velocity)^2 + RAP]. A RVSP ≥35 mm Hg is generally considered abnormal.
- RVSP estimation is feasible in a majority of subjects and should be calculated from the highest velocity with a dense Doppler envelope, regardless of the window used to record this signal.
- An average of three consecutive beats should be used in sinus rhythm to account for beat-to-beat variability and five to 10 beats in patients with arrhythmias obtained from the same acoustic window. The highest single velocity after a premature atrial or ventricular contraction, or a pause should be avoided.
- Agitated saline, blood-saline contrast, or UEA can be used to enhance the Doppler signal. Overgaining should be avoided.
- Resting peak TR velocity of ≥2.9 or ≥2.8 m/s with at least two adjunctive echocardiographic signs suggests PH and warrants further investigation.
- Healthy physiologic aging and increasing BSA may elevate RVSP without necessarily indicating PH.

Recommendations

1. RVSP can be easily obtained noninvasively and should always be included in the standardized report when an adequate TR signal is present.
2. In patients at risk for PH or being monitored for PH with an inadequate Doppler signal, agitated saline, blood-saline contrast, or UEA should be used to augment the Doppler signal.

Pulmonary Artery End-Diastolic Pressure

Pulmonary artery end-diastolic pressure (PAEDP) can be estimated from the CW Doppler end-diastolic PR velocity using the modified Bernoulli equation:

PAEDP = [4 × (peak end − diastolic PR velocity)^2] + RAP.

The PR signal is easily acquired from the PSAX view at the level of the aortic valve and angling upward to visualize the PV annulus and RVOT. CW Doppler is then used to measure the peak end-diastolic PR velocity at a sweep speed of 75 to 100 mm/s. A resting end-diastolic PR velocity of ≥2.2 m/s is generally considered abnormal.

CW Doppler alignment that is not parallel to the angle of PR flow can lead to underestimation or overestimation of PAEDP. In cases of severe PR and constrictive or restrictive RV physiology, the rapid deceleration slope can cause the end-diastolic PR velocity to influence the accuracy of PAEDP.[79,80] PAEDP measurements can also be influenced by arrhythmias and tachycardia. As with RVSP estimation, the highest single velocity after a premature contraction or pause should be avoid. In patients with arrhythmia, an average of five to 10 beats should be used.

Key Points

- Using the modified Bernoulli equation, PAEDP is estimated by the following formula: is PAEDP = [4 × (PR peak velocity)^2 + RAP]. A resting PR peak end-diastolic velocity of ≥2.2 m/s is generally considered abnormal.
- Severe PR and constrictive or restrictive RV physiology are common sources of under- and overestimation of PAEDP, respectively.

Recommendations

1. PAEDP is readily obtainable from the PSAX PA-focused view when an adequate PR Doppler signal is present.
2. PAEDP should be reported in patients at risk for PH or being monitored for PH in conjunction with RVSP.

Mean Pulmonary Artery Pressure

Although there are several formulas that can be used to estimate mean PA pressure (mPAP, reported in mm Hg), the most common is
mPAP = [1/3 × (PASP) + 2/3 × (PAEDP)].

Other formulas include the following:
mPAP = 79 − (0.45 × AccT) or
mPAP = 90 − (0.62 × AccT) when AccT < 120 ms,[81]
mPAP = 4 × (early PR velocity)^2 + RAP,[82]
mPAP = VTI$_{(TR)}$ + RAP,[83]
and
mPAP = [PASP × 0.61] + 2 mm Hg.[84]

As with other Doppler-based techniques, estimation of PR and TR velocities depends on dense CW Doppler signals, accurate Doppler alignment, and confirmation of the highest signal using multiple imaging planes. Although there are several echocardiographic methods to calculate mPAP, standard reporting of RVSP is generally preferred for several reasons. First, RVSP is directly measured from the peak velocity of the TR jet, making it a more straightforward and reliable estimate of RVSP. In contrast, methods like AccT and the integration of PASP and PAEDP within mPAP equations rely on indirect calculations and assumptions, which can introduce measurement errors. Definitive mPAP assessment for PH diagnosis and classification, and therapeutic initiation requires direct hemodynamic measurement by invasive right heart catheterization (RHC).[2,75]

Key Point

- The most common formula to noninvasively derive mPAP is: mPAP = [1/3 × (PASP) + 2/3 × (PAEDP)]. A mPAP > 20 mm Hg is considered abnormal.

Recommendations

1. Standard reporting includes RVSP estimation. Although multiple formulas exist to calculate mPAP noninvasively, the reliance on indirect measurements and additional calculations makes this technique less favorable.
2. When clinically relevant, such as screening and monitoring of patients with PH, reporting of mPAP can be considered when RVSP estimation is limited.
3. Definitive diagnosis and classification of PH requires invasive hemodynamic confirmation by RHC.

Pulmonary Vascular Resistance

PVR describes the resistive afterload on the RV from the pulmonary circulation[85] and is a key component for diagnosing, grading, and classifying PH.[2,69,3] In PH, PVR is a marker of disease chronicity and the extent of adverse pulmonary vascular remodeling. Notably, elevated RVSP and/or PASP does not always imply increased PVR, as appreciated from the relationship:

$$\Delta \text{ pressure } = \text{Flow} \times \text{Resistance.}$$

Therefore, PVR may offer a better assessment of intrinsic resistive properties of the pulmonary vasculature. PVR elevation may help distinguish between elevated PASP due to PVD and elevated PASP from a high-output state or other post-capillary etiology. The Abbas formula[82] is used to estimate PVR noninvasively, defined as

$$\text{PVR (reported in Wood Units} = \{[(\text{Peak TR velocity }/\text{VTI}_{RVOT}) \times 10] + 0.16 \text{ Wood units}\}.$$

This formula reports peak TR velocity in meters per second and VTI_{RVOT} in centimeters. A normal PVR is <1.5 Wood units (120 dynes · cm/s^2), while PVR > 2.0 Wood units (160 dynes · cm/s^2) is abnormal and suggestive of PH.[2,3]

However, several factors may limit widespread acquisition and reporting of PVR by echocardiography. Similar to mPAP, PVR calculation depends on indirect measurements that may be influenced by variability and accuracy of Doppler image acquisition. Small errors in either peak TR velocity or RVOT VTI can significantly influence the accuracy of PVR estimation. Furthermore, the Abbas equation is unreliable in patients with very high PVR (>8 Wood units), as this formula was derived within a specific range of PVR encountered in clinical practice.[86] Precise assessment of PVR is crucial for diagnosis and guiding treatment decisions in PH, and therefore, direct invasive hemodynamic measurements are generally preferred over noninvasive measures.

Key Points

- PVR is calculated noninvasively using the Abbas formula: PVR = [(Peak TR velocity/VTI$_{RVOT}$) × 10 + 0.16]. PVR >2.0 Wood units is considered abnormal.
- Calculating PVR may help distinguish distinguish if elevated PASP is due to pre-capillary or post-capillary etiologies. PVD or to left heart disease.

Recommendations

1. Although echocardiography-derived PVR can be obtained in most cases, it is not recommended for routine use, because as it depends on indirect measures and have accuracy in patients with advanced PVD.
2. Noninvasive PVR estimates do not substitute for invasive hemodynamic assessment for the diagnosis, grading, and classification of PH.

Pulmonary Capillary Wedge Pressure

"Pulmonary capillary wedge pressure" (PCWP) and "PA wedge pressure" are interchangeable terms and both provide different hemodynamic information than LV end-diastolic pressure (LVEDP).[87] The mean PCWP reflects the cumulative hemodynamic effect of left atrial pressure throughout the cardiac cycle and the impact of left-sided ventriculoarterial coupling on pulmonary compliance. In contrast, LVEDP is the instan-taneous LV pressure just before the onset of ventricular contraction, serving as a surrogate measure of LV preload and diastolic compliance. Differences between LVEDP and mean PCWP are also exaggerated in AF, hemodynamically significant mitral regurgitation (leading to a large V wave), and left atrial myopathies.[87] Mitral stenosis, pulmonary vein stenosis, pulmonary veno-occlusive disease, or chronic thromboembolic PH may also result in higher PCWP than LVEDP.

Therefore, PCWP represents an integrative measure of LV preload, diastolic function, and cumulative hemodynamic burden on the pulmonary circulation, offering a more comprehensive assessment of LV filling pressures across the cardiac cycle. There are several methods to calculate PCWP. Most commonly, PCWP is estimated from the mitral inflow method using the following formula[88]:

$$\text{PCWP } = [1.24 \times (\text{mitral E/e' ratio}) + 1.9].$$

PCWP can also be estimated using the SV method. SV is calculated as $\text{SV} = \pi r^2 \times \text{VTI}_{LVOT}$, where r is the radius (half the cross-sectional diameter) of the LV outflow tract (LVOT). Pulse pressure is calculated as $4 \times [(\text{peak TR velocity})^2 - (\text{PR end-diastolic velocity})^2]$. The ratio of SV to pulse pressure is then used in the following formula: PCWP = SV/pulse pressure.

A normal PCWP is <12 to 15 mm Hg. However, estimates of PCWP have limited value in certain clinical conditions, such as the presence of LV assist devices, left bundle branch block, paced rhythms, atrial arrhythmias, mitral prostheses, significant mitral annular calcification, mitral stenosis, and/or mitral regurgitation.[88] There are a number of limitations in estimating PCWP, requiring caution and careful consideration of the clinical context when interpreting these measurements.

Key Points

- PCWP is calculated noninvasively using the following formula: PCWP = [1.24 × (mitral E/e' ratio) + 1.9]. A normal PCWP is <12 to 15 mm Hg.
- PCWP is an integrated measure of LV preload, diastolic function, and the cumulative hemodynamic impact of the left heart on pulmonary circulation.
- Several common clinical scenarios may limit the routine use of this equation.

Recommendation

1. It is recommended to avoid routine reporting of PCWP, as it may be redundant given that averaged or medial mitral E/e' values, which are already included in the standard diastolic assessment.

Limitations of Doppler-Based Techniques

There are inherent limitations to the noninvasive assessment of hemodynamics, as shown in Table 5. First, Doppler measurements are angle dependent and require optimal alignment (<20° Θ angle), requiring interpretation of the highest velocity across multiple optimized imaging windows. Errors in gain settings may also affect the accuracy of hemodynamic measurements. Overgaining can exponentially amplify the measured pressures, while undergaining low can lead to inadequate detection of the Doppler signal. In patients at risk for PH or being monitored for PH, agitated saline,

blood-saline contrast, or UEA should be used to augment the Doppler signal instead of excessively increasing the gain. Hemodynamic factors, arrhythmia, valvular heart disease, and right heart adaptation may also impact the accuracy and precision of these noninvasive measurements. Secondary signs of PH such as abnormal LVEI, RV dysfunction and/or dilatation, dilated MPA, short RVOT AccT (≤105 ms), and RVOT VTI contour, may improve probability of PH diagnosis.[76] While RHC remains essential for PH diagnosis and classification, echocardiography plays a fundamental role in screening and early detection of PH.

D. RIGHT VENTRICULAR DIASTOLIC FUNCTION

Assessment of RV diastolic function is frequently excluded from standard echocardiographic reporting, despite increasing recognition of its relevance in many acute and chronic conditions, including PH.[89] RV diastolic dysfunction is a sensitive and measurable marker of subclinical RV dysfunction, often manifesting before overt systolic dysfunction, RV dilatation, or RV hypertrophy (RVH).[89,90] Table 6 highlights common clinical conditions associated with RV diastolic dysfunction.

Standard RV diastolic evaluation includes PW Doppler assessment of transtricuspid inflow (E- and A-wave velocities, tricuspid E/A ratio, deceleration time), PW Doppler of HV flow patterns, and lateral tricuspid annulus TDI (e' and a' velocities, e'/a' ratio). IVRT can also be included into diastolic assessment and is typically ≤73 ms in normal healthy adults. Doppler assessments are integrated with standard morphologic evaluations of the RA, RV, and IVC, as shown in Table 3. Grading of diastolic dysfunction relies on the tricuspid E/A ratio, deceleration time (normal range, 120-230 ms), abnormal tricuspid E/e' ratio (>6), and HVd flow predominance in the hepatic veins, as detailed in Table 6. TDI e' and a' velocities are generally less load dependent compared with tricuspid inflow velocities, which are affected by loading conditions and RV stiffness and compliance.[90]

Transtricuspid flow velocity measurements are generally feasible in most patients, with low inter- and intraobserver variability,[91] requiring measurements at end-expiration and averaging of at least five consecutive beats.[92] Physiologic conditions, heart rate, and respiratory rate may affect different RV diastolic parameters. Inspiration increases E wave velocity, resulting in a higher E/A ratio, while tachycardia increases E wave velocity but raises A wave velocity more, thereby lowering the tricuspid E/A ratio.[93] A normal physiologic response to exercise leads to proportional increases in both early rapid filling (E) and atrial contribution (A), generally maintaining the E/A ratio. Hemodynamically significant TV disease and atrial arrhythmias can also confound diastolic parameters. Last, age- and sex-specific differences in E/A ratio and TDI tricuspid e' velocities have been described, with higher inflow velocities seen in older healthy women.[92,94] When assessing RV diastolic function, it is important to consider these factors in an integrated fashion rather than considering any single diastolic parameter in isolation.

Several studies have evaluated the clinical impact of RV diastolic dysfunction in PH. In addition to correlating with invasive hemodynamics, derangements in diastolic parameters correlate with functional class, PH severity, 6-minute walk distance, N-terminal pro–brain-type natriuretic peptide, and poor clinical outcomes.[89,90,95] Diastolic filling patterns also reflect therapeutic response and in pulmonary arterial hypertension (PAH), can improve acutely with directed therapies.[96]

Key Points

- RV diastolic dysfunction is an early marker of subclinical disease that correlates with hemodynamic and functional variables in PH.
- RV diastolic assessment includes evaluating the morphologic features of the right heart, transtricuspid inflow velocities, TDI lateral annular velocities, and HV flow patterns.
- RV diastolic assessment is affected by age, sex, and physiologic factors such as respiratory rate and heart rate.

Recommendation

1. Although RV diastolic function is generally feasible in most patients, standardized assessment and reporting are limited mostly to select populations such as patients with or at risk for PH.

E. RIGHT HEART REMODELING IN PULMONARY HYPERTENSION

Defining Pulmonary Hypertension

The hemodynamic definition of PH was recently revised to a resting mPAP >20 mm Hg,[2,3] on the basis of extensive epidemiologic evidence of adverse clinical outcomes and heightened mortality in adults with mPAP of 21 to 24 mm Hg.[97] The current PH clinical classification includes five different groups, as shown in Table 7, with PVR > 2 Wood units distinguishing between pre- and postcapillary forms.[2,3]

Right Heart Adaptation to Pulmonary Vascular Disease

The RV adaptation to increased afterload is the main determinant of outcome in PH, a chronic disease marked by progressive vasoconstriction and adverse pulmonary vascular remodeling.[85] Physiologic matching of RV contractility to increased afterload, known as RV-PA coupling,[9] induces a series of adaptive chamber-level structural and morphologic changes (Figure 4, A). Effective RV adaptation and ventricular remodeling is a complex process influenced by the severity, duration, and rapidity of PVD, as well as the degree of hemodynamic derangements, neurohormonal activation, coronary perfusion, and myocardial metabolism.[85,98]

Although less muscular than the LV, the RV is able to maintain the same SV with approximately 25% of the stroke work due to the low resistance and high compliance of the pulmonary vascular bed. Initially, the RV chamber adapts to increasing afterload by enhancing muscle contractilty and mass up to four- to fivefold through the addition of sarcomeres aligned in parallel with cardiomyocytes.[9] Adaptive RV remodeling is defined by concentric RVH with minimal RV dilatation or fibrosis, preserved RVEF and cardiac output (CO), normal RV filling pressures, and preserved or mildly impaired exercise capacity. However, these adaptive mechanisms fail when afterload exceeds the compensatory gain of contractility, and the chambers begin to dilate to increase SV and maintain CO.[9,85]

Maladaptive RV remodeling is characterized by chamber dilatation, lower RV mass, increased RV volumes, RV tissue fibrosis, diminished RV function, and decreased exercise capacity.[9] Several key echocardiographic features can be seen during this phase of remodeling.[8] First, as the RV chamber dilates, the chamber contour shifts from

Table 6 RV diastolic function assessment

	Normal	Abnormal		
		Impaired	Pseudonormal	Restrictive
Morphologic assessment				
RAV index (method of disks), mL/m^2	<30		≥30	
RVWT, cm	<0.5		≥0.5	
IVC size, cm	≤2.1		>2.1	
IVC inspiratory variation	≥50%		<50%	
Doppler assessment				
E/A ratio	≥0.8 to <2.0	<0.8	0.8 to 2.1	>2.1
DT, ms	≥120 to ≤230	>230	120 to 230	<120
PA diastolic antegrade flow	No	No	Yes	Yes
Hepatic vein flow S/D ratio	≥1	≥1	<1	<1
Hepatic vein diastolic predominance	No	No	Yes	Yes
TDI				
e′/a′ ratio	≥0.5 to <1.8		<1	
E/e′ ratio	<6.0		>6	
RV IVRT, ms	≤73		>73	
Conditions associated with RV diastolic dysfunction (alphabetical order)				
Acute hypoxia				
Aging				
Amyloidosis				
Antiphospholipid antibody syndrome				
Aortic regurgitation				
Aortic stenosis				
Arrhythmogenic RV cardiomyopathy				
Behçet's vasculitis				
β-thalassemia				
Cardiac transplantation				
Cardiomyopathy				
Chagas disease				
Chronic heart failure				
Chronic obstructive pulmonary disease				
Congenitally corrected transposition of the great arteries				
Cystic fibrosis				
Diabetes mellitus				
Essential hypertension				
Hepatopulmonary syndrome				
Hypothyroidism				
Mitral regurgitation				
Myocardial infarction due to left anterior descending coronary artery lesion				
Myocardial infarction or ischemia due to (proximal) right coronary artery lesion				
PAH				
Pulmonary embolism				
Pulmonic stenosis				
Repaired tetralogy of Fallot depending on surgical approach				
Repaired transposition of the great arteries				
Renal transplantation				
Rheumatoid arthritis				
Smoking				
Stenosis of MPA and branch arteries				
Systemic sclerosis (scleroderma)				

DT, deceleration time; *IVC*, inferior vena cava; *IVRT*, isovolumetric relaxation time; *MPA*, main pulmonary artery; *PA*, pulmonary artery; *PAH*, pulmonary arterial hypertension; *RAV*, right atrial volume; *RV*, right ventricle; *RVWT*, right ventricular wall thickness

Table 7 PH definition and classification

PH	Characteristics	Clinical group
PH	mPAP > 20 mm Hg	All groups
Precapillary PH	mPAP > 20 mm Hg PCWP ≤ 15 mm Hg PVR > 2 WU	Group 1 PAH Group 3 PH associated with lung disease and/or hypoxia Group 4 PH associated with PA obstruction Group 5 PH with mixed/unclear etiology
Isolated postcapillary PH	mPAP > 20 mm Hg PCWP > 15 mm Hg PVR ≤ 2 WU	Group 2 PH associated with left heart disease Group 5 PH with unclear/multifactorial mechanisms
Combined pre- and postcapillary PH	mPAP > 20 mm Hg PCWP > 15 mm Hg PVR > 2 WU	
Exercise PH	mPAP/CO slope between rest and exercise > 3-3.5 mm Hg · min/L	Group 1 PAH Group 2 PH associated with left heart disease Group 3 PH associated with lung disease and/or hypoxia Group 4 PH associated with PA obstruction Group 5 PH with mixed/unclear etiology

Group 1 PAH

  1.1. Idiopathic

    1.1.1. Long-term responders to calcium channel blockers

  1.2. Heritable (*BMPR2* or other mutation)

  1.3. Associated with drugs and toxins

  1.4. Associated with:

    1.4.1. Connective tissue disease

    1.4.2. HIV infection

    1.4.3. Portal hypertension

    1.4.4. Congenital heart disease

    1.4.5. Schistosomiasis

  1.5. PAH with features of venous/capillary (PVOD/PCH) involvement

  1.6. Persistent PH of the newborn

Group 2 PH associated with left heart disease

  2.1. Heart failure

    2.1.1. With preserved ejection fraction

    2.1.2. With reduced or mildly reduced ejection fraction

    2.1.3. Cardiomyopathies with specific etiologies (hypertrophic, amyloid, Fabry disease, Chagas disease)

  2.2. Valvular heart disease

    2.2.1. Aortic valve disease

    2.2.2. Mitral valve disease

    2.2.3. Mixed valvular disease

  2.3. Congenital/acquired cardiovascular conditions leading to postcapillary PH

Group 3 PH associated with lung diseases and/or hypoxia

  3.1. Obstructive lung disease or emphysema

  3.2. Interstitial lung disease

  3.3. Lung disease with mixed restrictive/obstructive pattern

  3.4. Other parenchymal lung diseases (not included in group 5)

  3.5. Nonparenchymal restrictive lung diseases

    3.5.1. Hypoventilation syndromes

    3.5.2. Pneumonectomy

  3.6. Hypoxia without lung disease (e.g., high altitude)

  3.7. Developmental lung disorders

(Continued)

Table 7 (*Continued*)

Group 4 PH associated with PA obstructions
4.1. Chronic thromboembolic PH
4.2. Other PA obstructions
Group 5 PH with unclear and/or multifactorial mechanisms
5.1. Hematologic disorders
5.2. Systemic disorders: sarcoidosis, pulmonary Langerhans cell histiocytosis, and neurofibromatosis type 1
5.3. Metabolic disorders
5.4. Chronic renal failure with or without hemodialysis
5.5. Pulmonary tumor thrombotic microangiopathy
5.6. Fibrosing mediastinitis
5.7. Complex congenital heart diseases
Conditions that contribute to PH and warrant screening
BMPR2 mutations, a first-degree relative with a *BMPR2* mutation
HIV infection
Congenital heart disease with shunt
Connective tissue diseases: systemic sclerosis
Sickle-cell disease
Chronic lung diseases with hypoxia: interstitial lung disease, obstructive sleep apnea, obesity hypoventilation syndrome
Acute and recurrent pulmonary embolism
Hematologic disorders: chronic hemolytic anemia, myeloproliferative disease, splenectomy
Systemic disorders: sarcoidosis, pulmonary histiocytosis, lymphangioleiomyomatosis
Metabolic disorders: glycogen storage diseases, Gaucher disease, thyroid disorders

BMPR2, Bone morphogenic protein receptor 2; *CO*, cardiac output*HIV*, human immunodeficiency virus; *mPAP*, mean pulmonary arterial pressure; *PCH*, pulmonary capillary hemangiomatosis; *PCWP*, pulmonary capillary wedge pressure; *PVOD*, pulmonary veno-occlusive disease; *PVR*, pulmonary vascular resistance; *WU*, Wood units.

crescentic to spherical, with the end-diastolic midventricular linear dimension increasing relative to the longitudinal dimension (Figure 4, B). These changes typically precede an increase in the basal linear dimension. Additionally, there will be an increase in RVESA, occurring before increases in RVEDA. Diastolic dysfunction may also develop at this stage, as the RV becomes less compliant, leading to impaired filling and increased diastolic pressures. Mechanistically, RV chamber dilation likely occurs because the thinner RV wall experiences greater wall stress for a similar pressure increase compared with the LV.[9] Abnormal wall stress combined with progressive contractile dysfunction can also result in leftward tethering of the RV apex, a phenomenon known as apical traction.[46,99] In this stage of maladaptation, basal RV function is often preserved, resulting in potential overestimation of RV systolic function by parameters such as TAPSE and TDI S′ velocity.[99]

In advanced stages, there is continued right heart chamber enlargement and progressive contractile dysfunction against elevated afterload, known as RV-PA uncoupling (Figure 4, C). Clinically, RV-PA uncoupling is marked by congestive right heart failure, diminished CO due to ventricular interdependence,[100] increased filling pressures, restrictive RV diastolic dysfunction, and interventricular mechanical dysynchrony.[9,24] Adverse remodeling can also lead to TVA dilatation and poor leaflet coaptation, leading to significant FTR, further affecting RV performance and clinical outcomes in patients with PH.

Evaluation and Prognostic Significance of RV Maladaptation in PH

The precise mechanisms and timing of adaptive and maladaptive right heart remodeling are highly complex, occur along a continuum, and differ across various disease etiologies, independent of the degree of afterload elevation. As many imaging parameters are dependent on hemodynamic loading conditions, echocardiographic ratios that integrate contractile response at a given afterload may be more representative of deficient RV-PA coupling. The TAPSE/PASP ratio is an important noninvasive physiologic index of RV-PA coupling that has prognostic significance in a number of clinical settings,[47] including pre- and postcapillary PH[48-50,69] and heart failure.[51] However, previous studies have shown that TAPSE decreases during the early stages of RV remodeling, but remains relatively stable in advanced disease, highlighting its limited capacity to distinguish between adaptive and maladaptive remodeling.[8,101] As a result, the optimal numerator within echocardiographic ratios of RV-PA coupling may vary according to age, sex, race/ethnicity, body habitus, comorbid conditions, and severity of PH. In a recent study of patients with PAH, RVFWS/PASP outperformed TAPSE/PASP and independently predicted a combined end point of death and heart or lung transplantation using a cutoff of 0.19%/mm Hg.[70] Recent studies have also demonstrated that FAC/PASP has improved prognostic value over other numerators, reflecting age- and sex-specific adaptation to increased

afterload.[50,59] These studies underscore that echocardiographic RV-PA coupling ratios offer valuable insights into quantifying and prognosticating right heart adaptation to a given afterload across the disease continuum, yet are dependent on the specific numerator used.

Key Points

- Effective right heart adaptation to increased afterload is the main determinant of morbidity and mortality in PH and occurs along a continuum.
- Adaptive remodeling is characterized by concentric RVH with minimal RV dilatation and preserved function.
- Maladaptive RV remodeling is marked by chamber dilatation and progressive contractile dysfunction, known as RV-PA uncoupling, and is associated with onset of clinical heart failure.

Recommendations

1. A comprehensive assessment that incorporates structural changes and functional measures should be used to systematically evaluate RV adaptation to PH.
2. Echocardiographic coupling measures that integrate the contractile response to a given afterload can improve prognostication in clinical practice.

F. SPECIAL TOPICS

Precapillary vs Postcapillary Pulmonary Hypertension

A common clinical challenge in PH is distinguishing between precapillary and postcapillary phenotypes, which requires confirmatory diagnosis through invasive RHC. However, echocardiography can identify relevant adaptive and maladaptive changes in right heart morphology and function, providing insights into the predominant phenotype and underlying pathophysiology.[76] Table 8 summarizes common clinical and echocardiographic features observed across different PH phenotypes.

Fluid Challenge

A fluid challenge stresses the pulmonary circulation and can potentially differentiate between pre- and postcapillary PH, enhancing diagnostic accuracy.[102] Although the specifics may vary based on clinical context, a fluid challenge typically involves the administration of 250 to 500 mL of crystalloid solution over 15 to 30 minutes, and adjusted based on the observed hemodynamic response. A positive fluid challenge is generally defined as an increase in PCWP >18 mm Hg and/or an increase in mitral E/e′ ratio >12, indicating elevated left atrial pressure and supporting a diagnosis of occult LV diastolic dysfunction.[102,103] Further studies are needed to validate the routine use of fluid challenge during standard echocardiography for identifying occult LV diastolic dysfunction and unmasking postcapillary etiologies.

Assessment of Exercise Hemodynamics and Right Ventricular Functional Reserve

Assessing ventricular coupling with the pulmonary circuit during stress provides significant insight into cardiopulmonary physiology in healthy and diseased subjects, by evaluating symptoms such as dyspnea and fatigue and identifying characteristic echocardiographic pre- and post-capillary phenotypes that improve prognostication.[104-106] Semirecumbent bicycle stress is the preferred noninvasive method for assessing cardiopulmonary hemodynamics and contractile reserve.

Exercise-induced elevation in pulmonary pressures predicts outcomes in individuals at risk for PH. An abnormal pulmonary vascular response to exercise has been previously defined as a rest-stress RVSP difference ≥20 mm Hg and/or a peak RVSP ≥50 mm Hg.[104,107] A rest-stress mitral E/e′ ratio >12 suggests a component of postcapillary disease, with E/e′ ratios ≥15 indicating higher mortality risk, independent of ischemia or LV dysfunction.[108] Worsening mitral and/or tricuspid regurgitation with increased RVSP during exercise may further suggest a postcapillary phenotype. It is important to note that PASP can be influenced by various factors such as age, physical conditioning, and
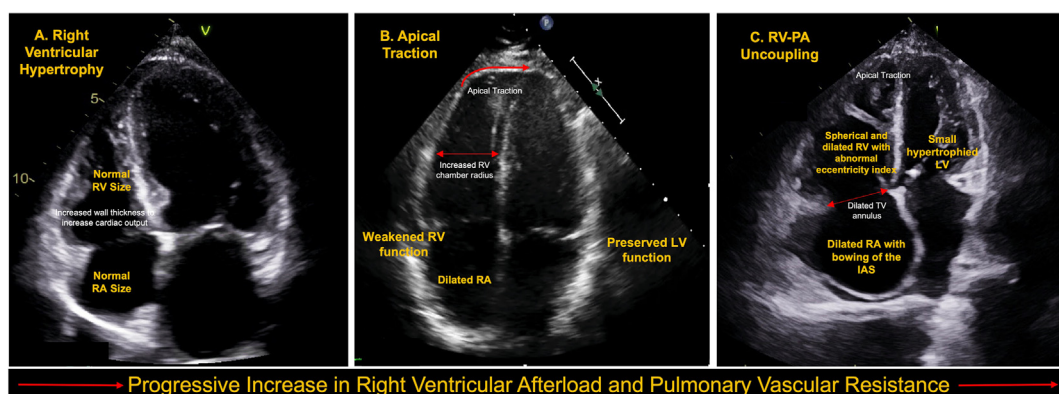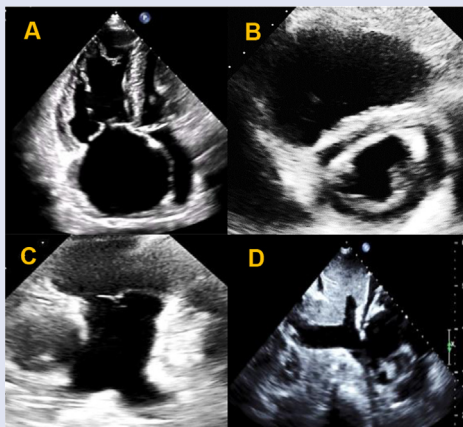

Figure 4 Right heart remodeling in PH. **(A)** The right ventricle initially responds to increased afterload by increasing RVWT to increase contractility and maintain CO. **(B)** With progressive PH, the contractile increases are insufficient to maintain CO, and the chamber dilates to increase SV. There may also be signs of apical traction, where the RV apex is tethered leftward because of weakened RV function and the inability to counteract LV forces. **(C)** Ultimately, there is an increase in right heart chamber sizes and RV systolic dysfunction, and abnormal LVEI, leading to diminished left ventricular performance, ventricular interdependence, and RV-PA uncoupling. TVA dilatation and FTR may also be present. *IAS*, Interatrial septum.

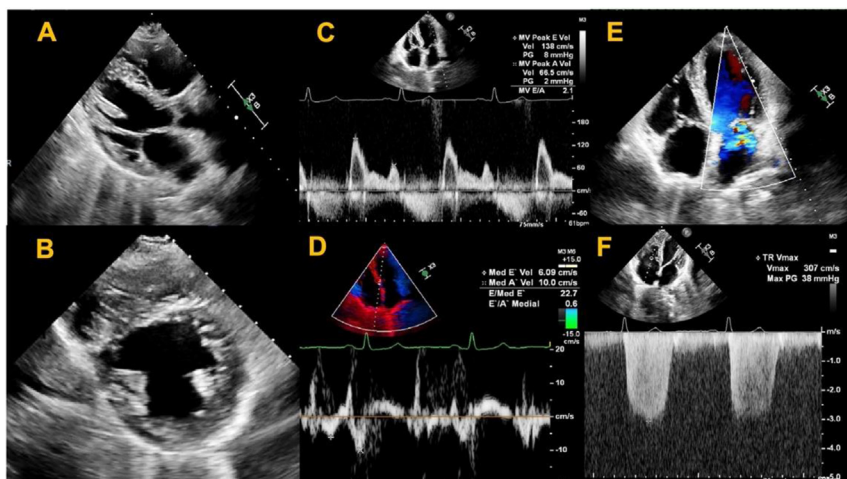**Table 8** Common clinical and echocardiographic features across ph phenotypes

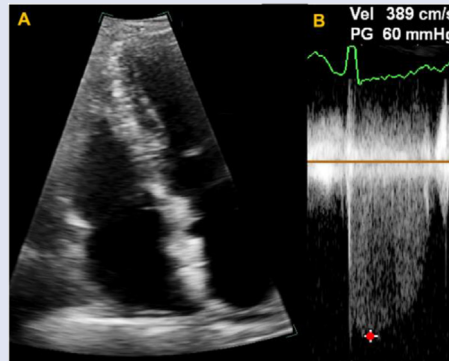|	
Group 1 Pre-capillary pulmonary arterial hypertension	Normal or small left heart Normal mitral E/e' ratio (<8) Dilated right heart: RV/LV>1, dilated RA (≥19 cm^2), RVH (**A**) LVEI>1.1, flattening of the interventricular septum in systole ± diastole based on hemodynamic conditions (**B**) RVOT AccT ≤105 msec Abnormal peak TR velocity ≥2.9 m/s* Abnormal end-diastolic PR ≥ 2.2 m/s TAPSE/PASP ratio <0.55 mm/mm Hg, <0.3-0.4 mm/mm Hg is associated with RV/PA uncoupling and increased mortality Dilated PA >25 mm (**C**) Dilated IVC with abnormal respirophasic variation, may have dilated hepatic veins with abnormal HVs/HVd ratio < 1 and holosystolic flow reversal (**D**). Typically, younger patients without cardiovascular co-morbidities
Group 2 Post-capillary pulmonary venous hypertension	LV hypertrophy (**A**) and/or LV chamber dilatation Reduced or preserved LV ejection fraction Normal LV eccentricity index <1.2 (**B**) Dilated LA Abnormal diastolic function, typically ≥ Grade 2 LV diastolic dysfunction (**C**) Pathological mitral E/e' ratio >14 (**D**) ≥mild-moderate mitral or aortic disease (**E**) Abnormal peak TR velocity ≥2.9 m/s* (**F**) Normal right heart until late in disease course Typically, older patients with cardiovascular co-morbidities

(Continued)

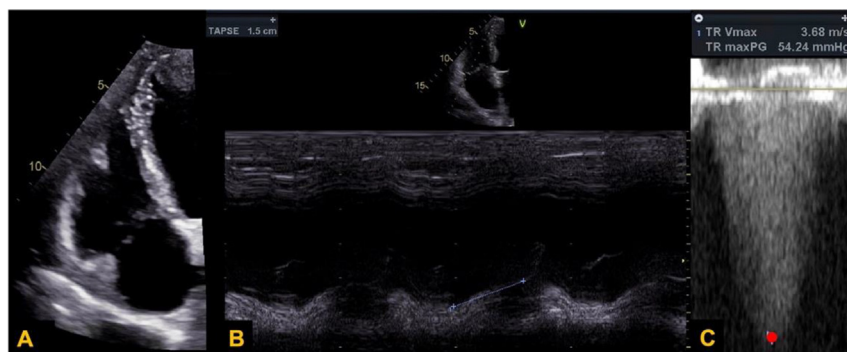**Table 8** (*Continued*)

Group 3 Pre-capillary pulmonary hypertension due to lung disease	Patients may have difficult acoustic windows due to lung interference that can be optimized through the utilization of subcostal imaging planes Due to shared risk factors with Group 2 PH including smoking and obesity, there may be varying degrees of left heart disease such as LV hypertrophy and LA enlargement Abnormal diastolic function, typically ≥ Grade 1 LV diastolic dysfunction Normal mitral E/e' ratio unless there is concomitant Group 2 disease. Typically, normal or small RV with RVH until late in the disease course (**A**) RV function is typically preserved until late in the disease course Abnormal RVSP with peak TR velocity ≥ 2.9 m/s* (**B**)
Group 4 Pre-capillary pulmonary hypertension due to chronic thromboembolic disease	*Chronic Thromboembolic Disease* Due to shared risk factors with Group 2 PH including smoking and obesity, there may be varying degrees of left heart disease such as LV hypertrophy and LA enlargement Normal mitral E/e' ratio unless there is concomitant Group 2 disease Mild RA and RV enlargement with RVH until late in the disease course, may appear similar to Group 1 PAH (**A**) Abnormal RV function (**B**) Abnormal RVSP with peak TR velocity ≥2.9 m/s* (**C**)

Of note, there may be a combined echo phenotype with shared features depending on stage of disease, disease duration, and co-morbid conditions. Further, echo phenotypes may change depending on stage and disease duration.
*Abnormal RVSP is defined as ≥2.9 m/s or ≥2.8 m/s with two adjunctive echo signs.

underlying health conditions, and defining the threshold of abnormality requires careful consideration of these variables in the clinical context.[109] Previous studies have shown that well-trained athletes and healthy adults >55 years may reach a peak PASP levels of 55-60 mm Hg that is physiologic rather than pathologic, driven by enhanced adaptation, increased CO, augmented RV inotropy due to heightened sympathetic tone, and pulmonary vasodilation.[110]

Increased PASP during exercise may also reflect preserved RV contractile reserve,[111] as evidenced by improved survival in patients with severe PH who can augment PASP by ≥30 mm Hg during exertion.[109] In this context, exercise stress echocardiography can evaluate RV contractile reserve, defined as the ability to enhance contractility with stress provocation. Global RV contractile reserve is measured by an exertional increase in RV functional parameters (TAPSE, DTI S' velocity, FAC), though specific numerical values are not well defined and may vary by sex.[104,111] Additionally, exercise-induced impairments in regional and global RVFWS can identify deficient contractile reserve in patients with connective tissue disease and PVD, serving as predictors of incident PH.[112,113]

Given the relative load dependence of many functional measures, echo-derived RV-PA coupling metrics may more effectively identify abnormal contractile responses to exertional changes in afterload, which may not be evident through conventional measures alone. These findings underscore the need to define exercise-induced pressure-flow relationships to detect pressure- and flow-dependent PVR changes. The European Society of Cardiology (ESC) and European Respiratory Society (ERS) guidelines define exercise-induced PH as an abnormal mPAP/CO slope of >3 mm Hg/L/min, emphasizing the dynamic relationship between mPAP and CO rather than an absolute mPAP threshold.[2,3] Defining abnormal pulmonary pressures during exercise is challenging without considering RV contractile function. Poiseuille's equation ($Q = \Delta P/R$) highlights that an abnormal pressure increase during exercise could stem from either high CO (e.g., in athletes) or elevated resistance (e.g., in PVD). In normal individuals, exercise increases SV and reduces PVR through pulmonary vasodilation. A recent study using bicycle stress echocardiography established the upper limit of normal for an echo derived mPAP/CO slope at 3.0 to 3.5 mm Hg/L/min,[105] accounting for variations by age, sex, and race/ethnicity.[114]

Key parameters obtained during a hemodynamic stress test include RV functional measures (TAPSE, DTI S′ velocity, FAC) from an RV-focused apical four-chamber view, RVSP, and LV diastology obtained at each stage of exertion. RVSP is calculated using RAP obtained at rest. CO is derived from the diameter measured at rest, and LVOT VTI is obtained at rest and stress. The most common formula to calculate mPAP during exercise stress is mPAP = [PASP*0.61] + 2 mm Hg.[84,105] RVFWS and FAC can be assessed offline if there is adequate RV visualization throughout the cardiac cycle. If significant mitral and/or tricuspid regurgitation is present at baseline, detailed valvular assessment should also be performed at each stage.[106]

Key Points

- Semirecumbent bicycle stress is the preferred noninvasive method for assessment of cardiopulmonary hemodynamics.
- Exertional changes in cardiopulmonary hemodynamics may help distinguish precapillary and postcapillary PH phenotypes.
- A precapillary PH phenotype is characterized by an exertional PASP increase without significant changes in LV diastolic parameters and the degree of aortic and/or mitral regurgitation or stenosis. There may also be diminished RV contractile reserve, defined by absent augmentation of RV functional parameters.
- A postcapillary PH phenotype is characterized by exertional PASP increase with worsening of LV diastolic parameters with or without an increase in degree of mitral regurgitation and/or TR.
- Integrating pressure-flow relationships using mPAP/CO may help identify exertional PH. The normal echo derived mPAP/CO slope range is 3.0 to 3.5 mm Hg · min/L with exercise.
- Stress echocardiography can also provide important information regarding RV contractile reserve in PH and at-risk populations.

Recommendation

1. Semirecumbent bicycle stress echocardiography is recommended for evaluating unexplained dyspnea, distinguishing cardiopulmonary causes, and identifying PH phenotypes. Using bicycle stress provides real-time continuous assessment of exercise-induced hemodynamic changes, improving detection of abnormal RV-PA coupling and PVR in patients with suspected PH.

G. TRICUSPID VALVE DISEASE

The integrity of the TVA is critical for optimal right heart performance. Comprehensive echocardiographic assessment is crucial to accurately determine TR severity and identify the mechanism and underlying valvular pathology. TR is highly prevalent, categorized into three main morphologic subtypes: primary, arising from a primary abnormality of the TVA; FTR, secondary to adverse right heart remodeling; and isolated atriofunctional TR (AFTR), due to adverse RA remodeling and long-standing atrial arrhythmia, such as AF.[115,116]

Anatomically, the TV typically has three leaflets: anterior, septal, and posterior. In healthy individuals, the relative circumferential length ratio of the anterior/septa/posterior leaflets is 1:1:0.75. The anterior leaflet is the longest radially and most mobile, while the septal leaflet is the shortest and least mobile. However, there can be considerable variation in the number of leaflets and three (type I, 54% of patients), four (type III, 39%), two (type II, 5%), and five (type IV, 2%) leaflets have been described.[117]

Primary TR is caused by an abnormality of any of the components of the TVA and commonly include myxomatous leaflet degeneration, leaflet prolapse, infective endocarditis, procedural iatrogenic perforation, and leaflet impingement from indwelling intracardiac leads. Primary TR also occurs in patients with ACHD due to congenital malformations such as Ebstein's anomaly, TV dysplasia, endocardial cushion defects, and structural involvement related to the specific underlying ACHD defect. Ebstein's anomaly is characterized by the apical displacement of the TV leaflets, which arise directly from the RV endocardium without any identifiable chordae. Primary TR resulting from leaflet damage can also occur secondary to anorectic drugs and ergot alkaloids, radiation, and systemic diseases such as carcinoid syndrome.[115]

FTR and AFTR are the predominant forms of TR, accounting for >80% of cases[115] and result from adverse right atrioventricular remodeling with a morphologically normal TVA. In the setting of PH and right heart maladaptation, TR severity and etiology both have important prognostic roles in determining the type and timing of therapy. Both qualitative and quantitative methods for assessing TR severity have been described.[118] Adjunctive signs frequently seen in severe TR include right heart dilatation and dysfunction, IVC enlargement and impaired respirophasic variation, abnormal HVs/HVd ratio<1, and holosystolic flow reversal.[118]

Functional Tricuspid Regurgitation

FTR results from adverse right heart remodeling, leading to TVA distortion and leaflet tethering, with displacement of the papillary muscles and chordae tendineae from the center of the coaptation plane.[119] TR severity is intricately linked to RV afterload, however

the relationship between elevated pulmonary pressures and the degree of TR is complex and multifaceted. With maladaptive remodeling to increased afterload, there is progressive dilation of the RV chamber to maintain CO, resulting in TVA deformation and FTR. The increased volume associated with FTR creates a vicious circle, leading to further dilatation and adverse remodeling of the right heart chambers. Pressure and volume overload in PH can also lead to IVS flattening, contributing to TVA dilatation and worsening FTR severity.[120] Although approximately 60% of patients with PAH have moderate or severe TR, many with severe PAH may or may not exhibit significant TR.[121] Different PH etiologies also result in distinct patterns of remodeling that affect the geometry and function of the TVA in different ways, thereby influencing the severity of FTR.[29,122-124] PAH generally leads to more severe FTR compared with other PH etiologies. In patients with RVSP >70 mm Hg, worsening FTR is associated with RA enlargement, abnormal TVA diameter, and increased valve tethering area.[121,125]

Assessment of FTR requires a thorough analysis of the anatomy and structure of the TVA and leaflets. Transthoracic echocardiography is the preferred initial imaging modality for evaluating right heart anatomy and function. When the acoustic window is adequate, transthoracic imaging may offer superior imaging of the TV when compared with TEE due to the anterior positioning of the valve structure. 3DE acquisition can be performed from standard transthoracic acoustic windows (parasternal, apical, and subcostal), offering high-resolution imaging (0.5 mm) of cardiac structures in the y (depth) and azimuthal (lateral orientation) dimensions. On 3DE, the TV is best visualized from an axial (cross-sectional) plane, providing an "en face surgical" view. In the 3D en face display of the TV, the interatrial septum is positioned inferiorly (at the 6 o'clock position), irrespective of the atrial or ventricular orientation.[116] However, systematic leaflet identification is not always possible, and TEE may be needed for comprehensive assessment of leaflet and TVA pathology, in accordance with the ASE guidelines.[31]

The TVA has a complex and dynamic saddle shape that flattens and dilates with maladaptive remodeling.[117,126] As the TVA dilates, it becomes more circular, particularly in the direction of the unsupported lateral and posterior regions. The TVA diameter is measured most commonly in end-diastole from the RV-focused apical four-chamber view with a normal cutoff value of ≤40 mm (21 mm/m² indexed to BSA). However, current societal recommendations[118] are limited by the assumption of a flat, circular annulus and the lack of standardization on when measures within the diastole period should be acquired.[126]

Following TVA measurement, the next step in evaluating FTR severity is the assessment of location and extent of leaflet coaptation. Normally, TV leaflet coaptation occurs at the TVA level or slightly below, with 5 to 10 mm of the leaflet edges in contact during systole. When the coaptation surface decreases in the setting of TVA dilation or leaflet tethering, coaptation occurs more apically, forming a triangular area between the coapted leaflets and the annular plane. Current recommendations suggest measuring two parameters to estimate the extent of leaflet tethering: the distance between the leaflet coaptation point and annular plane (tethering distance) and the area between the closed leaflet and annular plane (tenting area). Significant leaflet tethering is defined by tethering distance > 8 mm and tenting area > 1.6 cm².[116,127]

Atriofunctional Tricuspid Regurgitation

Isolated AFTR is increasingly recognized as a distinct etiology of TR given the absence of associated leaflet tethering.[115,128,129] In AFTR,

leaflet coaptation occurs at or near the annular plane. The RV will typically maintain a normal length while dilating at the base in a process known as conical remodeling.[119] With RA enlargement and annular dilatation, there is a decrease in leaflet coaptation surface resulting in leaflet malcoaptation and AFTR. The ratio of tricuspid leaflet area to closure area is a strong indicator of TR severity, reflecting leaflet adaptation, annular dilatation, and tethering geometry.[127]

AFTR typically occurs in patients with long-standing AF, who are more often older and female, with a higher RV FAC, a higher LV ejection fraction, and smaller LV cavity.[129] Approximately 25% of patients with lone AF duration of >10 years will have significant AFTR, of whom 28% will also have concomitant mitral regurgitation. In general, patients with AFTR have significantly better long-term survival and lower rates of mortality and HF hospitalizations compared to those with nonatrial TR.[129] However, the combination of AF and significant TR is associated with a poor prognosis, and restoring sinus rhythm may reverse adverse right heart remodeling and improve clinical outcomes.[130] Table 9 demonstrates the key differences between AFTR and FTR.

Tricuspid Regurgitation and Pulmonary Hypertension

The etiology of TR is frequently multifactorial, with primary and secondary mechanisms often coexisting and interacting to varying degrees, ultimately influencing TR severity. For example, the degree of TVA dilatation may be a stronger determinant of FTR severity than the amount of leaflet tethering and papillary muscle displacement.[125] In patients with PH, structural parameters such as TVA, tethering area, and eccentricity index are more closely associated with FTR severity than RV systolic function or PASP.[120] However, it is important to note that the severity of one condition does not reliably predict the severity of the other, as severe PH can occur in the absence of severe TR, and conversely, severe TR may develop in the absence of severe PH. Pathophysiologic variability, along with the timing and progression of right heart adaptation, can independently influence FTR severity. Factors such as chamber dilation and dysfunction, TVA involvement, and leaflet tethering contribute to this process, regardless of pulmonary pressures and severity of PH. Additionally, severely elevated RV afterload can create a counteracting force that mechanically opposes regurgitant flow, promoting leaflet coaptation and potentially reducing FTR severity.[125,126] High RV systolic pressure increases intracavitary forces, which may temporarily improve leaflet apposition despite underlying annular dilation or tethering. However, the effect is dynamic and may vary based on loading conditions and disease progression.[126,127]

Key Points

- Primary TR results from intrinsic abnormalities affecting the leaflets, mechanical interference from intracardiac devices, and congenital or acquired leaflet pathology.
- FTR typically results from adverse right atrioventricular remodeling, leading to annular dilatation and leaflet tethering without primary structural valvular abnormalities.
- The severity of FTR in PH is closely related to the extent of RV dysfunction, TVA dilation, and the degree of leaflet tethering, independent of the severity of PH.
- AFTR is a distinct etiology of TR driven predominantly by annular dilation without tricuspid leaflet tethering. AFTR generally has a better prognosis compared with FTR.

Recommendations

> 1. Comprehensive echocardiographic assessment, using several 2DE imaging planes and 3DE when feasible, is crucial for identifying the mechanism and severity of TR.
> 2. Distinguishing the etiology and contribution of adverse right heart remodeling and abnormalities of the TVA should be part of standardized reporting.
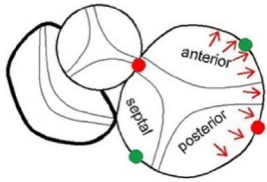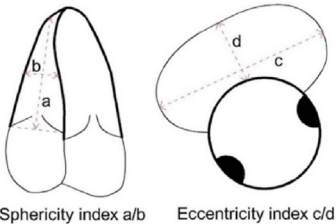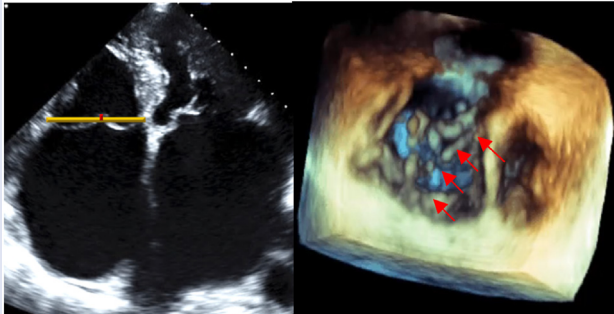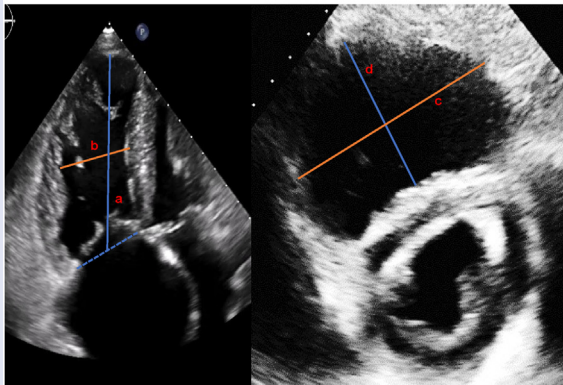
H. PULMONIC VALVE

The PV is the most superiorly positioned cardiac valve, located anterior and slightly left of the aorta, forming an approximately 30-degree angle with the aortic trunk. The PV consists of the anterior, left, and right cusps, which are anatomically thinner than the aortic valve. The left cusp is the closest to the aortic root, the aortic valve, and the basal LV septum. The anterior and right cusps, located above anterolateral free wall, are considered nonseptal cusps. However, there are several anatomic variants, such as bicuspid or quadricuspid valves. The PV annulus is a ring-shaped connective tissue structure with a mean diameter of 20 mm that defines the junction between the distal RVOT and the MPA trunk. The PV annulus, MPA, and proximal PA bifurcation are best visualized from the PSAX view at the level of the aortic valve, and angling upwards. Physiologic trivial or mild PR is a common and normal finding in healthy individuals.[118]

Transthoracic evaluation of PV anatomy may be difficult because of limited acoustic imaging planes. The optimal views for visualizing the PV include the subcostal view and the PSAX view at the level of RVOT. By tilting and rotating the transducer counterclockwise from the PSAX, the MPA and main left and right branches can also be visualized from the PA-focused view. By adding color Doppler, it may be possible to identify branch stenoses and congenital

---

Table 9 Mechanisms of FTR

Atriofunctional Tricuspid Regurgitation	Functional Tricuspid Regurgitation
Primary Right Atrial Remodeling remodeling	**Primary Right Ventricular remodeling**
AFTR typically results from RA enlargement without leaflet tethering. Progressive RA dilatation causes the annulus to become more planar and circular, with greater anteroposterior than mediolateral dilatation. Normal coaptation occurs at or just below the annulus, with a 5- to 10-mm coaptation length. TVA dilatation reduces leaflet coaptation and increases malcoaptation. • Tenting $\leq$ 10 mm • RV midventricular dimension $\leq$ 38 mm • LVEF $\geq$ 50% AFTR is commonly associated with long-standing AF, RA > LA enlargement, and moderate or greater TR.	The sphericity index of the RV is measured from the apical 4Ch view and is calculated by dividing the longitudinal diameter (*a*) by the short-axis diameter (*b*) in end-diastole. A normal RV sphericity index is 0.49 $\pm$ 0.11. An increased ratio indicates RV remodeling or dilatation. RVEI is calculated from the parasternal midventricular short-axis images and is equal to the ratio of the largest RV width (*c*) to the midpoint of the IVS to the RVFW (*d*). RVEI = *c/d* and is abnormal if >1. However, by convention, LVEI is used more commonly than RVEI. • Tethering height: 5-10 mm • Leaflet tethering is considered significant if there is a tethering height >8 mm or a tenting area >1.6 cm

A4C, Apical four-chamber; *LVEF*, LV ejection fraction; *RVEI*, RV eccentricity index.

abnormalities such as PS and patent ductus arteriosus. If visualization of the PV is adequate, biplane imaging and 3DE can identify potential abnormalities in leaflet morphology and structure. Live 3DE from the parasternal window is particularly useful for visualizing the PV en face. Additionally, 3DE biplane imaging formats enables the simultaneous display of orthogonal 2DE views, enhancing comprehensive assessment of PV structure and function. TEE may be necessary for further evaluation of leaflet pathology and annular structure in patients with suboptimal acoustic windows, following ASE guidelines.[31] Table 9 outlines technical considerations for PV assessment by transthoracic approaches. Echocardiographic methods for assessing the severity of pulmonary insufficiency and stenosis have been previously described.[118,131]

Pulmonic Regurgitation and Pulmonary Hypertension

Although rare, primary PR may result from pathologic leaflet abnormalities, such as congenital abnormalities, leaflet bowing and restricted mobility in rheumatic diseases, myxomatous degeneration, or carcinoid disease. More commonly, PR occurs as an iatrogenic complication following valvotomy for PS and repaired tetralogy of Fallot in patients with ACHD. Diagnosing and treating PR in the ACHD population can be challenging due to the lack of well-validated echocardiographic methods to assess severity.[132]

Secondary or functional PR occurs in patients with morphologically normal PVs. With adverse right heart remodeling, particularly in PAH, there can be disproportionate dilation of the RVOT and PV annulus, resulting in functional PR. PR is generally well tolerated until late in the disease course, when maladaptive chamber remodeling develops, associated clinically with signs and symptoms of right heart failure. Chronic PR typically causes RV volume overload and dilatation of the right heart chambers and impaired cardiac function. In contrast to FTR, the severity of PR is closely linked to elevated RV afterload, resulting from PH and PVD, and contributes to further adverse remodeling of the right heart.

Key Points

- The PV can be visualized from the PSAX PA-focused view or the subcostal view.
- Physiologic trivial or mild PR is a normal finding in healthy individuals. Primary PR results from morphologic abnormalities of the valve leaflets, while functional PR occurs secondary to MPA dilatation with or without severe PH.
- Chronic PR leads to volume overload and adverse chamber remodeling and dysfunction, and closely linked to the degree and chronicity of RV afterload elevation.

Recommendation

1. A comprehensive echocardiographic assessment of the PV and MPA should be performed when there is known or suspected PV pathology that may be contributing to right heart maladaptation in PH.

I. SCREENING, EARLY DETECTION, PROGNOSTICATION, AND THERAPEUTIC GUIDANCE IN PULMONARY HYPERTENSION

Echocardiography in Screening and Early Detection

Early screening and detection of PH and associated adaptive right heart changes can prevent disease and lessen adverse clinical outcomes. The widespread availability and noninvasive characteristics of echocardiography facilitate early PH identification, enabling timely diagnosis and intervention. Table 7 illustrates specific medical and genetic conditions that contribute to the onset of PH.[2] Due to the heterogenous nature of right heart adaptation to PH and varying subtypes, comprehensive echocardiographic assessment is essential for effective screening and noninvasive phenotyping and should integrate hemodynamic findings with detailed evaluation of chamber remodeling and contractile function.[76]

Table 10 demonstrates key recommendations for PH screening, which include evaluation of right heart structure and function, noninvasive hemodynamic estimation, and identification of significant pericardial effusions. A resting TR velocity value ≥2.9 or ≥ 2.8 m/s with at least two adjunctive echocardiographic signs suggests PH and warrants further evaluation.[2] Additional echocardiographic signs that may be present in precapillary PH include dilatation of the right heart chambers, RVH, short AccT, elevated PAEDP, and abnormal LVEI.[133] Including STE in screening echocardiographic examinations can also enhance the detection of subtle RV dysfunction not apparent by conventional metrics alone, improving the early identification of emerging PH.[134,135] Although bicycle stress echocardiography is not currently recommended as a screening tool,[104] some studies suggest that it may be useful to unmask subclinical PH and abnormalities in contractile reserve in at-risk populations, such as patients with systemic sclerosis[112] or heritable causes of PH.[136] Patients with a high suspicion of PH on the basis of screening echocardiography, even in the absence of risk factors, should be referred for diagnostic RHC for definitive hemodynamic confirmation of PH status.

Key Points

- Echocardiography is the first-line noninvasive screening tool for PH by estimating hemodynamics, assessing right heart size and function, and detecting associated cardiac abnormalities. Additionally, distinct echocardiographic characteristics may indicate specific PH phenotypes.
- A resting TR velocity value ≥2.9 or ≥2.8 m/s with at least two adjunctive echocardiographic signs suggests PH.
- Bicycle stress echocardiography may be a useful tool for early detection of subclinical PH and exertional abnormalities in pulmonary pressures and RV contractile reserve.

Echocardiography in Prognostication

Recent studies underscore the prognostic importance of right heart performance across the spectrum of PVD and PH across underlying disease etiologies. The association of echocardiographic measures with clinical outcomes is influenced by many factors including age, sex, the presence of concomitant cardiovascular disease, and PH disease duration, etiology, and severity.

Table 10 Recommendations for key echocardiographic imaging parameters

Screening for PH	Established PH
At a minimum, screening PH echocardiography should include Hemodynamics • Peak TRV • RVSP • LV E/e′ ratio Structure • Left atrial volume index • RA area and/or volume index • RV basal dimension: if abnormal, complete RV chamber assessment including quantification and grading of size (mild, moderate, severely dilated), presence or absence of septal flattening (diastole only suggestive of volume overload vs systole and diastole suggestive of pressure and volume overload) Function • LV ejection fraction (biplane from apical 4Ch, 2Ch) • RV systolic function (TAPSE, TDI, RVFWS*): if abnormal and/or there is evidence of RV structural abnormality such as dilation and presence of apical traction, calculate FAC Valves • Comprehensive assessment of ≥ moderate regurgitant lesions (mitral, tricuspid, aortic), aortic and mitral stenosis Other • Presence/absence of any pericardial effusion and if present, size and location in end-diastole, signs of cardiac tamponade	At a minimum, established PH echocardiography should include Hemodynamics • Peak TRV • RVSP with RAP and compare with prior • LV E/e′ ratio for group 2 PH or mixed pre- and postcapillary PH Structure • RA area and/or volume index • RV basal dimension: if abnormal, complete RV chamber assessment including quantification and grading of size (mild, moderate, severely dilated), presence or absence of septal flattening (diastole only suggestive of volume overload vs systole and diastole suggestive of pressure and volume overload) • RV volumes using 3DE if feasible Function • LV ejection fraction (biplane from 4Ch, 2Ch) • RV systolic function (TAPSE, TDI, FAC, RVFWS*): if abnormal and/or there is evidence of RV structural abnormality such as dilation and presence of apical traction, calculate FAC Valves • Change in valvular severity from prior (regurgitant lesions [mitral, tricuspid, aortic], aortic and mitral stenosis) • For FTR, evaluation of etiologies, presence of malcoaptation, presence of leaflet tethering, quantitative measures (annular size, tethering distance and length), presence of HVs reversal Other • Presence/absence of moderate or greater pericardial effusion and if present, size and location in end-diastole, signs of cardiac tamponade

2Ch, Two-chamber; *4Ch*, four-chamber; *TRV*, TR velocity.

PH screening and established PH echocardiograms should trigger comprehensive visualization, quantification, and assessment of the right heart chambers. When available, trained sonographers and echocardiologists should standardize image acquisition and interpretation, with consistent reporting using echocardiographic features above.

*RVFWS requires dedicated software either on the ultrasound machine and acquired at the time of image acquisition and/or dedicated offline analytic software, in addition to adequate visualization of the RVFW throughout the cardiac cycle.

Echo-derived hemodynamics are crucial for prognosticating PH, with multiple studies linking abnormal pulmonary pressures to adverse clinical outcomes. However, previous research often included patients with prevalent PH, variable degrees of right heart remodeling, significant valve disease, and frequently lacked invasive validation. Additionally, measures such as mPAP, RVSP, and PASP are influenced by CO, PCWP, and PVR, which limits their specificity as indicators of PVD severity when compared to PVR. While these findings highlight that no single hemodynamic parameter can accurately prognosticate PH, the grade of TR alone, and in combination with other echocardiographic parameters may enhance diagnostic accuracy.[137-139]

Several studies have evaluated the clinical impact of RV diastolic dysfunction in PH, including the presence of diastolic dysfunction, elevated tricuspid E/e′ values, and abnormal filling patterns. RV diastolic dysfunction correlates with diminished functional capacity in PH and is predictive of morbidity and mortality across pre- and postcapillary forms.[89,90,140] RV diastolic filling patterns also reflect therapeutic responsiveness and can improve acutely with institution of PAH-directed therapies.[96] Although tricuspid E/e′ ratio has a reasonable relationship to RAP on a population level, its prognostic value at the individual level is limited, particularly in patients with atrial arrhythmias or TV disease.[89,141] Additionally, the tricuspid E/e′ ratio has not been validated across a wide range of RAP values.

Pericardial effusions in PH indicate advanced disease and poor prognosis, often resulting from elevated RAP and right heart failure, leading to increased systemic venous pressure and fluid accumulation in the pericardial space. The presence of a pericardial effusion is incorporated into prognostic scores for PH, reflecting the strong association with disease progression and adverse clinical outcomes.[142]

Echocardiographic metrics of right heart adaptation provide notable prognostic insights in PH. A recent meta-analysis demonstrated that both RA area and area indexed to BSA predict morbidity and in PH, with each 1-cm^2 increase conferring a 6% increased risk.[4] STE-derived RA strain can also provide insights into RV end-diastolic pressures and adverse remodeling[40] while demonstrating independent predictive value in precapillary PH.[38] RA strain, although a valuable marker of right heart performance,[50] is limited by the absence of standardized reference values and significant variability, even in healthy populations.[41-43] The RA plays a pivotal role as a key indicator of RV diastolic function, offering insights into chronic pressure-volume changes and the adaptive ventricular response. The presence of RV diastolic dysfunction carries substantial clinical implications in PH, serving as a predictor of morbidity and mortality in both precapillary and postcapillary PH.[25,26]

In PAH, thresholds such as end-diastolic RV basal dimension > 5.5 cm, midventricular dimension > 5.0 cm, indexed

RVEDA >21 cm^2/m^2, and indexed RVESA > 17 cm^2/m^2 are associated with reduced 1-year survival.[143] Multiple studies have underscored the importance of RV functional measures, including TAPSE, TDI S$'$ velocity, RV MPI, and RV FAC, for prognosticating PH by assessing and quantifying the degree of right heart adaptation. STE-derived measures of RV function may reduce the angle dependency seen with conventional metrics, such as TDI S$'$ velocity and TAPSE. Further, STE parameters are predictive of morbidity, mortality, and therapeutic response across both pre- and postcapillary PH subtypes.[144-149] A RVFWS value less than-13.5% is associated with increased mortality in PAH.[69,146] However, across both pre- and postcapillary PH, even an RVFWS greater than-20% (i.e., less negative) is linked to increased mortality, underscoring the prognostic value of RVFWS across various forms of PH.[69]

Newer modalities such as 3DE-derived RV volumes and RVEF may enhance prognostic capability in PH by improving visualization of the right heart, reducing the geometric assumptions inherent to 2DE techniques, and increasing precision in volumetric measurements.[12,29,122-124] Regardless of the specific echocardiographic parameter used, serial changes in these parameters improves predictive capacity compared with a single assessment.[133,150-152]

Integrative echocardiographic measures that assess RV contractile response to variable afterloads may serve as stronger predictors of adverse events than any single measure of right heart function or hemodynamics. Various echocardiographic parameters for approximating RV-PA coupling have been proposed, with some studies indicating that FAC/PASP and RVFWS/PASP may outperform the predictive value of TAPSE/PASP.[50,59,69,70] The ESC/ERS guidelines recommend a TAPSE/PASP <0.36 mm/mm Hg as suggestive of PH, with a ratio of <0.19 mm/mm Hg indicating a 1-year mortality risk of $>20\%$.[2,3] Across pre- and postcapillary PH, even a mildly reduced TAPSE/PASP ratio is associated with a 37% higher mortality risk.[69] Other important metrics associated with increased 1-year mortality included in the ERS/ESC guidelines include RA area > 26 cm^2 and the presence of a moderate pericardial effusion.

Key Points

- Although echocardiographic measures of right heart chamber size, function, and hemodynamics may predict morbidity and mortality across WSPH classifications, no single measure alone can fully prognosticate outcomes.
- Integrative indices of RV-PA coupling such as TAPSE/PASP offer enhanced prediction of adverse clinical events in PH by reflecting abnormal contractile response to increased afterload.

Echocardiography in Guiding Therapy

Abnormal right heart imaging parameters should prompt invasive hemodynamic assessment and therapeutic institution or escalation. The ESC/ERS guidelines recommend classifying PH into low-, intermediate-, and high-probability categories at diagnosis and follow-up.[2] Risk stratification combines clinical, functional, cardiac performance and hemodynamic parameters to guide therapy or treatment escalation if there is poor therapeutic response. Echocardiography is a key feature of many of these risk scores, incorporating assessments of RA size, RV function, noninvasive hemodynamic estimates, and the presence of pericardial effusion. Recent studies have also defined the minimal detectable difference in right heart metrics in PAH to quantify thera-

peutic response.[148,153] Although improvement in imaging parameters is a key goal of targeted therapies, trends over time are more clinically relevant than any single measurement. Echocardiography is typically performed annually although may be appropriate at more frequent intervals when initiating or titrating treatments.[142] Table 10 demonstrates key echocardiographic parameters recommended for patients with established PH.

Key Point

- Echocardiographic metrics of right heart chamber size and function are integral to PH classification and severity grading, guiding risk stratification, and monitoring treatment response.

Use of Additional Imaging Techniques

The diagnostic classification of PH is enhanced by multimodality cardiac imaging, with each technique providing unique insights for a comprehensive assessment of underlying etiologies.[135,154]

CMR has emerged as the gold standard for the assessment of right heart structure and function due to excellent spatial and temporal resolution, flexible imaging planes with freedom from acoustic windows, and signal-to-noise ratio without exposure to harmful ionizing radiation.[155] The standard CMR data set allows the assessment of chamber-level volumes, function, SV, ventricular mass, myocardial perfusion, and valvular and vascular flow in a single examination. CMR imaging is valuable for assessing PH associated with congenital heart disease[156] infiltrative cardiomyopathies, and autoimmune diseases.[135,154,157] In PH, SV deterioration and increased RV chamber dimensions may be observed before clinically apparent right heart failure.[8] Diminished RV perfusion, dilation of the MPA, and adverse right heart remodeling can be seen on CMR in PAH and correlate with hemodynamic severity, although assessment of RVWT and delayed enhancement may be challenging because of partial volume effects.[154] When monitoring treatment response to PH therapies, longitudinal CMR-derived volumetric measurements of the right heart chambers serve as a key therapeutic target because of high reproducibility and low interobserver variability. CMR is also an effective modality for myocardial tissue characterization, providing detailed insights into structural abnormalities in myocardial composition through the administration of gadolinium. In PH, late gadolinium enhancement at the RV insertion points into the left ventricle suggest tissue fibrosis and myocardial stress due to increased pressure.[154,155] The degree of late gadolinium enhancement can predict time to clinical worsening in PH[158] but does not predict mortality.[159]

Chest CT is a standard component in the diagnostic workup for PH and offers several key benefits, including the evaluation of interstitial and parenchymal lung disease, quantification of pulmonary fibrosis, and detection of adverse pulmonary vascular remodeling. Chest CT also allows for precise MPA measurements, which compared with ascending aorta diameter correlates with PH severity.[34] Dual-energy CT is a recent advancement that provides CT angiographic images of the pulmonary vasculature at two different energy levels after the administration of iodine-based contrast.[134,154] The pulmonary vasculature is more clearly visualized due to differences in attenuation properties, facilitating the diagnosis and evaluation of chronic thromboembolic PH and potentially serving as an alternative to ventilation/perfusion scanning. Recent advances in computational and machine learning algorithms have been used to identify pulmonary vascular
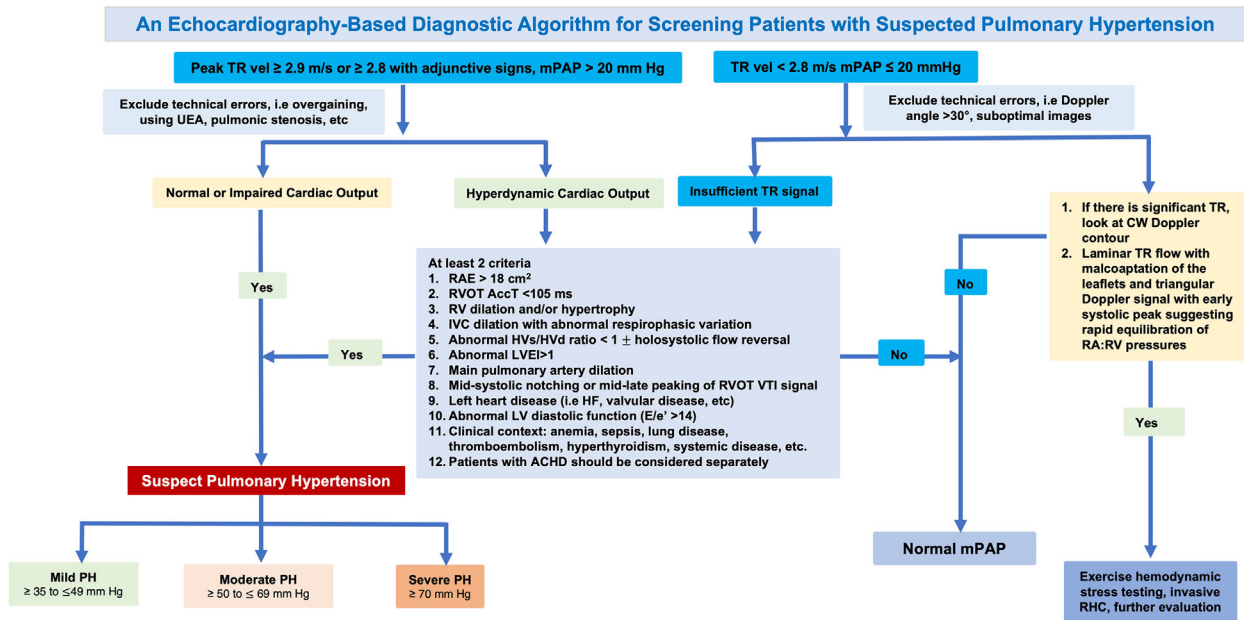
Figure 5 Echocardiographic diagnostic algorithm for screening patients with suspected PH. An echocardiographic algorithm is provided for patients with PVD at risk for or with suspected PH. *ASD*, Atrial septal defect; *HF*, heart failure; *PAP*, pulmonary artery pressure; *PHTN*, pulmonary hypertension; *RAE*, RA enlargement; *RH*, right heart; *TOF*, tetralogy of Fallot; *vel*, velocity; *VSD*, ventricular septal defect.

morphologic features on CT, revealing distal pruning of the small PAs in patients with PAH.[134]

Positron emission tomography (PET) has an emerging role in the evaluation of PH. The most widely used PET tracer is 2-deoxy-2-[^{18}F] fluorodeoxyglucose (FDG), which is used to measure glucose metabolism and abnormalities in cellular activity. In PH, cellular metabolism shifts from predominately fatty acid oxidation to increased glycolysis, serving as a compensatory adaptive mechanism to meet the heightened energy demands from increased afterload.[85] Through the detection of myocyte glycolysis, increased FDG uptake can be seen in the RV in patients with PH and is associated with hemodynamic severity, time to clinical deterioration, and death.[160] Quantifying the degree of FDG uptake serves as a valuable therapeutic end point by assessing treatment efficacy in PH and tailoring management strategies on the basis of metabolic response.[161]

Given the ability to integrate anatomic, functional, and metabolic data, there is increased utility of hybrid imaging in PH to refine diagnostic accuracy and therapeutic monitoring.[134,135,154] The two most commonly used hybrid imaging techniques in PH are CMR/PET and PET/CT. Simultaneous CMR/PET allows molecular imaging of impaired myocardial glycolysis and simultaneous structural imaging of the right heart. Increased FDG uptake within the RV myocardium and decreased CMR-derived RVEF can identify patients with PAH at greatest risk for clinical deterioration or death.[162] PET/CT is not commonly used in routine clinical practice for evaluation of PH because of cost and availability, however is an area of active investigation. PET/CT may be valuable for identifying vascular inflammation and assessing impaired coronary flow reserve, which may elucidate the underlying mechanisms contributing to PH in select populations.[134,135,154]

Key Points

- Although echocardiography is the primary remains the primary tool for screening, prognostication, and monitoring of therapeutic response in PH, multimodality cardiac imaging provides important adjunctive value in diagnostic classification and investigation of underlying etiologies.

J. FUTURE DIRECTIONS

Despite advances in PH-directed therapies through improved screening and early detection, PH is associated with unacceptably high morbidity and mortality. Echocardiographic assessment of right heart morphology and function provides crucial prognostic information, reinforcing its role as a key clinical tool. Emerging clinical techniques such as 3DE and STE offer comprehensive quantification of chamber-level systolic and diastolic function, refined valvular assessment, and established age- and sex-specific thresholds across diverse populations. Integrating these methodologies into routine clinical evaluation enhances diagnostic accuracy and enables tailored management strategies. However, an upfront multimodal approach in PH is limited by cost, availability, and the complexity of integrating diverse imaging metrics into a cohesive diagnostic and prognostic framework.

Moreover, no single parameter comprehensively reflects right heart function across the spectrum of PVD. Future research should prioritize optimizing relevant echocardiographic data, emphasizing quantitative measurements and leveraging automated software packages. There is an urgent need to identify the most effective

echocardiographic variables using machine learning and artificial intelligence to enhance risk stratification. A personalized approach that focuses on key variables and incorporates a "right heart composite score" could improve risk stratification by addressing individual variability in right heart adaptation and identifying intermediate-risk groups. Ultimately, an integrated multiparametric approach combining detailed assessments of right heart structure, function, and cardiopulmonary hemodynamics is likely to be more effective for diagnosing and prognosticating PH than any single echocardiographic feature. Figure 5 presents a high-yield and clinically applicable diagnostic algorithm for PH.

NOTICE AND DISCLAIMER

This report is made available by the ASE as a courtesy reference source for its members. It contains recommendations only and should not be used as the sole basis for making medical practice decisions or for taking disciplinary action against any employee. The statements and recommendations contained in this report are based primarily on the opinions of experts rather than on scientifically verified data.

The ASE makes no express or implied warranties regarding the completeness or accuracy of the information in this report, including the warranty of merchantability or fitness for a particular purpose. In no event shall the ASE be liable to you, your patients, or any other third parties for any decision made or action taken by you or such other parties in reliance on this information. Nor does your use of this information constitutes offering of medical advice by the ASE or create any physician-patient relationship between the ASE and your patients or anyone else.

REVIEWERS

This document was reviewed by members of the 2024–2025 ASE Guidelines and Standards Committee, the ASE Board of Directors, and the ASE Executive Committee.

CONFLICTS OF INTEREST

ACKNOWLEDGMENTS

SUPPLEMENTAL APPENDIX

We systematically searched PubMed to identify published studies that reported right-sided echocardiographic parameters in a cohort or a subgroup of healthy men or women ≥ 18 years of age with no known cardiovascular disease or significant acute or chronic comorbidity (as defined in the various studies). We extracted study-level data, notably, the mean and SD of each echocardiographic parameter, as well as the number of men and women studied. These study-level data are publicly available at https://bit.ly/3JY51X3. We used a Bayesian hierarchical model to derive the pooled mean and the pooled SD values for each echocardiographic parameter. These pooled mean and SD values were then used to determine the lower reference value (mean $- 1.96$ SDs), upper reference value (mean $+ 1.96$ SDs), moderate cutoff value (mean ± 3 SDs), and severe cutoff value (mean ± 4 SDs). For each statistic, we computed the posterior median and 95% equal-tailed credible interval. Our model was stratified by measurement technique when relevant differences were expected. The number of studies reporting values separately in men and women was insufficient to reliably stratify our meta-analysis by sex. We used a Python codebase with the JAGS package (https://github.com/tmiasko/pyjags) to perform the meta-analysis.

REFERENCES

1. Rudski LG, Lai WW, Afilalo J, et al. Guidelines for the echocardiographic assessment of the right heart in adults: a report from the American Society of Echocardiography endorsed by the European Association of Echocardiography, a registered branch of the European Society of Cardiology, and the Canadian Society of Echocardiography. J Am Soc Echocardiogr 2010;23:685-713.
2. Humbert M, Kovacs G, Hoeper MM, et al. 2022 ESC/ERS guidelines for the diagnosis and treatment of pulmonary hypertension. Eur Respir J 2023;61:2200879.
3. Kovacs G, Bartolome S, Denton CP, et al. Definition, classification and diagnosis of pulmonary hypertension. Eur Respir J 2024;64:2401324.
4. Richter MJ, Fortuni F, Alenezi F, et al. Imaging the right atrium in pulmonary hypertension: a systematic review and meta-analysis. J Heart Lung Transplant 2023;42:433-46.

5. Lang RM, Badano LP, Mor-Avi V, et al. Recommendations for cardiac chamber quantification by echocardiography in adults: an update from the American Society of Echocardiography and the European Association of Cardiovascular Imaging. J Am Soc Echocardiogr 2015;28:1-39.e14.

6. Kebed K, Kruse E, Addetia K, et al. Atrial-focused views improve the accuracy of two-dimensional echocardiographic measurements of the left and right atrial volumes: a contribution to the increase in normal values in the guidelines update. Int J Cardiovasc Imaging 2017;33:209-18.

7. Genovese D, Mor-Avi V, Palermo C, et al. Comparison between four-chamber and right ventricular-focused views for the quantitative evaluation of right ventricular size and function. J Am Soc Echocardiogr 2019;32:484-94.

8. Vonk Noordegraaf A, Haddad F, Bogaard HJ, et al. Noninvasive imaging in the assessment of the cardiopulmonary vascular unit. Circulation 2015;131:899-913.

9. Vonk Noordegraaf A, Westerhof BE, Westerhof N. The relationship between the right ventricle and its load in pulmonary hypertension. J Am Coll Cardiol 2017;69:236-43.

10. Braams NJ, van Leeuwen JW, Vonk Noordegraaf A, et al. Right ventricular adaptation to pressure-overload: differences between chronic thromboembolic pulmonary hypertension and idiopathic pulmonary arterial hypertension. J Heart Lung Transplant 2021;40:458-66.

11. Grapsa J, Tan TC, Nunes MCP, et al. Prognostic impact of right ventricular mass change in patients with idiopathic pulmonary arterial hypertension. Int J Cardiol 2020;304:172-4.

12. Grapsa J, O'Regan DP, Pavlopoulos H, et al. Right ventricular remodelling in pulmonary arterial hypertension with three-dimensional echocardiography: comparison with cardiac magnetic resonance imaging. Eur J Echocardiogr 2010;11:64-73.

13. Lang RM, Badano LP, Tsang W, et al. EAE/ASE recommendations for image acquisition and display using three-dimensional echocardiography. J Am Soc Echocardiogr 2012;25:3-46.

14. van der Zwaan HB, Geleijnse ML, McGhie JS, et al. Right ventricular quantification in clinical practice: two-dimensional vs. three-dimensional echocardiography compared with cardiac magnetic resonance imaging. Eur J Echocardiogr 2011;12:656-64.

15. Myhr KA, Kristensen CB, Pedersen FHG, et al. Accuracy and sensitivity of three-dimensional echocardiography to detect changes in right ventricular volumes: comparison study with cardiac magnetic resonance. Int J Cardiovasc Imaging 2021;37:493-502.

16. Shimada YJ, Shiota M, Siegel RJ, et al. Accuracy of right ventricular volumes and function determined by three-dimensional echocardiography in comparison with magnetic resonance imaging: a meta-analysis study. J Am Soc Echocardiogr 2010;23:943-53.

17. Knight DS, Grasso AE, Quail MA, et al. Accuracy and reproducibility of right ventricular quantification in patients with pressure and volume overload using single-beat three-dimensional echocardiography. J Am Soc Echocardiogr 2015;28:363-74.

18. Wang S, Wang S, Zhu Q, et al. Reference values of right ventricular volumes and ejection fraction by three-dimensional echocardiography in adults: a systematic review and meta-analysis. Front Cardiovasc Med 2021;8:709863.

19. Maffessanti F, Muraru D, Esposito R, et al. Age-, body size-, and sex-specific reference values for right ventricular volumes and ejection fraction by three-dimensional echocardiography: a multicenter echocardiographic study in 507 healthy volunteers. Circ Cardiovasc Imaging 2013;6:700-10.

20. McGhie JS, Menting ME, Vletter WB, et al. Quantitative assessment of the entire right ventricle from one acoustic window: an attractive approach. Eur Heart J Cardiovasc Imaging 2017;18:754-62.

21. Tamborini G, Marsan NA, Gripari P, et al. Reference values for right ventricular volumes and ejection fraction with real-time three-dimensional echocardiography: evaluation in a large series of normal subjects. J Am Soc Echocardiogr 2010;23:109-15.

22. Addetia K, Miyoshi T, Amuthan V, et al. Normal values of three-dimensional right ventricular size and function measurements: results of the World Alliance Societies of Echocardiography Study. J Am Soc Echocardiogr 2023;36:858-66.e1.

23. Manganaro R, Cusma-Piccione M, Carerj S, et al. Echocardiographic patterns of abnormal septal motion: beyond myocardial ischemia. J Am Soc Echocardiogr 2023;36:1140-53.

24. Marcus JT, Gan CT, Zwanenburg JJ, et al. Interventricular mechanical asynchrony in pulmonary arterial hypertension: left-to-right delay in peak shortening is related to right ventricular overload and left ventricular underfilling. J Am Coll Cardiol 2008;51:750-7.

25. Bossone E, Duong-Wagner TH, Paciocco G, et al. Echocardiographic features of primary pulmonary hypertension. J Am Soc Echocardiogr 1999;12:655-62.

26. Raymond RJ, Hinderliter AL, Willis PW, et al. Echocardiographic predictors of adverse outcomes in primary pulmonary hypertension. J Am Coll Cardiol 2002;39:1214-9.

27. Brierre G, Blot-Souletie N, Degano B, et al. New echocardiographic prognostic factors for mortality in pulmonary arterial hypertension. Eur J Echocardiogr 2010;11:516-22.

28. Ryan T, Petrovic O, Dillon JC, et al. An echocardiographic index for separation of right ventricular volume and pressure overload. J Am Coll Cardiol 1985;5:918-27.

29. Addetia K, Maffessanti F, Yamat M, et al. Three-dimensional echocardiography-based analysis of right ventricular shape in pulmonary arterial hypertension. Eur Heart J Cardiovasc Imaging 2016;17:564-75.

30. Badagliacca R, Poscia R, Pezzuto B, et al. Pulmonary arterial dilatation in pulmonary hypertension: prevalence and prognostic relevance. Cardiology 2012;121:76-82.

31. Hahn RT, Abraham T, Adams MS, et al. Guidelines for performing a comprehensive transesophageal echocardiographic examination: recommendations from the American Society of Echocardiography and the Society of Cardiovascular Anesthesiologists. J Am Soc Echocardiogr 2013;26:921-64.

32. Truong QA, Massaro JM, Rogers IS, et al. Reference values for normal pulmonary artery dimensions by noncontrast cardiac computed tomography: the Framingham Heart Study. Circ Cardiovasc Imaging 2012;5:147-54.

33. Kawel-Boehm N, Hetzel SJ, Ambale-Venkatesh B, et al. Reference ranges ("normal values") for cardiovascular magnetic resonance (CMR) in adults and children: 2020 update. J Cardiovasc Magn Reson 2020;22:87.

34. Mahammedi A, Oshmyansky A, Hassoun PM, et al. Pulmonary artery measurements in pulmonary hypertension: the role of computed tomography. J Thorac Imaging 2013;28:96-103.

35. Narendra Kumar K, Singh NG, P SN, et al. Transesophageal echocardiographic assessment of pulmonary artery-to-ascending aorta ratio for the detection of pulmonary hypertension in cardiac surgical patients. J Cardiothorac Vasc Anesth 2017;31:1702-6.

36. Alenezi F, Mandawat A, Il'Giovine ZJ, et al. Clinical utility and prognostic value of right atrial function in pulmonary hypertension. Circ Cardiovasc Imaging 2018;11:e006984.

37. Bhave NM, Visovatti SH, Kulick B, et al. Right atrial strain is predictive of clinical outcomes and invasive hemodynamic data in group 1 pulmonary arterial hypertension. Int J Cardiovasc Imaging 2017;33:847-55.

38. Hasselberg NE, Kagiyama N, Soyama Y, et al. The prognostic value of right atrial strain imaging in patients with precapillary pulmonary hypertension. J Am Soc Echocardiogr 2021;34:851-61.e1.

39. Saha SK, Soderberg S, Lindqvist P. Association of right atrial mechanics with hemodynamics and physical capacity in patients with idiopathic pulmonary arterial hypertension: insight from a single-center cohort in Northern Sweden. Echocardiography 2016;33:46-56.

40. Lang IM, Binder T. Right atrial strain is a surrogate of coupling in the right heart. Eur Heart J Cardiovasc Imaging 2020;21:863-4.

41. Badano LP, Kolias TJ, Muraru D, et al. Standardization of left atrial, right ventricular, and right atrial deformation imaging using two-dimensional speckle tracking echocardiography: a consensus document of the EACVI/ASE/Industry task force to standardize deformation imaging. Eur Heart J Cardiovasc Imaging 2018;19:591-600.

42. Soulat-Dufour L, Addetia K, Miyoshi T, et al. Normal values of right atrial size and function according to age, sex, and ethnicity: results of the World Alliance Societies of Echocardiography Study. J Am Soc Echocardiogr 2021;34:286-300.

43. Krittanawong C, Maitra NS, Hassan Virk HU, et al. Normal ranges of right atrial strain: a systematic review and meta-analysis. JACC Cardiovasc Imaging 2023;16:282-94.

44. Peluso D, Badano LP, Muraru D, et al. Right atrial size and function assessed with three-dimensional and speckle-tracking echocardiography in 200 healthy volunteers. Eur Heart J Cardiovasc Imaging 2013;14:1106-14.

45. Raina A, Vaidya A, Gertz ZM, et al. Marked changes in right ventricular contractile pattern after cardiothoracic surgery: implications for post-surgical assessment of right ventricular function. J Heart Lung Transplant 2013;32:777-83.

46. Motoji Y, Tanaka H, Fukuda Y, et al. Association of apical longitudinal rotation with right ventricular performance in patients with pulmonary hypertension: insights into overestimation of tricuspid annular plane systolic excursion. Echocardiography 2016;33:207-15.

47. Guazzi M, Bandera F, Pelissero G, et al. Tricuspid annular plane systolic excursion and pulmonary arterial systolic pressure relationship in heart failure: an index of right ventricular contractile function and prognosis. Am J Physiol Heart Circ Physiol 2013;305:H1373-81.

48. Tello K, Wan J, Dalmer A, et al. Validation of the tricuspid annular plane systolic excursion/systolic pulmonary artery pressure ratio for the assessment of right ventricular-arterial coupling in severe pulmonary hypertension. Circ Cardiovasc Imaging 2019;12:e009047.

49. Gorter TM, van Veldhuisen DJ, Voors AA, et al. Right ventricular-vascular coupling in heart failure with preserved ejection fraction and pre- vs. post-capillary pulmonary hypertension. Eur Heart J Cardiovasc Imaging 2018;19:425-32.

50. Gami A, Jani VP, Mombeini H, et al. Prognostic value of echocardiographic coupling metrics in systemic sclerosis-associated pulmonary vascular disease. J Am Soc Echocardiogr 2024;Oct 1:S0894-7317(24)00468-1.

51. Gami A, Jani VP, Mombeini H, et al. Prognostic Value of Echocardiographic Coupling Metrics in Systemic Sclerosis-Associated Pulmonary Vascular Disease. J Am Soc 2024 Oct 1:S0894-7317(24)00468-1.

52. Jani V, Kapoor K, Meyer J, et al. Unsupervised machine learning demonstrates the prognostic value of TAPSE/PASP ratio among hospitalized patients with COVID-19. Echocardiography 2022;39:1198-208.

53. D'Alto M, Marra AM, Severino S, et al. Right ventricular-arterial uncoupling independently predicts survival in COVID-19 ARDS. Critical care 2020;24:1-10.

54. Lillo R, Graziani F, Ingrasciotta G, et al. Right ventricle systolic function and right ventricle-pulmonary artery coupling in patients with severe aortic stenosis and the early impact of TAVI. Int J Cardiovasc Imaging 2022;38:1761-70.

55. Brener MI, Lurz P, Hausleiter J, et al. Right ventricular-pulmonary arterial coupling and afterload reserve in patients undergoing transcatheter tricuspid valve repair. J Am Coll Cardiol 2022;79:448-61.

56. Besler C, Orban M, Rommel KP, et al. Predictors of procedural and clinical outcomes in patients with symptomatic tricuspid regurgitation undergoing transcatheter edge-to-edge repair. JACC Cardiovasc Interv 2018;11:1119-28.

57. Mukherjee M, Ogunmoroti O, Jani V, et al. Characteristics of right ventricular to pulmonary arterial coupling and association with functional status among older aged adults from the multi-ethnic study of atherosclerosis. Am J Cardiol 2023;196:41-51.

58. Tan Y, Manouras A, Lund LH, et al. Feasibility and accuracy of tricuspid annular displacement assessed by speckle tracking echocardiography and Doppler tissue imaging. Echocardiography 2019;36:2004-9.

59. Jani VP, Strom JB, Gami A, et al. Optimal method for assessing right ventricular to pulmonary arterial coupling and subclinical right ventricular dysfunction in older aged healthy adults: the multi-ethnic study of atherosclerosis. Am J Cardiol 2024;222:11-9.

60. Anavekar NS, Gerson D, Skali H, et al. Two-dimensional assessment of right ventricular function: an echocardiographic-MRI correlative study. Echocardiography 2007;24:452-6.

61. Kavurt AV, Pac FA, Koca S, et al. The evaluation of right ventricular systolic function in patients with repaired tetralogy of fallot by conventional echocardiographic methods and speckle tracking echocardiography: compared with the gold standard cardiac mangenetic resonance. Echocardiography 2019;36:2251-8.

62. Focardi M, Cameli M, Carbone SF, et al. Traditional and innovative echocardiographic parameters for the analysis of right ventricular performance in comparison with cardiac magnetic resonance. Eur Heart J Cardiovasc Imaging 2015;16:47-52.

63. Marra A. Reference ranges and determinants of right ventricle outflow tract acceleration time in healthy adults by two-dimensional echocardiography. Int J Cardiovasc Imaging 2017;33:219-26.

64. Haddad F, Amsallem M. Full circle on pulmonary flow dynamics in pulmonary arterial hypertension. JACC Cardiovasc Imaging 2017;10:1278-80.

65. Ameloot K, Palmers PJ, Vande Bruaene A, et al. Clinical value of echocardiographic Doppler-derived right ventricular dp/dt in patients with pulmonary arterial hypertension. Eur Heart J Cardiovasc Imaging 2014;15:1411-9.

66. Tei C, Dujardin KS, Hodge DO, et al. Doppler echocardiographic index for assessment of global right ventricular function. J Am Soc Echocardiogr 1996;9:838-47.

67. Geyer H, Caracciolo G, Abe H, et al. Assessment of myocardial mechanics using speckle tracking echocardiography: fundamentals and clinical applications. J Am Soc Echocardiogr 2010;23:351-69.

68. Landzaat JWD, van Heerebeek L, Jonkman NH, et al. The quest for determination of standard reference values of right ventricular longitudinal systolic strain: a systematic review and meta-analysis. J Echocardiogr 2023;21:1-15.

69. Mukherjee M, Mathai SC, Jellis C, et al. Defining echocardiographic degrees of right heart size and function in pulmonary vascular disease from the PVDOMICS study. Circ Cardiovasc Imaging 2024;17:e017074.

70. Unlu S, Bezy S, Cvijic M, et al. Right ventricular strain related to pulmonary artery pressure predicts clinical outcome in patients with pulmonary arterial hypertension. Eur Heart J Cardiovasc Imaging 2023;24:635-42.

71. Farsalinos KE, Daraban AM, Unlu S, et al. Head-to-Head comparison of global longitudinal strain measurements among nine different vendors: the EACVI/ASE inter-vendor comparison study. J Am Soc Echocardiogr 2015;28:1171-81.e2.

72. Yock PG, Popp RL. Noninvasive estimation of right ventricular systolic pressure by Doppler ultrasound in patients with tricuspid regurgitation. Circulation 1984;70:657-62.

73. Jue J, Chung W, Schiller NB. Does inferior vena cava size predict right atrial pressures in patients receiving mechanical ventilation? J Am Soc Echocardiogr 1992;5:613-9.

74. Akintoye E, Wang TKM, Nakhla M, et al. Quantitative echocardiographic assessment and optimal criteria for early intervention in asymptomatic tricuspid regurgitation. JACC Cardiovasc Imaging 2022;16:13-24.

75. Lara-Breitinger KM, Miranda WR, Eleid MF, et al. Critical appraisal of pulmonary artery systolic pressure by Doppler echocardiography in patients with severe tricuspid regurgitation. J Am Soc Echocardiogr 2024;37:708-11.

76. D'Alto M, Di Maio M, Romeo E, et al. Echocardiographic probability of pulmonary hypertension: a validation study. Eur Respir J 2022;60:2102548.

77. Lam CS, Borlaug BA, Kane GC, et al. Age-associated increases in pulmonary artery systolic pressure in the general population. Circulation 2009;119:2663-70.

78. Mukherjee M, Strom JB, Afilalo J, et al. Normative values of echocardiographic chamber size and function in older healthy adults: the multi-ethnic study of atherosclerosis. Circ Cardiovasc Imaging 2024;17:e016420.

79. Masuyama T, Kodama K, Kitabatake A, et al. Continuous-wave Doppler echocardiographic detection of pulmonary regurgitation and its application to noninvasive estimation of pulmonary artery pressure. Circulation 1986;74:484-92.

80. Kaga S, Mikami T, Takamatsu Y, et al. Quantitative and pattern analyses of continuous-wave Doppler-derived pulmonary regurgitant flow velocity for the diagnosis of constrictive pericarditis. J Am Soc Echocardiogr 2014;27:1223-9.

81. Dabestani A, Mahan G, Gardin JM, et al. Evaluation of pulmonary artery pressure and resistance by pulsed Doppler echocardiography. Am J Cardiol 1987;59:662-8.

82. Abbas AE, Franey LM, Marwick T, et al. Noninvasive assessment of pulmonary vascular resistance by Doppler echocardiography. J Am Soc Echocardiogr 2013;26:1170-7.

83. Aduen JF, Castello R, Lozano MM, et al. An alternative echocardiographic method to estimate mean pulmonary artery pressure: diagnostic and clinical implications. J Am Soc Echocardiogr 2009;22:814-9.

84. Chemla D, Castelain V, Humbert M, et al. New formula for predicting mean pulmonary artery pressure using systolic pulmonary artery pressure. Chest 2004;126:1313-7.

85. Vonk Noordegraaf A, Chin KM, Haddad F, et al. Pathophysiology of the right ventricle and of the pulmonary circulation in pulmonary hypertension: an update. Eur Respir J 2019;53:1801900.

86. Rajagopalan N, Simon MA, Suffoletto MS, et al. Noninvasive estimation of pulmonary vascular resistance in pulmonary hypertension. Echocardiography 2009;26:489-94.

87. Reddy YNV, El-Sabbagh A, Nishimura RA. Comparing pulmonary arterial wedge pressure and left ventricular end diastolic pressure for assessment of left-sided filling pressures. JAMA Cardiol 2018;3:453-4.

88. Nagueh SF, Smiseth OA, Appleton CP, et al. Recommendations for the evaluation of left ventricular diastolic function by echocardiography: an update from the American Society of Echocardiography and the European Association of Cardiovascular Imaging. J Am Soc Echocardiogr 2016;29:277-314.

89. Rain S, Handoko ML, Trip P, et al. Right ventricular diastolic impairment in patients with pulmonary arterial hypertension. Circulation 2013;128:2016-25. 1-10.

90. Jung YH, Ren X, Suffredini G, et al. Right ventricular diastolic dysfunction and failure: a review. Heart Fail Rev 2022;27:1077-90.

91. Pye MP, Pringle SD, Cobbe SM. Reference values and reproducibility of Doppler echocardiography in the assessment of the tricuspid valve and right ventricular diastolic function in normal subjects. Am J Cardiol 1991;67:269-73.

92. Klein AL, Leung DY, Murray RD, et al. Effects of age and physiologic variables on right ventricular filling dynamics in normal subjects. Am J Cardiol 1999;84:440-8.

93. Berman GO, Reichek N, Brownson D, et al. Effects of sample volume location, imaging view, heart rate and age on tricuspid velocimetry in normal subjects. Am J Cardiol 1990;65:1026-30.

94. Carvalho SC, Singh A, Miyoshi T, et al. Sex-, age-, and race-related normal values of right ventricular diastolic function parameters: data from the World Alliance Societies of Echocardiography Study. J Am Soc Echocardiogr 2022;35:426-34.

95. Trip P, Rain S, Handoko ML, et al. Clinical relevance of right ventricular diastolic stiffness in pulmonary hypertension. Eur Respir J 2015;45:1603-12.

96. Gan CT, Holverda S, Marcus JT, et al. Right ventricular diastolic dysfunction and the acute effects of sildenafil in pulmonary hypertension patients. Chest 2007;132:11-7.

97. Kolte D, Lakshmanan S, Jankowich MD, et al. Mild pulmonary hypertension is associated with increased mortality: a systematic review and meta-analysis. J Am Heart Assoc 2018;7:e009729.

98. Sanz J, Sánchez-Quintana D, Bossone E, et al. Anatomy, function, and dysfunction of the right ventricle: JACC state-of-the-art review. J Am Coll Cardiol 2019;73:1463-82.

99. Unlu S, Farsalinos K, Ameloot K, et al. Apical traction: a novel visual echocardiographic parameter to predict survival in patients with pulmonary hypertension. Eur Heart J Cardiovasc Imaging 2016;17:177-83.

100. Motoji Y, Tanaka H, Fukuda Y, et al. Interdependence of right ventricular systolic function and left ventricular filling and its association with outcome for patients with pulmonary hypertension. Int J Cardiovasc Imaging 2015;31:691-8.

101. Rako ZA, Yogeswaran A, Lakatos BK, et al. Clinical and functional relevance of right ventricular contraction patterns in pulmonary hypertension. J Heart Lung Transplant 2023;42:1518-28.

102. D'Alto M, Badesch D, Bossone E, et al. A fluid challenge test for the diagnosis of occult heart failure. Chest 2021;159:791-7.

103. Agrawal V, D'Alto M, Naeije R, et al. Echocardiographic detection of occult diastolic dysfunction in pulmonary hypertension after fluid challenge. J Am Heart Assoc 2019;8:e012504.

104. Rudski LG, Gargani L, Armstrong WF, et al. Stressing the cardiopulmonary vascular system: the role of echocardiography. J Am Soc Echocardiogr 2018;31:527-50.e11.

105. Gargani L, Pugliese NR, De Biase N, et al. Exercise stress echocardiography of the right ventricle and pulmonary circulation. J Am Coll Cardiol 2023;82:1973-85.

106. Lancellotti P, Pellikka PA, Budts W, et al. The clinical Use of stress echocardiography in non-Ischaemic heart disease: recommendations from the European association of cardiovascular imaging and the American Society of echocardiography. J Am Soc Echocardiogr 2017;30:101-38.

107. Bidart CM, Abbas AE, Parish JM, et al. The noninvasive evaluation of exercise-induced changes in pulmonary artery pressure and pulmonary vascular resistance. J Am Soc Echocardiogr 2007;20:270-5.

108. Luong CL, Anand V, Padang R, et al. Prognostic significance of elevated left ventricular filling pressures with exercise: insights from a cohort of 14,338 patients. J Am Soc Echocardiogr 2024;37:382-93.e1.

109. Grünig E, Tiede H, Enyimayew EO, et al. Assessment and prognostic relevance of right ventricular contractile reserve in patients with severe pulmonary hypertension. Circulation 2013;128:2005-15.

110. Bossone E, Rubenfire M, Bach DS, et al. Range of tricuspid regurgitation velocity at rest and during exercise in normal adult men: implications for the diagnosis of pulmonary hypertension. J Am Coll Cardiol 1999;33:1662-6.

111. D'Alto M, Pavelescu A, Argiento P, et al. Echocardiographic assessment of right ventricular contractile reserve in healthy subjects. Echocardiography 2017;34:61-8.

112. Mukherjee M, Mercurio V, Hsu S, et al. Assessment of right ventricular reserve utilizing exercise provocation in systemic sclerosis. Int J Cardiovasc Imaging 2021;37:2137-47.

113. Lu J, Jani V, Mercurio V, et al. Stress echocardiographic prediction of emerging pulmonary vascular disease in systemic sclerosis. J Am Soc Echocardiogr 2023;36:259-61.

114. Zeder K, Banfi C, Steinrisser-Allex G, et al. Diagnostic, prognostic and differential-diagnostic relevance of pulmonary haemodynamic parameters during exercise: a systematic review. Eur Respir J 2022;60:2103181.

115. Prihadi EA, Delgado V, Leon MB, et al. Morphologic types of tricuspid regurgitation: characteristics and prognostic implications. JACC Cardiovasc Imaging 2019;12:491-9.

116. Hahn RT. State-of-the-art review of echocardiographic imaging in the evaluation and treatment of functional tricuspid regurgitation. Circ Cardiovasc Imaging 2016;9:e005332.

117. Hahn RT, Weckbach LT, Noack T, et al. Proposal for a standard echocardiographic tricuspid valve Nomenclature. JACC Cardiovasc Imaging 2021;14:1299-305.

118. Zoghbi WA, Adams D, Bonow RO, et al. Recommendations for noninvasive evaluation of native valvular regurgitation: a report from the American Society of Echocardiography developed in collaboration with the Society for Cardiovascular Magnetic Resonance. J Am Soc Echocardiogr 2017;30:303-71.

119. Florescu DR, Muraru D, Florescu C, et al. Right heart chambers geometry and function in patients with the atrial and the ventricular phenotypes of functional tricuspid regurgitation. Eur Heart J Cardiovasc Imaging 2021.

120. Kim HK, Kim YJ, Park JS, et al. Determinants of the severity of functional tricuspid regurgitation. Am J Cardiol 2006;98:236-42.

121. Mutlak D, Aronson D, Lessick J, et al. Functional tricuspid regurgitation in patients with pulmonary hypertension: is pulmonary artery pressure the only determinant of regurgitation severity? Chest 2009;135:115-21.

122. Addetia K, Maffessanti F, Muraru D, et al. Morphologic analysis of the normal right ventricle using three-dimensional echocardiography-derived curvature indices. J Am Soc Echocardiogr 2018;31:614-23.

123. Bidviene J, Muraru D, Maffessanti F, et al. Regional shape, global function and mechanics in right ventricular volume and pressure overload conditions: a three-dimensional echocardiography study. Int J Cardiovasc Imaging 2021;37:1289-99.

124. Grapsa J, Gibbs JS, Dawson D, et al. Morphologic and functional remodeling of the right ventricle in pulmonary hypertension by real time three dimensional echocardiography. Am J Cardiol 2012;109:906-13.

125. Spinner EM, Lerakis S, Higginson J, et al. Correlates of tricuspid regurgitation as determined by 3D echocardiography: pulmonary arterial pressure, ventricle geometry, annular dilatation, and papillary muscle displacement. Circ Cardiovasc Imaging 2012;5:43-50.

126. Addetia K, Muraru D, Veronesi F, et al. 3-Dimensional echocardiographic analysis of the tricuspid annulus provides new insights into tricuspid valve geometry and dynamics. JACC Cardiovasc Imaging 2019;12:401-12.

127. Afilalo J, Grapsa J, Nihoyannopoulos P, et al. Leaflet area as a determinant of tricuspid regurgitation severity in patients with pulmonary hypertension. Circ Cardiovasc Imaging 2015;8.

128. Muraru D, Badano LP, Hahn RT, et al. Atrial secondary tricuspid regurgitation: pathophysiology, definition, diagnosis, and treatment. Eur Heart J 2024;45:895-911.

129. Schlotter F, Dietz MF, Stolz L, et al. Atrial functional tricuspid regurgitation: novel definition and impact on prognosis. Circ Cardiovasc Interv 2022;15:e011958.

130. Soulat-Dufour L, Lang S, Addetia K, et al. Restoring sinus rhythm reverses cardiac remodeling and reduces valvular regurgitation in patients with atrial fibrillation. J Am Coll Cardiol 2022;79:951-61.

131. Baumgartner H, Hung J, Bermejo J, et al. Echocardiographic assessment of valve stenosis: EAE/ASE recommendations for clinical practice. J Am Soc Echocardiogr 2009;22:1-23.

132. Yang H, Pu M, Chambers CE, et al. Quantitative assessment of pulmonary insufficiency by Doppler echocardiography in patients with adult congenital heart disease. J Am Soc Echocardiogr 2008;21:157-64.

133. D'Alto M, Romeo E, Argiento P, et al. Pulmonary arterial hypertension: the key role of echocardiography. Echocardiography 2015;32(Suppl 1):S23-37.

134. Alenezi F, Covington TA, Mukherjee M, et al. Novel approaches to imaging the pulmonary vasculature and right heart. Circ Res 2022;130:1445-65.

135. Weber BN, Paik JJ, Aghayev A, et al. Novel imaging approaches to cardiac manifestations of systemic inflammatory diseases: JACC scientific statement. J Am Coll Cardiol 2023;82:2128-51.

136. Montani D, Girerd B, Jaïs X, et al. Screening for pulmonary arterial hypertension in adults carrying a BMPR2 mutation. Eur Respir J 2021;58:2004229.

137. Chen L, Larsen CM, Le RJ, et al. The prognostic significance of tricuspid valve regurgitation in pulmonary arterial hypertension. Clin Respir J 2018;12:1572-80.

138. Ghio S, Mercurio V, Fortuni F, et al. A comprehensive echocardiographic method for risk stratification in pulmonary arterial hypertension. Eur Respir J 2020;56:2000513.

139. Dardi F, Boucly A, Benza R, et al. Risk stratification and treatment goals in pulmonary arterial hypertension. Eur Respir J 2024;64:2401323.

140. Cubero Salazar IM, Lancaster AC, Jani VP, et al. Poor cardiac output reserve in pulmonary arterial hypertension is associated with right ventricular stiffness and impaired interventricular dependence. Eur Respir J 2024;64:2400420.

141. Fletcher AJ, Robinson S, Rana BS. Echocardiographic RV-E/e' for predicting right atrial pressure: a review. Echo Res Pract 2020;7:R11-20.

142. Forfia P, Benza R, D'Alto M, et al. The heart of the matter: right heart imaging indicators for treatment escalation in pulmonary arterial hypertension. Pulm Circ 2023;13:e12240.

143. Celestin BE, Bagherzadeh SP, Ichimura K, et al. Identifying consistent echocardiographic thresholds for risk stratification in pulmonary arterial hypertension. Pulm Circ 2024;14:e12361.

144. Rajagopal S, Forsha DE, Risum N, et al. Comprehensive assessment of right ventricular function in patients with pulmonary hypertension with global longitudinal peak systolic strain derived from multiple right ventricular views. J Am Soc Echocardiogr 2014;27:657-65.e3.

145. Mukherjee M, Chung SE, Ton VK, et al. Unique abnormalities in right ventricular longitudinal strain in systemic sclerosis patients. Circ Cardiovasc Imaging 2016;9:e003792.

146. Mukherjee M, Mercurio V, Tedford RJ, et al. Right ventricular longitudinal strain is diminished in systemic sclerosis compared with idiopathic pulmonary arterial hypertension. Eur Respir J 2017;50:1701436.

147. Li AL, Zhai ZG, Zhai YN, et al. The value of speckle-tracking echocardiography in identifying right heart dysfunction in patients with chronic thromboembolic pulmonary hypertension. Int J Cardiovasc Imaging 2018;34:1895-904.

148. Mercurio V, Mukherjee M, Tedford RJ, et al. Improvement in right ventricular strain with ambrisentan and tadalafil upfront therapy in Scleroderma pulmonary arterial hypertension. Am J Respir Crit Care Med 2017;197:388-91.

149. Fine NM, Chen L, Bastiansen PM, et al. Outcome prediction by quantitative right ventricular function assessment in 575 subjects evaluated for pulmonary hypertension. Circ Cardiovasc Imaging 2013;6:711-21.

150. Schuijt MTU, Blok IM, Zwinderman AH, et al. Mortality in pulmonary arterial hypertension due to congenital heart disease: serial changes improve prognostication. Int J Cardiol 2017;243:449-53.

151. Grigioni F, Potena L, Galiè N, et al. Prognostic implications of serial assessments of pulmonary hypertension in severe chronic heart failure. J Heart Lung Transplant 2006;25:1241-6.

152. Nickel N, Golpon H, Greer M, et al. The prognostic impact of follow-up assessments in patients with idiopathic pulmonary arterial hypertension. Eur Respir J 2012;39:589-96.

153. Mukherjee M, Mercurio V, Balasubramanian A, et al. Defining minimal detectable difference in echocardiographic measures of right ventricular function in systemic sclerosis. Arthritis Res Ther 2022;24:146.

154. Farrell C, Balasubramanian A, Hays AG, et al. A clinical approach to multimodality imaging in pulmonary hypertension. Front Cardiovasc Med 2021;8:794706.

155. Hahn RT, Lerakis S, Delgado V, et al. Multimodality imaging of right heart function: JACC scientific statement. J Am Coll Cardiol 2023;81:1954-73.

156. Steele JM, Moore RA, Lang SM. Use of advanced cardiac imaging in congenital heart disease: growth, indications and innovations. Curr Opin Pediatr 2021;33:495-502.

157. Mavrogeni S, Pepe A, Nijveldt R, et al. Cardiovascular magnetic resonance in autoimmune rheumatic diseases: a clinical consensus document by the European Association of Cardiovascular Imaging. Eur Heart J Cardiovasc Imaging 2022;23:e308-22.

158. Freed BH, Gomberg-Maitland M, Chandra S, et al. Late gadolinium enhancement cardiovascular magnetic resonance predicts clinical worsening in patients with pulmonary hypertension. J Cardiovasc Magn Reson 2012;14:11.

159. Swift AJ, Rajaram S, Capener D, et al. LGE patterns in pulmonary hypertension do not impact overall mortality. JACC Cardiovasc Imaging 2014;7:1209-17.

160. Ahmadi A, Ohira H, Mielniczuk LM. FDG PET imaging for identifying pulmonary hypertension and right heart failure. Curr Cardiol Rep 2015;17:555.

161. Li W, Wang L, Xiong CM, et al. The prognostic value of 18F-FDG uptake ratio between the right and left ventricles in idiopathic pulmonary arterial hypertension. Clin Nucl Med 2015;40:859-63.

162. Kazimierczyk R, Szumowski P, Nekolla SG, et al. Prognostic role of PET/MRI hybrid imaging in patients with pulmonary arterial hypertension. Heart 2021;107:54-60.

163. Huston JH, Maron BA, French J, et al. Association of Mild Echocardiographic Pulmonary Hypertension with Mortality and Right Ventricular Function. JAMA Cardiology 2019;4:1112-21.